ROLE OF INNATE HOST DEFENSES IN ACUTE AND VACCINATION MODELS OF PNEUMONIC TULAREMIA

by

Deanna Marie Schmitt

Bachelor of Science, The Pennsylvania State University, 2005

Submitted to the Graduate Faculty of

the School of Medicine in partial fulfillment

of the requirements for the degree of

Doctor of Philosophy

University of Pittsburgh

2012

UNIVERSITY OF PITTSBURGH

SCHOOL OF MEDICINE

This dissertation was presented

by

Deanna Marie Schmitt

It was defended on

August 8, 2012

and approved by

Dr. L. Antoinette Darville, M.D.
Professor, Department of Pediatrics

Dr. JoAnne L. Flynn, Ph.D.
Professor, Department of Microbiology and Molecular Genetics

Dr. Tim D. Oury, M.D., Ph.D.
Professor, Department of Pathology

Dr. Russell D. Salter, Ph.D.
Professor, Department of Immunology

Dissertation Advisor:
Dr. Gerard J. Nau, M.D., Ph.D.
Assistant Professor, Department of Microbiology and Molecular Genetics

ROLE OF INNATE HOST DEFENSES IN ACUTE AND VACCINATION MODELS OF PNEUMONIC TULAREMIA

Deanna Marie Schmitt, Ph.D.

University of Pittsburgh, 2012

The innate immune system is the first line of defense against invading pathogens. In order to establish a productive infection, microorganisms must effectively evade host defenses. The intracellular bacterium *Francisella tularensis* possesses multiple strategies to actively and passively avoid recognition and clearance by the host. Moreover, *F. tularensis* elicits a delayed innate immune response compared to other respiratory pathogens such as *Klebsiella pneumoniae*. Whether this immune response plays a beneficial or detrimental role in tularemia pathogenesis is not known. In this thesis, the contribution of innate host defenses against *F. tularensis* was evaluated in two different settings: acute infection of naïve animals with a type A strain and after vaccination with the live vaccine strain (LVS). First, a comprehensive comparison of the early host response to the virulent type A *F. tularensis* strain Schu S4 and the attenuated type B strain LVS revealed several unique features of type A *F. tularensis* infection. The most significant immunological difference between these strains was a reduction in the number of viable lung cells, particularly NK cells and T cells, in Schu S4-infected mice. Since the decline in NK cells correlated with morbidity and mortality, the role of these cells in host defense against Schu S4 infection was evaluated. Modulation of NK cells did not have a demonstrable effect on Schu S4 infection *in vivo* suggesting these cells do not contribute to immunity against type A *F. tularensis*. In the final part of this thesis, LVS was genetically modified in order to better

stimulate antigen-presenting cells and improve vaccine efficacy. Although LVS FTL_0883 mutants elicited increased proinflammatory cytokine production and costimulatory molecule expression by macrophages and DCs, they failed to provide better protection against Schu S4 challenge than wild-type LVS. The data presented in this thesis expands our current knowledge of the innate immune response to *F. tularensis* and provides insight into tularemia vaccine development and immunotherapy.

TABLE OF CONTENTS

LIST OF TABLES

LIST OF FIGURES

PREFACE

First and foremost, I want to acknowledge my parents, Donna and Walter Tarwacki, for their constant love and support over the past 29 years. I appreciate all the sacrifices you have made to allow me to follow my dreams and become "Dr. Dee". To my husband, Matt, being the spouse of a graduate student isn't easy, particularly with the odd work hours and the constant frustrations that come with scientific research. Your continuous encouragement helped me get through some tough times and I could not have achieved this doctorate without you. To my daughter Ally, your beautiful smiling face constantly motivates me to be a better person, scientist, and mother. To my mentor, Dr. Jerry Nau, without your guidance, this project would never have progressed into the solid body of work found in this dissertation. Thank you for helping me to develop into an independent scientist. To both past and present members of the Nau lab, thank you for providing endless amounts of laughter, advice, and technical support. I will miss interacting with each of you on a daily basis. To my thesis committee, Dr. Flynn, Dr. Darville, Dr. Salter, and Dr. Oury, your insight and suggestions at each committee meeting provided an invaluable contribution to this dissertation. Lastly, to all my graduate school friends, thank you for being there to celebrate in my accomplishments and commiserate in my failures. I am grateful for meeting and knowing each one of you.

1.0 INTRODUCTION

1.1 *FRANCISELLA TULARENSIS*

Originally named “Bacterium tularense”, *Francisella tularensis* was first isolated from ground squirrels exhibiting a “plaguelike disease” in Tulare County, CA in 1911 (Francis, 1925). The first cases of human *F. tularensis* infection were reported in Ohio in 1914 (Wherry, 1914) and by 1928; more than 600 cases had been documented (Francis, 1928). Currently, *F. tularensis* has been isolated from over 250 animal species including fish, birds, rodents, lagomorphs, and arthropods (Oyston et al., 2004). *F. tularensis* is also capable of infecting protozoans such as amoeba, which may serve as natural reservoirs (Abd et al., 2003; Oyston et al., 2004).

Infection with *F. tularensis* results in the potentially fatal illness, tularemia. Less than 10 organisms can cause disease and up to 60% of individuals with *F. tularensis* pneumonia die in the absence of antibiotic therapy (Dennis et al., 2001; McLendon et al., 2006). Transmission of tularemia can occur through an arthropod vector, handling of infected animals, or inhalation of infectious particles (Oyston, 2008). In the United States, approximately 100-200 cases of tularemia are diagnosed each year (Barry et al., 2009; Feldman et al., 2001). Worldwide, there also is a low incidence of disease although tularemia outbreaks are common, particularly in Eastern Europe (Ryden et al., 2012). Large outbreaks involving up to 900 people have been regularly reported in Sweden and Finland since 2000 (Ryden et al., 2012). Due to its

aerosolization potential and high infectivity and mortality, the Centers for Disease Control and Prevention designated *F. tularensis* a Category A bioterrorism agent (Barry et al., 2009). Following the events of September 2001 and the subsequent anthrax attacks in the United States, increased biodefense funding resulted in a renewed interest in this bacterium (Oyston, 2008).

1.1.1 *F. tularensis* subspecies

F. tularensis consists of four subspecies: *tularensis, holarctica, novicida,* and *mediasiatica*. Subspecies classification is based on degree of virulence and geographic location (Table 1). *F. tularensis* subspecies *mediasiatica* is the only subspecies that has not been associated with human disease (Oyston et al., 2004). This subspecies has been isolated in Central Asia and some parts of the former Soviet Union. *F. tularensis* subspecies *novicida* (*F. novicida*) rarely causes human disease, though it can infect immunocompromised individuals (Oyston et al., 2004). Isolates of this subspecies have been found in North America and Australia (Oyston et al., 2004). A moderately virulent *F. tularensis* subspecies prevalent in Europe, Asia, and North America, *F. tularensis* subspecies *holarctica* (Type B *Francisella*), causes a mild, protracted disease typically involving infection through the skin (Oyston et al., 2004). *F. tularensis* subspecies *tularensis* (Type A *Francisella*) is the most virulent subspecies with an estimated LD_{50} of less than 10 colony forming units (CFU) in humans when inhaled (Pechous et al., 2009). This subspecies is responsible for approximately 90% of all tularemia cases documented in North America (Choi, 2002). Type A *Francisella* can be further divided into two distinct clades: A.I and A.II (Keim et al., 2007). These two clades differ in their geographic distribution in the United States, disease outcome, and transmission route (Keim et al., 2007). Clade A.II, found in the Rocky Mountain

region, is less virulent than clade A.I, found in the eastern United States and California (Keim et al., 2007; Staples et al., 2006).

Table 1: *F. tularensis* subspecies

***F. tularensis* subspecies**		**Virulence in humans**	**Global Distribution**
tularensis	clade A.I	+++++	North America (Eastern United States)
	clade A.II	++++	North America (Western United States)
holarctica		+++	Europe, Asia, North America
mediasiatica		ND[a]	Central Asia and some parts of the former Soviet Union
novicida		+	North America and Australia

[a]ND, not determined
[b]modified from Oyston et al. 2004 with permission from Nature Publishing Group

1.1.2 Tularemia

Tularemia can present in various forms depending on the route of *F. tularensis* infection (Table 2). Ulceroglandular tularemia is the most common and involves infection through the skin (Oyston et al., 2004). Typically, an individual acquires this disease by the bite of infected arthropod vector or direct contact with an infected animal (Oyston et al., 2004). Three to five days later, the patient develops flu-like symptoms including fever, chills, malaise, headache, and sore throat (Oyston, 2008). An ulcer also forms at the site of infection (Titball and Oyston, 2003). The draining lymph nodes may become enlarged and suppuration occurs in 30% of cases if left untreated (Oyston, 2008). The mortality rate for this specific form of tularemia is less than 5% (Pechous et al., 2009). Typhoidal tularemia is diagnosed in cases where an individual

presents with the flu-like symptoms but the route of infection remains unknown (Dennis et al., 2001). In rare instances, *F. tularensis* can infect the eye resulting in oculoglandular tularemia (Oyston et al., 2004). The eye becomes inflamed and a purulent secretion surrounds the area (Oyston, 2008). If antibiotic therapy is not administered, the infection can spread to the local lymph nodes (Oyston, 2008). Ingestion of food or water contaminated with *F. tularensis* is known as oropharyngeal or gastrointestinal tularemia (Oyston, 2008). Oropharyngeal tularemia is diagnosed when symptoms are localized to the upper gastrointestinal tract including ulcers, pharyngitis, swollen cervical lymph nodes and the development of a yellow-white pseudomembrane over the pharynx (Oyston, 2008). Depending on the infectious dose, gastrointestinal tularemia can present as mild to moderate diarrhea or extensive bowel ulceration (Oyston, 2008). The most severe form of tularemia involves inhalation of *F. tularensis* known as pneumonic tularemia. Farmers and landscapers are most at-risk due to occupational exposure through hay-making, lawn-mowing, and brush cutting (Oyston, 2008). Presentation of this disease varies depending on the infecting *F. tularensis* strain. Type B *Francisella* causes mild pneumonia, while infection with Type A *Francisella* results in severe illness with high fever, malaise, chills, cough, delirium, and pulse-temperature dissociation (Oyston, 2008). Without administration of antibiotics, pneumonic tularemia has a case fatality rate of 30-60% (Dennis et al., 2001). Outbreaks of pneumonic tularemia are rare although one occurred recently in Martha's Vineyard in 2000 (Feldman et al., 2001; Oyston, 2008). Fifteen cases of tularemia were reported with one fatality (Feldman et al., 2001). The largest recorded outbreak of pneumonic tularemia occurred in Sweden from 1966-1967 and involved more than 600 individuals (Oyston et al., 2004; Pechous et al., 2009). Today, cases of tularemia are often underreported due to the non-specific symptoms associated with disease (Pechous et al., 2009).

Table 2: Clinical forms of tularemia

Form	Route of Acquisition	Mortality Rate[b]
Ulceroglandular	Bite of infected arthropod vector or direct contact with an infected animal	< 5%
Oculoglandular	Touching the eye with a contaminated finger	ND[c]
Oropharyngeal or Gastrointestinal	Ingestion of contaminated food or water	ND[c]
Pneumonic	Inhalation of aerosolized *F. tularensis*	30-60%
Typhoidal	Unknown	30-60%

[a]Information presented in this table obtained from (Oyston, 2008; Oyston and Quarry, 2005; Oyston et al., 2004)
[b]Without antibiotic treatment
[c]ND = Not Determined

1.1.3 *F. tularensis* as a bioterrorism agent

Based on historical records, *F. tularensis* has been used for thousands of years as a biowarfare agent. In 1300 B.C., infected Neshite soldiers deliberately spread the disease to their Arzawan enemies during the Anatolian war (Trevisanato, 2007). *F. tularensis* was investigated by the Japanese as part of their biological weapons development program from 1932-1945 (Barry et al., 2009). During World War II, a tularemia outbreak among thousands of Soviet and German soldiers was attributed to an intentional release of this pathogen (Dennis et al., 2001). The United States and Soviet Union worked to develop a weapon that could disseminate *F. tularensis* aerosols during the Cold War (Nigrovic and Wingerter, 2008). By the late 1960s, *F. tularensis* was one of several biological weapons stockpiled by the United States military (Christopher et al., 1997). While the United States terminated its biological weapons program in 1970, the Soviet Union continued its program until the early 1990s (Dennis et al., 2001). Ken Alibek, a

former Soviet Union scientist, claimed that antibiotic- and vaccine-resistant *F. tularensis* strains were generated during this time (Sjostedt, 2007). The World Health Organization predicted that aerosolization of *F. tularensis* within a metropolitan area containing five million people would result in 19,000 deaths and leave another 250,000 individuals incapacitated (McLendon et al., 2006). Currently, *F. tularensis* is one of six agents characterized as the most likely biological threats to the United States (Sjostedt, 2007).

1.1.4 Bacteriology of *F. tularensis*

F. tularensis is a non-motile Gram-negative coccobacillus capable of infecting numerous cell types including macrophages, dendritic cells, neutrophils, hepatocytes, fibroblasts, epithelial cells, and endothelial cells (Cowley and Elkins, 2011; Oyston, 2008). It is a nutritionally fastidious organism and requires the amino acid cysteine for growth (Sandstrom, 1994). Based on 16S ribosomal RNA sequencing, *F. tularensis* is assigned to the class Gammaproteobacteria with its closest relatives being endosymbionts like *Wolbacchia persica* (Oyston, 2008). This bacterium is also distantly related to the human pathogens *Coxiella burnetti* and *Legionella pneumophila* (Oyston, 2008). Given its success at causing severe disease and invading a wide repertoire of host cells, *F. tularensis* must possess numerous virulence factors.

1.1.5 *F. tularensis* virulence factors

1.1.5.1 *Francisella* Pathogenicity Island (FPI)

First identified in 2004, the FPI is a 30kb region of the *F. tularensis* genome that is essential for intracellular growth and virulence in mice (Nano et al., 2004). Type A and Type B *Francisella*

contain two copies of the FPI, while *F. novicida* contains only one (Oyston, 2008). For this reason, most investigations on the function of different FPI genes have been conducted with *F. novicida* (Oyston, 2008). The FPI contains approximately 19 genes including the intracellular growth locus (*iglA-J, iglF* is also known as *clpV*), the pathogenicity determinant protein family (*pdpA-E, pdpB* and *pdpE* are also known as *icmF* and *hcp* respectively), *vsrG* (valine glycine repeat), *dotU* (defect in organelle trafficking), and *anmK* (anhydro-N-acetylmuramic acid kinase) (Fig. 1). The best characterized FPI protein is IglC. It is highly expressed in macrophages and is required to inhibit phagosome maturation and for escape into the cytosol (Golovliov et al., 1997; Lindgren et al., 2004a; Santic et al., 2005b). It also plays a role in the downregulation of NF-κB signaling and induction of apoptosis in macrophages (Lai et al., 2004; Telepnev et al., 2003). Similar to *iglC* mutants, *pdpA* mutants colocalize with lysosomal markers suggesting this gene also plays a role in phagosomal escape (Schmerk et al., 2009). The genes *pdpB, vgrG, iglF/clpV, pdpE/hcp*, and *dotU* are homologous to members of the type VI secretion system found in *P. aeruginosa* and *V. cholera* (Barker et al., 2009). Conventionally, IcmF, ClpV, and DotU mediate secretion of Hcp and VgrG (Oyston, 2008). In *F. tularensis*, VgrG and IglI are secreted into macrophages and are required for phagosomal escape and replication in the cytosol (Barker et al., 2009). IglA and IglB have also been implicated in type VI secretion (de Bruin et al., 2007). PdpD localizes to the outer membrane and interacts with members of the type VI secretion system, IglA, IglB, and IglC (Ludu et al., 2008). AnmK is only fully expressed in *F. novicida* and it is not essential for intracellular growth *in vitro* or *in vivo* (Ludu et al., 2008). Other FPI genes, *iglE, iglG, iglH,* and *iglJ,* have no known function and have not been confirmed to play a role in *F. tularensis* intracellular growth (Barker et al., 2009; Broms et al., 2010).

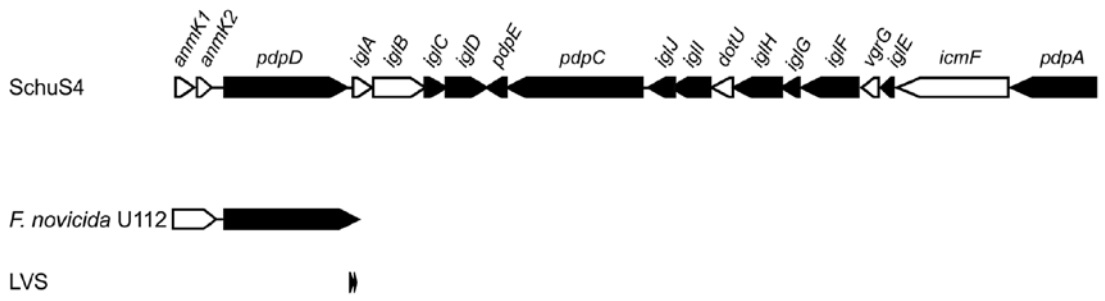

Figure 1. Schematic representation of the *Francisella* pathogenicity island.

The ORFs of the FPI are essentially the same in all subspecies, with the exception of the anmK-pdpD region. Compared to *F. novicida*, the pdpD gene in Schu S4 is slightly smaller and the anmK gene is separated into two distinct ORFs. LVS lacks anmK and most of the pdpD gene due to a large deletion within this region. The open reading frames represented by black arrows indicate gene products with no significant homology to other proteins; while white arrows represent products with homologs in other bacterial systems. Adapted from (Broms et al., 2010) with permission.

FPI gene expression is regulated by a variety of transcription factors. MglA (macrophage growth locus A) is a global transcription factor in *F. tularensis,* regulating the expression of more than 100 genes (Brotcke et al., 2006; Lauriano et al., 2004). This protein forms a complex with SspA (stringent starvation protein A) to associate with the RNA polymerase and regulate transcription (Charity et al., 2007). PmrA was identified as an orphan two-component response regulator in *F. tularensis* that regulates the expression of genes within and outside the FPI (Mohapatra et al., 2007). Very few genes are regulated by both PmrA and MglA (Brotcke and Monack, 2008). In addition, PmrA does not regulate MglA and vice versa suggesting these two transcription factors function independently of each other (Mohapatra et al., 2007). FevR (*Francisella* effector of virulence regulation) is regulated by the MglA/SspA complex and functions in parallel to MglA to positively regulate FPI genes (Brotcke and Monack, 2008). Another transcription element, MigR (macrophage intracellular growth

regulator), regulates FevR as well as the *iglABCD* operon (Buchan et al., 2009). The only negative regulator of the FPI is Hfq which functions to downregulate the *pdp* operon (Meibom et al., 2009).

1.1.5.2 Capsule

The existence of an *F. tularensis* capsule is controversial. Several researchers have successfully visualized the capsule using electron microscopy (Golovliov et al., 2003; Hood, 1977; Sandstrom et al., 1988). Others question its presence due to an inability to detect or isolate this electron dense material (Clay et al., 2008; Clemens et al., 2005; Raynaud et al., 2007). *F. tularensis* possesses orthologs of the *Bacillus anthracis capBCA* operon which encodes the poly-D-glutamic acid capsule biosynthesis machinery (Larsson et al., 2005). While poly-D-glutamic acid could not be detected in *F. tularensis* extracts or on the surface of the bacteria (Michell et al., 2010; Raynaud et al., 2007), deletion of *capB* or the entire operon attenuates *F. tularensis in vivo* (Jia et al., 2010; Michell et al., 2010; Su et al., 2007). This suggests that while *capBCA* may not encode components necessary for capsule assembly, this locus contributes to virulence. Apicella and colleagues isolated capsular material from *F. tularensis* and determined that it was comprised of repeating O-antigen subunits (Apicella et al., 2010). A subsequent study by Lindemann et al. identified the gene loci in the type A *F. tularensis* strain Schu S4 (FTT1236, FTT1237, and FTT1238) responsible for the synthesis of this O-antigen capsule (Lindemann et al., 2011). Mutations in any of the three genes resulted in increased sensitivity and reduced intracellular growth (Lindemann et al., 2011). Furthermore, macrophages infected with these mutants undergo rapid cell death suggesting these genes play a role in intramacrophage survival (Lindemann et al., 2011). More recently, a second capsular material has been described that is

distinct from the O-antigen capsule (Bandara et al., 2011). This capsule-like complex (CLC) is believed to consist of an unidentified glycoprotein (Bandara et al., 2011).

1.1.5.3 Lipopolysaccharide (LPS)

Compared to other Gram-negative bacteria, the LPS of *F. tularensis* has a unique structure (Fig. 2) and poorly activates proinflammatory responses due to lack of recognition by TLR2 and TLR4 (Gunn and Ernst, 2007). The lipid A component is missing free phosphate moieties and is hypoacylated compared to other LPS species (Phillips et al., 2004; Vinogradov et al., 2002; Wang et al., 2006). Removal of the 4'-phosphate is mediated by the lipid A phosphatase LpxF (Wang et al., 2007). The *lpxF* mutant is attenuated in a mouse model of infection suggesting the altered lipid A structure of *F. tularensis* contributes to its virulence (Wang et al., 2007). The LPS O-antigen is also important for *F. tularensis* pathogenesis. O-antigen mutants are more susceptible to complement-mediated killing by serum and are attenuated for growth *in vitro* (Raynaud et al., 2007; Thomas et al., 2007). Furthermore, two *F. tularensis* phase variants, blue and grey, which differ in their O-antigen structure, engender different immune responses (Cowley et al., 1996). Unlike the blue variant, the grey variant stimulated increased NO production resulting in limited growth in macrophages (Cowley et al., 1996).

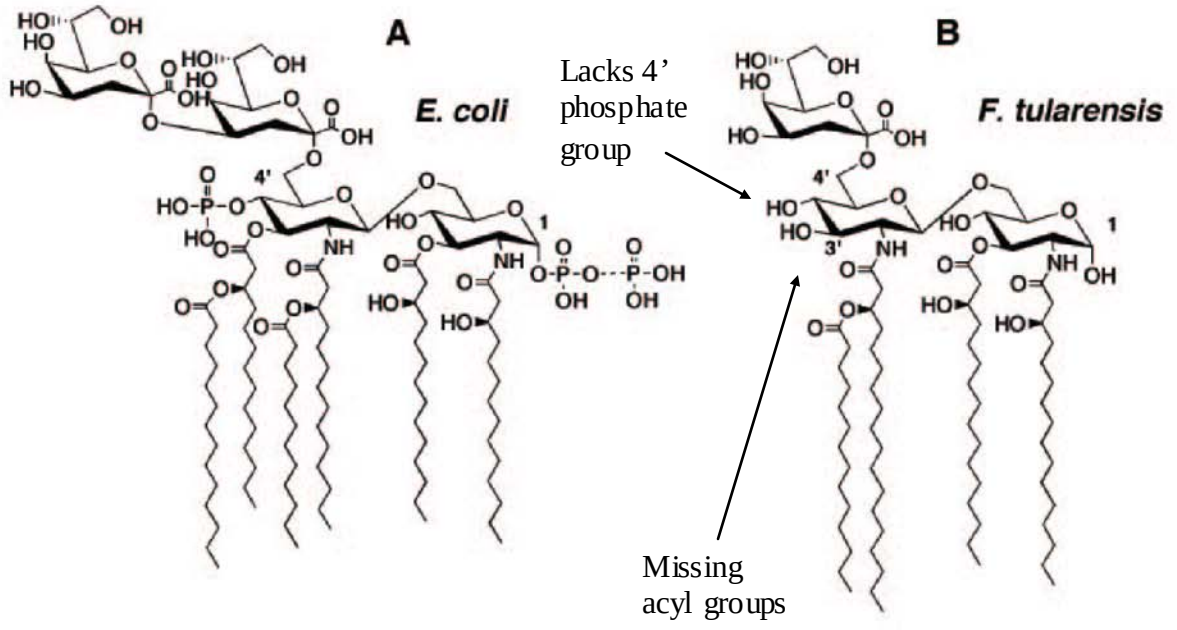

Figure 2. Lipid A structures for *E. coli* and *F. tularensis*.

The lipid A component of *F. tularensis* LPS is missing free phosphate moieties and is hypoacylated compared to *E. coli* LPS. Adapted from (Wang et al., 2004) with permission.

1.1.5.4 Type IV Pili

Pili are filamentous bacterial surface structures involved in many physiological processes including adhesion, biofilm formation, and protein secretion (Pechous et al., 2009). The type IV pilus is composed of one major pilin subunit, PilA, and several additional minor pilins, PilB, PilC, PilD, PilQ, and PilT (Forslund et al., 2010) (Fig. 3). Within the *F. tularensis* genome, homologs of all the pilin genes are present (Forsberg and Guina, 2007). Pili have also been observed on the surface of *F. tularensis* by electron microscopy (Gil et al., 2004). Deletion of any of the pilin genes in *F. tularensis* results in reduced virulence in mice (Chakraborty et al., 2008; Forslund et al., 2006; Forslund et al., 2010). Furthermore, the attenuation of the *F. tularensis* live vaccine strain, LVS, was attributed to loss of *pilA* (Salomonsson et al., 2009). The pilin genes, *pilB*, *pilC*, *pilQ*, and *pilD* are homologous to components of the type II secretion

system and are required for protein secretion in *F. novicida* (Hager et al., 2006; Salomonsson et al., 2011).

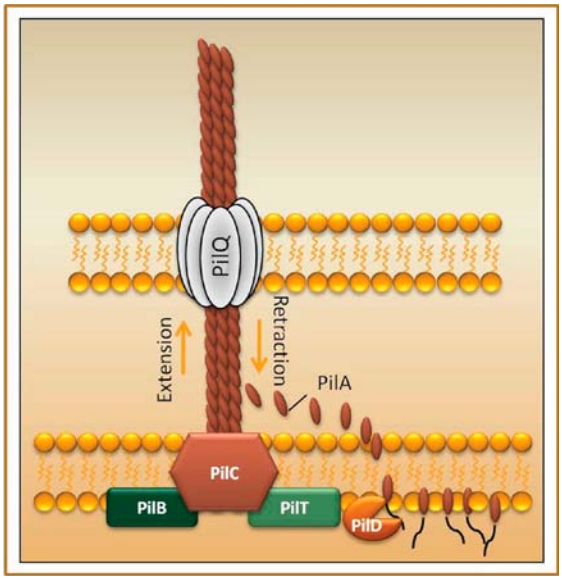

Figure 3. Schematic overview of the type IV pilin system.

PilA is synthesized in a prepilin form that requires cleavage by PilD for proper pilus assembly and function. Following translocation across the inner membrane, multiple PilA subunits assemble to form the pilus fiber within the periplasmic space. This multimeric structure is then secreted across the outer membrane by PilQ. The extension and retraction of the pilus is mediated by the ATPases PilB and PilT. PilC is an inner membrane protein of unknown function associated with the type IV complex. Adapted from (Salomonsson et al., 2011) with permission.

1.1.5.5 Additional Virulence Factors

In addition to the type II and type VI secretion systems, *F. tularensis* possesses orthologs of the type I secretion system (Gil et al., 2006). Both *tolC* and *ftlC* mutants were susceptible to different antibiotics and detergents *in vitro*, but only the *tolC* mutant was attenuated *in vivo* (Gil et al., 2006). *F. tularensis* also expresses the acid phosphatases, AcpA, AcpB, AcpC, and Hap, which catalyze the hydrolysis of phosphomonoesters at an acidic pH (Mohapatra et al., 2008).

While these enzymes contribute to the intracellular survival of *F. novicida* by dephosphorylating components of the NADPH oxidase complex thereby inhibiting the respiratory burst (Mohapatra et al., 2008; Reilly et al., 1996), deletion of the *acp* genes had no effect on intracellular growth or virulence in a mouse model of type A *Francisella* infection (Child et al., 2010). Genes typically associated with metabolism such as *deoB*, *pyrF*, *purMCD*, and *ctu* have also been shown to contribute to *Francisella* pathogenesis (Horzempa et al., 2008a; Horzempa et al., 2010; Mahawar et al., 2009; Pechous et al., 2006; Pechous et al., 2008). Deletion or disruption of any of these genes results in invasion, growth, and/or virulence defects (Horzempa et al., 2008a; Horzempa et al., 2010; Mahawar et al., 2009; Pechous et al., 2006; Pechous et al., 2008). To identify novel virulence factors, the genomes of attenuated and virulent *F. tularensis* strains have been sequenced and compared (Broekhuijsen et al., 2003; Svensson et al., 2005). Several regions of difference (RD) have been identified with two genetic loci of particular interest (Salomonsson et al., 2009). A portion of RD18 (FTT0918) and RD19 (*pilA*) are deleted from the genome of the attenuated type B stain LVS. Complementation of LVS with these two genes restored full virulence (Salomonsson et al., 2009). Identification and characterization of additional *F. tularensis* virulence genes is ongoing, as most encode hypothetical proteins (Oyston, 2008).

1.1.6 Regulation of *F. tularensis* virulence

For *F. tularensis* to be a successful intracellular pathogen, it must adapt to the host environment by altering virulence gene expression (Dai et al., 2010). *F. tularensis* senses its environment through various signals including temperature, iron, oxidative stress, and the polyamine spermine (Dai et al., 2010). To identify those genes regulated by mammalian body temperature, the gene expression profiles of *F. tularensis* cultured at 26ºC (environmental temperature) and 37ºC

(mammalian body temperature) were compared (Horzempa et al., 2008a). Forty percent of the LVS genes upregulated at 37ºC were previously identified or predicted to be important for intracellular growth and/or virulence (Horzempa et al., 2008a). Two genes of unknown function, FTL_1581 and FTL_1664, were further characterized and confirmed to play a role in *F. tularensis* pathogenesis (Horzempa et al., 2008a). Another transcriptomic study evaluated gene expression changes in response to iron limitation (Deng et al., 2006). Approximately 80 genes were differentially expressed in iron-restricted growth conditions, including many of the FPI and fig (*Francisella* iron-regulated gene) genes (Deng et al., 2006). Similar results were observed in a *F. tularensis* proteomics study (Lenco et al., 2007). A different proteomics study identified proteins regulated by oxidative stress (Ericsson et al., 1994). Following exposure to hydrogen peroxide, the most highly expressed proteins were the chaperones DnaK, GroEL, and GroES (Ericsson et al., 1994). Lenco and colleagues confirmed the upregulation of these proteins and identified 18 additional proteins that are synthesized at an increased level in response to oxidative stress (Lenco et al., 2005). Following invasion of eukaryotic cells, *F. tularensis* senses and responds to the host-specific polyamine, spermine, to change its global gene expression profile (Carlson et al., 2009). These modifications reduce the capacity of *F. tularensis* to stimulate cytokine production from macrophages (Carlson et al., 2009). A subsequent study identified FTL_0883/FTT_0615c as a gene necessary for *F. tularensis* spermine responsiveness (Russo et al., 2011). Mutation of this gene resulted in higher cytokine production from macrophages and attenuation of this mutant *in vitro* and *in vivo* (Russo et al., 2011).

1.1.7 *F. tularensis* intracellular life cycle

The intracellular life cycle of *F. tularensis* has primarily been studied in macrophages (Fig. 4). This bacterium is also capable of infecting other cell types including dendritic cells, neutrophils, hepatocytes, and lung epithelial cells (Pechous et al., 2009). To invade these cells, *F. tularensis* utilizes a novel phagocytosis strategy involving the engulfment of bacteria by pseudopod loops (Clemens et al., 2005). This process is dependent on complement factor C3 and complement receptor CR3 (Clemens et al., 2005). Additional host receptors can contribute to *F. tularensis* uptake including: complement receptor CR4, FcγR, mannose receptor, SP-A, class A scavenger receptors, and cell surface expressed nucleolin (Balagopal et al., 2006; Barel et al., 2008; Ben Nasr et al., 2006; Pierini, 2006; Schulert and Allen, 2006). Once inside the cell, *F. tularensis* resides in a membrane bound vacuole known as the *Francisella*-containing phagosome (FCP) (Checroun et al., 2006; Chong et al., 2008; Clemens et al., 2004; Santic et al., 2005b). Acidification of the FCP is transient, as phagosome maturation is arrested at the late endosomal stage (Chong et al., 2008; Clemens et al., 2009; Santic et al., 2008). Within 30-60 minutes, the phagosomal membrane degrades and *F. tularensis* enters the cytoplasm where it replicates exponentially (Checroun et al., 2006; Chong et al., 2008; Clemens et al., 2004; Golovliov et al., 2003; Santic et al., 2005b; Wehrly et al., 2009). Later in infection, bacteria have been found in vesicles that are structurally similar to autophagolysosomes (Checroun et al., 2006; Wehrly et al., 2009). These *Francisella*-containing vacuoles (FCV) have only been described in murine macrophages (Checroun et al., 2006; Wehrly et al., 2009). Bacterial egress likely occurs through apoptosis or pyroptosis, although the final stages of the *F. tularensis* life cycle are not well understood (Lai et al., 2001; Lai and Sjostedt, 2003; Mariathasan et al., 2005; Santic et al., 2009).

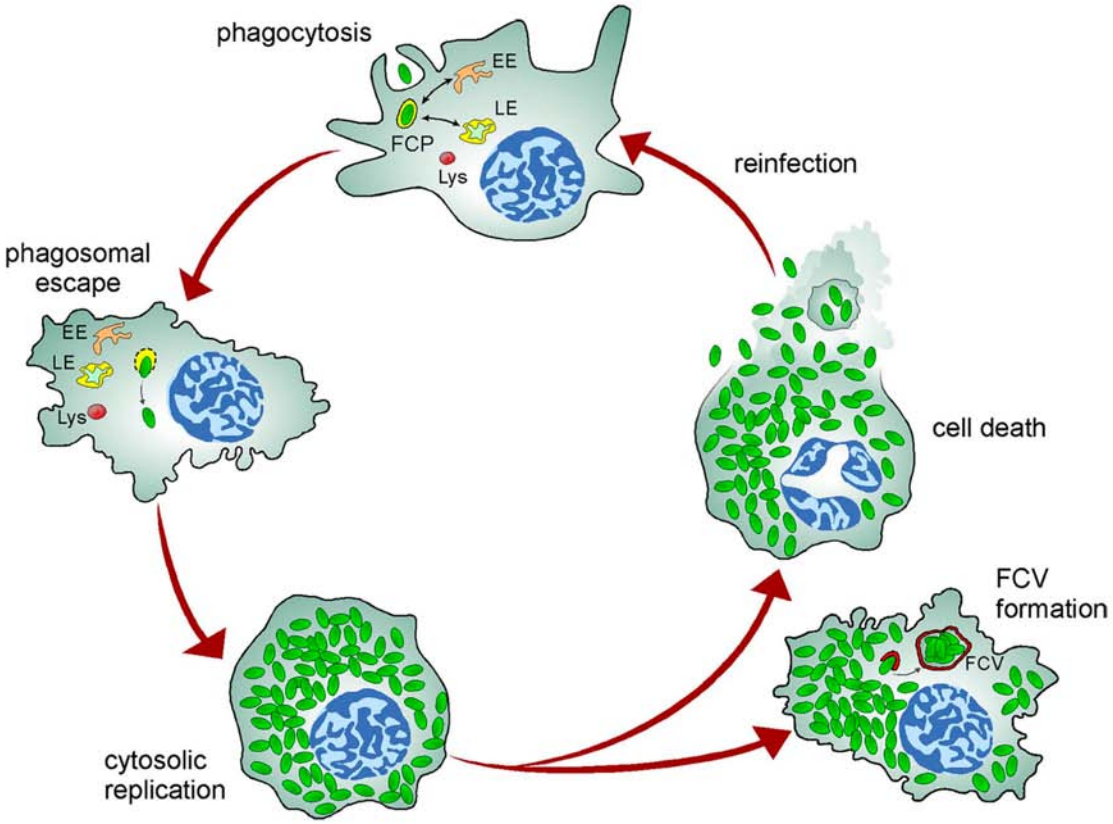

Figure 4. Model of the *Francisella* intracellular life cycle in macrophages.

F. tularensis invades macrophages through a process known as looping phagocytosis. Upon cell entry, bacteria reside in an early phagosome (FCP) that interacts with early (EE) and late (LE) endocytic compartments but not lysosomes (Lys). Bacteria rapidly degrade the FCP membrane and reach the cytosol where they undergo extensive replication, a process followed by cell death and bacterial release or reentry of cytosolic bacteria within *Francisella*-containing vacuoles (FCV) via autophagy. Adapted from (Chong and Celli, 2010) with permission.

Several genes have been identified to participate in specific stages of the *Francisella* life cycle. Mutation of *deoB, pilF*, or *pilT* results in reduced invasion of phagocytic and/or non-phagocytic cells (Chakraborty et al., 2008; Horzempa et al., 2008a). The mechanism by which these genes contribute to host cell entry is still being investigated. Escape of *F. tularensis* from the phagosome is mediated by FPI members (*iglABCD*), transcription regulators (*mglA*, *fevR*, and *migR*), and acid phosphatases (*acpABCH*) (Bosio et al., 2007; Broms et al., 2009; Buchan et

al., 2009; Mohapatra et al., 2008). While multiple genes are known to mediate replication of *F. tularensis* in the cytosol, only one has been characterized in detail. Expression of *ggt*, which encodes a putative γ-glutamyl transpeptidase, allows *F. tularensis* to utilize glutathione and γ-glutamyl-cysteine dipeptide as a source of cysteine, which is required for growth (Alkhuder et al., 2009). The genes FTT0584 and FTT0782 are known to play a role in regulating the induction of pyroptosis in infected cells and therefore, may facilitate the exit of *F. tularensis* (Weiss et al., 2007).

1.2 IMMUNE RESPONSE TO *FRANCISELLA*

For the past thirty years, most studies on *Francisella* immunology have involved the attenuated type B strain LVS (Conlan et al., 2003). While LVS is avirulent in humans, mice are very susceptible to LVS infection through various administration routes (Rick Lyons and Wu, 2007). Moreover, infection of mice with this strain mimics the course of infection observed in humans (Rick Lyons and Wu, 2007). Therefore, most of the discussion on the function of different immune cells, cytokines, and chemokines in *F. tularensis* infection will focus on this model system (Fig. 5). Differences in the immune response elicited to type A *Francisella* compared to LVS will be discussed at the end of this section.

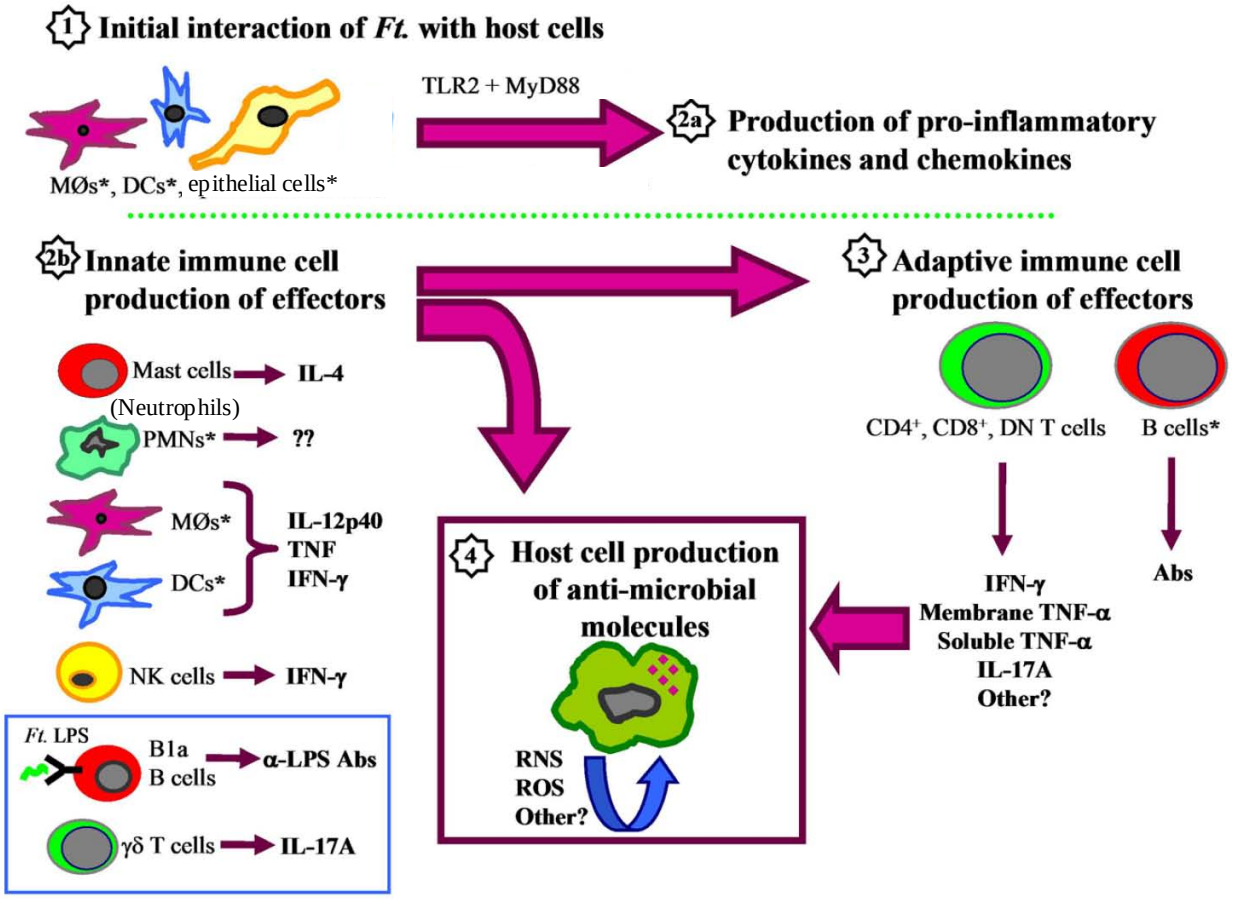

Figure 5. Components of murine innate and adaptive immune responses to *Francisella*.

(1) The initial interaction of *Francisella* with host cells, such as macrophages, dendritic cells, and epithelial cells, stimulates production of pro-inflammatory cytokines and chemokines (2a) in a manner that is dependent upon MyD88 and TLR2. Simultaneously, important innate immune cells recruited to the area of infection produce effector cytokines such as IL-12p40, TNF-α, IFN-γ, and IL-17A (2b) that influence T cell development (3), and induce host cell production of antimicrobial molecules (4). In addition to the classic Th1-type cytokines, other mediators include mast cell production of IL-4, which can directly inhibit *Francisella* intramacrophage growth, and B-1a B cell production of anti-LPS antibodies that limit intraperitoneal infection. Neutrophils or polymorphonuclear cells (PMNs) are essential for survival of *Francisella* infections initiated via some routes, but fail to eradicate intracellular organisms *in vitro*, so their contribution to infection remains unclear. After several days, activation and expansion of *Francisella*-specific T cells and B cells occurs (3). αβ T cells are essential for clearance of primary infection, and produce effector cytokines such as IL-17A, IFN-γ, and TNF-α. These factors activate infected host cells to produce reactive oxygen and nitrogen species, as well as other unidentified antimicrobials, and limit intracellular *F.*

tularensis growth (4). Asterisks (*) indicate host cells that have been shown to harbor intracellular *Francisella*. The blue box indicates cell types that are neither fully innate nor adaptive, based on classical definitions. Adapted from (Cowley and Elkins, 2011) with permission.

1.2.1 Role of innate immune cells in *F. tularensis* immunity

1.2.1.1 Macrophages

Macrophages have historically been considered the primary replicative niche of *F. tularensis* in the host (Elkins et al., 2007). In the absence of immune stimulation, bacterial replication proceeds exponentially, often resulting in death of the cell (Elkins et al., 2007). Cell death is believed to be caspase-3 dependent although this has only been shown at high multiplicities of LVS infection (Lai et al., 2001; Lai and Sjostedt, 2003). Treatment with IFN-γ is the most common way to activate macrophages and inhibit growth of *F. tularensis* (Anthony et al., 1992; Fortier et al., 1992; Lindgren et al., 2004a). IFN-γ induces the expression of iNOS and assembly of the NADPH oxidase complex resulting in robust production of reactive oxygen species (ROS) and reactive nitrogen species (RNS) (Lindgren et al., 2005). Mice deficient in $p47^{phox}$ or iNOS were more susceptible to intradermal challenge with LVS supporting a role for RNS and ROS *in vivo* (Lindgren et al., 2004b). Peroxynitrite, a compound generated by the interaction of nitric oxide with superoxide, is believed to be the major mediator of IFN-γ induced killing (Lindgren et al., 2005). IFN-γ also controls *F. tularensis* growth by promoting phagolysosome fusion (Lindgren et al., 2004a; Santic et al., 2005a).

F. tularensis evades host bactericidal mechanisms by suppressing the activation of macrophages (Bosio and Dow, 2005; Carlson et al., 2007; Loegering et al., 2006; Parsa et al., 2008; Telepnev et al., 2003; Telepnev et al., 2005). Macrophages produce little to no

proinflammatory cytokines *in vitro* in response to LVS and type A *F. tularensis* infection (Bosio and Dow, 2005; Carlson et al., 2007; Loegering et al., 2006; Russo et al., 2011; Telepnev et al., 2003; Telepnev et al., 2005), although they do express high levels of the immunosuppressive molecule prostaglandin E_2 (PGE_2) (Woolard et al., 2007). PGE_2 inhibits IL-2 production and promotes Th2 responses (Woolard et al., 2007). *F. tularensis*-infected macrophages also do not increase expression of the costimulatory molecule CD86 or MHCII (Bosio and Dow, 2005). Stimulation with TLR ligands such as *E. coli* LPS fails to restore cytokine secretion by these cells suggesting *F. tularensis* actively suppresses TLR signaling (Bosio and Dow, 2005; Carlson et al., 2007; Loegering et al., 2006; Telepnev et al., 2003). This suppression is due to the downregulation of critical inflammatory signaling pathways involved in MAPK and NF-κB activation (Telepnev et al., 2005). Furthermore, *F. tularensis* can inhibit IFN-γ signaling through the upregulation of SOCS3 which blocks the phosphorylation and activation of STAT1 (Parsa et al., 2008). While macrophages are the predominant cell infected by *F. tularensis*, replication within them is not essential for virulence (Horzempa et al., 2010). A *F. tularensis pyrF* mutant that was attenuated for growth in macrophages retained full virulence in a mouse model of pneumonic tularemia (Horzempa et al., 2010).

1.2.1.2 Dendritic Cells

Similar to macrophages, dendritic cells are preferentially targeted by *F. tularensis* (Bosio and Dow, 2005). *F. tularensis*-infected DCs are poor producers of proinflammatory cytokines, fail to upregulate costimulatory molecules, and are unresponsive to stimulation with TLR ligands (Bosio et al., 2007; Bosio and Dow, 2005; Chase et al., 2009; Schmitt et al., 2012). Suppression of these cells by *F. tularensis* was partially attributed to production of the immunosuppressive cytokine TGF-β (Bosio et al., 2007; Bosio and Dow, 2005). Elevated levels of TGF-β were

detected in the lungs of mice following pulmonary *F. tularensis* infection (Bosio et al., 2007). Neutralization of this cytokine had a minimal effect on reducing bacterial burdens in the lung of infected mice compared to isotype controls (Bosio et al., 2007). In an intranasal LVS mouse model, *F. tularensis*-infected DCs were found to migrate from the lung to the mediastinal lymph node suggesting DCs play a role in *F. tularensis* dissemination (Bar-Haim et al., 2008).

1.2.1.3 NK Cells

In bacterial infections, NK cells have two primary functions: secrete IFN-γ and lyse infected cells through the release of perforin and granzymes (Warren and Smyth, 1999). Following pulmonary LVS infection, NK cells are the primary early producers of IFN-γ (Bokhari et al., 2008; Lopez et al., 2004; Wickstrum et al., 2007). *In vitro*, NK cells control *F. tularensis* intramacrophage growth in an IFN-γ-dependent manner (Elkins et al., 2009; Sanapala et al., 2012; Skyberg et al., 2012). Depletion of NK cells using anti-asialo GM1 or anti-NK1.1 antibody shortened mouse survival following lethal LVS infection (Lopez et al., 2004; Metzger et al., 2007). A few studies have investigated the role of NK cell lytic activity in *F. tularensis* immunity. Beige mice, which are defective in NK cell cytotoxicity, are not more susceptible than wild-type to lethal LVS infection (Duckett et al., 2005). There was also no difference in survival between wild-type and perforin knockout mice infected with LVS (Sanapala et al., 2012).

A number of therapies that prolong survival in a mouse model of pneumonic tularemia are dependent on NK cells. In the absence of NK cells, recombinant IL-12 does not extend the survival time of mice infected with either *F. novicida* or LVS (Duckett et al., 2005; Pammit et al., 2004). The protective effect of both CpG DNA and acai polysaccharides against LVS and Schu S4 infection, respectively, was dependent on control of intramacrophage growth by NK cells (Elkins et al., 2009; Elkins et al., 1999b; Skyberg et al., 2012). Prolonged survival from

Schu S4 infection through treatment with cationic liposome-DNA complexes (CLDC) was abolished when NK cells were depleted (Troyer et al., 2009). These studies suggest that NK cells play a beneficial role in the host response to *F. tularensis*.

1.2.1.4 Mast Cells

While mast cells are classically known to mediate allergic responses, they also play a critical role in host defense against bacterial infections (Chan et al., 2012). Mast cell-deficient mice are more susceptible to pulmonary infection with LVS (Ketavarapu et al., 2008). *In vitro*, mast cells control the growth of *F. tularensis* in macrophages through the production of IL-4 (Ketavarapu et al., 2008). Inhibition of *F. tularensis* replication was associated with increased ATP levels and colocalization of bacteria with acidified organelles (Rodriguez et al., 2011). In the absence of IL-4 signaling, lung macrophages expressed elevated levels of caspase-3 suggesting mast cell-produced IL-4 regulates host cell death during *F. tularensis* infection (Rodriguez et al., 2011).

1.2.1.5 Neutrophils

Neutrophils are the first innate immune cells recruited to the site of infection. These cells ingest and kill invading microbes through the production of cationic peptides, proteases, ROS, and RNS (Appelberg, 2007). Following phagocytosis of *F. tularensis*, neutrophils fail to undergo a respiratory burst (McCaffrey and Allen, 2006). *F. tularensis* inhibits assembly of the NADPH oxidase complex, thereby allowing for phagosomal escape and replication in the cytosol (McCaffrey and Allen, 2006). Furthermore, *F. tularensis* prolongs the lifespan of the neutrophil by blocking caspase activation (Schwartz et al., 2012). In a mouse model of pneumonic tularemia, the recruitment of neutrophils is delayed and dependent on the production of IL-17 (Cowley et al., 2010; Hall et al., 2008; Lin et al., 2009; Mares et al., 2008). Limiting neutrophil

recruitment ameliorates disease as demonstrated by the enhanced resistance of MMP-9-/- mice to respiratory *F. tularensis* infection (Malik et al., 2007). MMP-9 is a metalloproteinase that cleaves extracellular matrix proteins to generate neutrophil chemoattractants (Malik et al., 2007). Complete depletion of neutrophils, however, has no effect on the susceptibility of mice to pulmonary LVS infection (Conlan et al., 2002). In contrast, neutropenic mice succumb to intradermal or intravenous LVS infection earlier than wild-type (Conlan et al., 2002; Elkins et al., 1996; Sjostedt et al., 1994), suggesting the role of neutrophils in host defense is dependent on the route of infection.

1.2.2 Role of cytokines and chemokines in *F. tularensis* infection

The production of proinflammatory cytokines essential for control of *F. tularensis* infection is dependent on MyD88 and TLR2 (Abplanalp et al., 2009; Collazo et al., 2006; Malik et al., 2006). Following intradermal or intraperitoneal *F. tularensis* infection, the Th1 cytokines IFN-γ, TNF-α, and IL-12 can be detected within 24-48 hours (Stenmark et al., 1999; Wickstrum et al., 2007). In comparison, these cytokines are not produced until three to four days post infection upon inhalation of *F. tularensis* (Abplanalp et al., 2009; Bokhari et al., 2008; Duckett et al., 2005). In *F. novicida*-infected mice, many of these cytokines and chemokines are produced at excessive levels, 10-500 fold greater than uninfected controls (Mares et al., 2008). This "cytokine storm" is believed to contribute to the pathology and mortality associated with respiratory *F. novicida* infection (Mares et al., 2008).

Survival from *F. tularensis* infection is dependent upon the production of TNF-α and IFN-γ (Cowley and Elkins, 2011). Neutralization of either cytokine renders mice more susceptible to LVS infection (Elkins et al., 1996; Leiby et al., 1992). Similar results were

observed with TNF-α and IFN-γ knockout mice (Chen et al., 2004; Collazo et al., 2009; Duckett et al., 2005). TNF-α mediates resistance to LVS infection through the induction of reactive nitrogen species (Cowley et al., 2008). One function of IFN-γ is to induce the expression of monocyte and T cell chemoattractants, such as MCP-1 and MIG (Park et al., 2002; Pietras et al., 2011). Mice deficient in CCR-2, the receptor for MCP-1, had higher bacterial burdens, correlating with reduced recruitment of monocytes and production of TNF-α and nitric oxide (Pietras et al., 2011). On the other hand, no difference in morbidity and mortality was observed in *F. tularensis*-infected $Mig^{-/-}$ mice (Park et al., 2002).

The role of IL-12 in the host response to *F. tularensis* is complex and appears dependent on the route of infection. IL-12 is a heterodimeric cytokine comprised of two subunits, p35 and p40. The p40 subunit can also interact with another protein, p19, to form the cytokine IL-23. Therefore, IL-12p40$^{-/-}$ mice are deficient in both IL-23 and IL-12, while IL-12p35$^{-/-}$ mice only lack IL-12. Both subunits contribute to host resistance against respiratory LVS infection (Duckett et al., 2005; Lin et al., 2009), although p35 and p40 have divergent roles in intradermal LVS infection (Elkins et al., 2002). IL-12p35$^{-/-}$ mice completely resolve the infection following intradermal inoculation, while IL-12p40$^{-/-}$ mice do not (Elkins et al., 2002). These data suggest IL-23, not IL-12, facilitates resistance to intradermal LVS infection. IL-23 also plays a role in pulmonary LVS infection as IL-23p19$^{-/-}$ mice are more susceptible than wild type to intranasal challenge (Lin et al., 2009). A recent study by Slight *et al*. demonstrated a novel role for IL-12p40 in the migration of DCs from the lung to the draining lymph node following intranasal LVS infection (Slight et al., 2011).

Several other cytokines and chemokines play an important role in *F. tularensis* immunity. IL-17 was detected in the lungs within three days of LVS infection (Lin et al., 2009). In the

absence of IL-17, mice are more susceptible to pulmonary, but not intradermal, LVS infection (Cowley et al., 2010; Lin et al., 2009). In a mouse model of pneumonic tularemia, IL-17 induces the secretion of IL-12 and IFN-γ from LVS-infected macrophages and DCs, promoting bacterial clearance and Th1 cell differentiation (Lin et al., 2009). IL-17 has also been shown to act synergistically with IFN-γ to control LVS growth in murine macrophages and ATII epithelial cells (Cowley et al., 2010). TGF-β is produced by airway cells following *F. tularensis* infection (Bosio et al., 2007; Bosio and Dow, 2005). Treatment of *F. tularensis*-infected mice with an anti-TGF-β neutralizing antibody had a minimal effect on reducing bacterial burden in the lung and spleen compared to isotype controls (Bosio et al., 2007). Type I IFNs negatively regulate the generation of IL-17-producing γδ T cells (Henry et al., 2010). $IFNAR^{-/-}$ mice possess an increased frequency of $IL\text{-}17^{+}$ γδ T cells and are resistant to *F. novicida* infection (Henry et al., 2010). Deletion of CX3CR1, a receptor for the T cell and monocyte chemoattractant CX3CL1, did not alter disease progression in a mouse model of pneumonic tularemia (Hall et al., 2009).

1.2.3 Adaptive immune responses of lymphocytes to *F. tularensis* infection

1.2.3.1 B Cells and Antibodies

In humans naturally infected with *F. tularensis*, production of IgM, IgA, and IgG antibodies begins around two weeks post infection and peaks at four to seven weeks (Koskela and Salminen, 1985). Antibodies are still present in individuals anywhere from six months to eleven years after exposure (Koskela and Salminen, 1985). Similar kinetics of antibody production were observed in LVS vaccinees (Koskela and Herva, 1982). In mice, antibodies can be detected as early as five days post LVS infection (Rhinehart-Jones et al., 1994). Antibody levels peak two weeks after infection and slowly decline thereafter, but can still be detected for up to four

months (Rhinehart-Jones et al., 1994). The role of *F. tularensis*-specific antibodies in *F. tularensis* immunity has been primarily been studied through the transfer of immune serum. Mice administered immune human or murine sera were protected against lethal challenge with LVS or a virulent type B strain (Drabick et al., 1994; Fortier et al., 1991; Kirimanjeswara et al., 2007; Stenmark et al., 2003). Serum from mice immunized with LVS LPS or heat-killed LVS was also protective (Fulop et al., 2001; Lavine et al., 2007). In a mouse model of pneumonic tularemia, the protective effect of immune serum was dependent upon FcγR as well as the presence of macrophages and neutrophils (Kirimanjeswara et al., 2007). These data suggest antibody opsonization of LVS is a critical mechanism for uptake and killing of bacteria by phagocytes (Kirimanjeswara et al., 2007).

Besides their role in antibody production, it is not well understood how B cells contribute to *F. tularensis* immunity. *F. tularensis* can infect and replicate in B cells resulting in apoptosis (Krocova et al., 2008). Compared to wild-type mice, B cell-deficient mice are equally susceptible to intradermal and pulmonary LVS infection, although higher bacterial burdens were measured in all organs (Chen et al., 2004; Elkins et al., 1999a). A unique innate population of B cells, known as B-1 cells, mediates protection elicited by immunization with *F. tularensis* LPS (Cole et al., 2009). B-1 cells are primarily located in the spleen, peritoneal cavity, and intestinal mucosa (Cowley and Elkins, 2011). They produce natural antibodies against T-independent antigens and are divided into two distinct populations: B-1a ($CD5^+$) and B-1b ($CD5^-$) (Cole et al., 2009). Immunization with LVS LPS stimulates the proliferation and differentiation of B-1a cells into plasma cells that secrete LPS-specific antibodies (Cole et al., 2009). Depletion of these cells renders LPS-immunized mice susceptible to lethal LVS infection (Cole et al., 2009).

1.2.3.2 T Cells

T cells are indispensable for resolution of *F. tularensis* infection. Athymic and TCR-β-deficient mice are able to control LVS growth for the first two weeks following infection (Elkins et al., 1993; Yee et al., 1996). LVS is never completely eradicated in the absence of T cells, however, and high bacterial burdens persist in all organs (Elkins et al., 1993; Yee et al., 1996). Eventually, these mice succumb to infection within 4-6 weeks (Elkins et al., 1993; Yee et al., 1996). Using knockout mice and antibody depletion, Yee *et al.* demonstrated that either $CD4^+$ or $CD8^+$ T cells are sufficient for clearance of *F. tularensis* (Yee et al., 1996). Interestingly, mice depleted of both T cell populations survive lethal LVS challenge but develop a chronic infection (Conlan et al., 1994; Cowley et al., 2005; Cowley et al., 2010; Yee et al., 1996). These data suggest a $CD4^-CD8^-$ T cell population contributes to control of *F. tularensis*. Subsequent studies demonstrated that these "double negative" T cells inhibit *in vitro* LVS intramacrophage growth in a TNF-α and IFN-γ dependent manner (Cowley and Elkins, 2003; Cowley et al., 2005). Control of LVS replication by $CD4^+$ and $CD8^+$ T cells is also dependent on the production of these cytokines (Cowley and Elkins, 2003; Cowley et al., 2007). Preliminarily, T cell cytotoxicity does not appear to contribute to inhibition of LVS growth in macrophages (Cowley and Elkins, 2011). The role of γδ T cells in *F.tularensis* immunity has also been investigated and determined to be insignificant (Markel et al., 2010; Yee et al., 1996).

To better characterize the T cell response to *F. tularensis*, researchers are also working to identify T cell epitopes. In one study, recombinant *F. tularensis* culture filtrate proteins were incubated with immune splenocytes to determine which proteins are capable of eliciting robust T cell proliferation and IFN-γ production (Lee et al., 2006). Three proteins, GroEL, KatG, and bacterioferritin, were identified to be immunostimulatory, although the specific epitopes within

these proteins has not been identified (Lee et al., 2006). A recent study discovered an immunodominant $CD4^+$ T cell epitope within the outer membrane protein Tul4 (amino acids 86-99) (Valentino et al., 2009). In *F. tularensis*-infected C57BL/6 mice, up to 20% of the responding $CD4^+$ T cell population is specific for Tul4 (Valentino et al., 2009).

Human T cell responses to *F. tularensis* have also been investigated using PBMCs from tularemia patients and LVS vaccinees. In *ex vivo* re-stimulation assays, PBMCs from infected and vaccinated individuals proliferate and produce IFN-γ, TNF-α, and IL-2 (Karttunen et al., 1991; Surcel et al., 1991). Peak responses were observed two to three weeks following immunization or the onset of symptoms (Karttunen et al., 1991; Surcel et al., 1991). PBMCs from LVS vaccinees also produce canonical Th17 cytokines, IL-17 and IL-22 (Paranavitana et al., 2010). Another study identified the rapid expansion of a unique population of γδ T cells in the blood of tularemia patients following infection (Poquet et al., 1998). For the first two weeks post infection, approximately 30% of the $CD3^+$ population in the blood was comprised of γδ T cells expressing the Vγ9/Vδ2 receptor which recognizes phosphorylated non-peptidic ligands on bacteria (Poquet et al., 1998). A homologous population of γδ T cells cannot be found in mice so the role of this specific T cell population in *F. tularensis* immunity has not been further investigated (Cowley and Elkins, 2011).

1.2.4 Immune Response to Type A *Francisella*

Compared to LVS, Schu S4 infection results in rapid morbidity and mortality in mice (Bosio, 2011). The enhanced virulence of this strain is attributed to its ability to evade and suppress the immune response (Bosio, 2011). Schu S4 avoids phagocytosis by binding plasmin to block antibody opsonization (Chase et al., 2009). Plasmin-bound Schu S4 also poorly elicits the

production of proinflammatory cytokines from macrophages (Chase et al., 2009). Schu S4 is resistant to the bactericidal effects of ROS and RNS, allowing for uncontrolled replication (Lindgren et al., 2007). *In vivo*, Schu S4-infected mice exhibit severe thymic atrophy and depletion of $CD4^+CD8^+$ thymocytes (Chen et al., 2005). All immunodeficient mice tested thus far, including those lacking IFN-γ and TNF-α, show no increased sensitivity to type A *F. tularensis* compared to immunocompetent mice (Chen et al., 2004; Zhang et al., 2008). This demonstrates that type A *F. tularensis* fails to elicit an effective host immune response.

1.3 VACCINES AND THERAPIES AGAINST *F. TULARENSIS*

If implemented early in infection, antibiotics are an effective treatment for tularemia (Barry et al., 2009). Antibiotic therapy has been shown to reduce the case fatality rate from 30-60% to 2% (Dennis et al., 2001). Aminoglycosides, specifically streptomycin or gentamicin, are the drugs of choice, although ciprofloxacin has also been prescribed in uncomplicated cases of tularemia (Nigrovic and Wingerter, 2008; Oyston, 2009). Since the symptoms of tularemia are non-specific, misdiagnoses are common resulting in delayed treatment and reduced survival (Barry et al., 2009). There is also a potential for the introduction of antibiotic-resistant strains (Oyston, 2009). Due to these concerns, there is a large interest in developing alternative anti-*F. tularensis* therapies. Another area of active research is development of an effective tularemia vaccine. The only tularemia vaccine known to elicit protection from virulent *F. tularensis*, LVS, is not currently licensed for use in the United States (Oyston, 2009).

1.3.1 Killed Vaccines

The earliest tularemia vaccine, referred to as the Foshay vaccine, consisted of *F. tularensis* that was killed through acid extraction and preservation in phenol (Pechous et al., 2009). Several thousand volunteers in Ohio were immunized with this vaccine between 1933 and 1941 (Foshay et al., 1942). While the Foshay vaccine reduced the incidence of laboratory-acquired tularemia cases by 70% in the 1950s, the majority of vaccinees still developed severe disease (Kadull et al., 1950). Fifty-seven percent of Foshay vaccinees displayed symptoms of tularemia following challenge with virulent *F. tularensis* compared to 17% of individuals vaccinated with a live attenuated *F. tularensis* strain (Saslaw et al., 1961). Failure of the Foshay vaccine to elicit protective immunity was attributed to poor stimulation of cell-mediated immune responses.

After those initial studies, little work has focused on the development of killed *F. tularensis* vaccines. Recently, several researchers have tried to improve the efficacy of the Foshay vaccine by testing different preparations and including adjuvants. Administration of heat killed LVS protected mice from homologous challenge (Lavine et al., 2007). Similarly, immunization of mice with UV-irradiated LVS in combination with recombinant IL-12 elicited protection against LVS (Baron et al., 2007). Neither vaccine, however, was tested in a mouse model of virulent *F. tularensis* infection (Baron et al., 2007; Lavine et al., 2007). UV-irradiated LVS mixed with immune-stimulating complexes (ISCOMS) and CpG was completely protective against challenge with virulent type B *F. tularensis*, but only minimally protective against type A (Eyles et al., 2008). Protection from LVS challenge mediated by chemically killed LVS could be enhanced by the addition of mouse anti-*F. tularensis* LPS monoclonal antibodies or cholera toxin B (Bitsaktsis et al., 2009; Rawool et al., 2008). Neither of these vaccine combinations afforded complete protection against Schu S4 challenge (Bitsaktsis et al., 2009; Rawool et al., 2008).

1.3.2 Subunit Vaccines

A number of *F. tularensis* antigens have been tested as subunit vaccines. LPS was a logical first choice as a subunit vaccine candidate because it is the primary target of the antibody response in LVS vaccinees (Oyston, 2009). LPS-immunized mice were protected against LVS challenge, but not Schu S4 (Fulop et al., 1995). Conjugation of the LPS O-antigen to BSA protected mice against intradermal, but not aerosol, challenge with virulent type B *F. tularensis* (Conlan et al., 2002). Little to no protection was elicited by O-antigen-BSA complexes against Schu S4 challenge (Conlan et al., 2002). Coupling LPS immunization with *N. meningitidis* PorB, a robust stimulator of TLR2, or an LVS boost improved vaccine efficacy but still did not afford complete protection against Type A *Francisella* challenge (Chiavolini et al., 2008; Fulop et al., 2001). The highly immunogenic protein Tul4 was also tested as a vaccine candidate and provided only modest protection against intravenous LVS challenge when administered with ISCOMS (Golovliov et al., 1995). Researchers tried to improve the immune response elicited to subunit vaccines by generating recombinant bacteria species that expressed *F. tularensis* proteins. IglC-expressing *Listeria monocytogenes* and FopA-expressing *Salmonella typhimurium* were comparable to LVS in the protection provided against Schu S4 challenge (Fulop et al., 1995; Jia et al., 2009). The best subunit vaccine candidate tested so far is a mixture of LVS outer membrane proteins (OMP). Tissue burdens were significantly reduced by OMP immunization and 50% of mice survived Schu S4 challenge (Huntley et al., 2008).

1.3.3 Live Attenuated Vaccines

The limited effectiveness of Foshay vaccines and subunit vaccines suggests an ideal tularemia vaccine would consist of multiple antigenic components capable of stimulating both humoral and cell-mediated immune responses (Pechous et al., 2009). A live attenuated *F. tularensis* vaccine possesses these characteristics. Thousands of people in the Soviet Union have been successfully immunized with live attenuated type B *Francisella* strains during and after World War II (De Pascalis et al., 2012). The United States received a few of these vaccine strains in the 1950s as part of a formal scientific exchange program (Wayne Conlan and Oyston, 2007). Repeated passage of one of these strains on peptone cysteine agar yielded two distinct colony variants, blue and grey (Wayne Conlan and Oyston, 2007). Immunization of mice and guinea pigs with the blue variant protected them against Schu S4 infection (Eigelsbach and Downs, 1961). Subsequently, the blue variant was lyophilized and serially passaged through mice before being designated LVS (Eigelsbach and Downs, 1961). In a vaccine trial conducted by Saslaw et al., 83% of LVS-vaccinated individuals were completely protected from aerosol challenge with type A *Francisella* (Saslaw et al., 1961). A similar rate of protection was observed against low dose, but not medium to high dose, aerosol challenge in another study of LVS-vaccinated individuals (McCrumb, 1961). In the 1960s, LVS reduced the incidence of tularemia from 5.7 cases to 0.27 cases per 1000 researchers and was subsequently given investigational new drug status by the Food and Drug Administration (FDA) (Burke, 1977).

While early vaccine studies demonstrated a protection rate for LVS of greater than 80%, additional human vaccine trials by Hornick and Eigelsbach have shown that protection afforded by this vaccine is incomplete and short-lived against aerosol challenge (Hornick and Eigelsbach, 1966). When LVS was administered by scarification, all individuals were protected from aerosol

challenge for up to two months following vaccination (Hornick and Eigelsbach, 1966), similar to previous studies (McCrumb, 1961; Saslaw et al., 1961). However, when subjects were challenged with aerosolized virulent *Francisella* 1-3 years post LVS vaccination, only 25-50% were protected (Hornick and Eigelsbach, 1966). Immunization of individuals with a high dose (10^6-10^8 bacteria) of aerosolized LVS improved its efficacy but commonly resulted in severe adverse side effects (Hornick and Eigelsbach, 1966). This variable efficacy may be due to reversion of the blue variant to grey, since certain preparations of LVS contained as much as 20% of the grey variant (Sandstrom, 1994). For this reason, in addition to its undefined attenuation and mechanism of protection, LVS is not licensed for public use by the FDA (Wayne Conlan and Oyston, 2007).

Researchers are currently working to obtain licensure of LVS by addressing the concerns of the FDA. Two genetic loci were identified to be responsible for the attenuation of LVS (Salomonsson et al., 2009). Expression of pilA and FTT0918 in LVS restored virulence in mice, resembling infection with a virulent type B strain (Salomonsson et al., 2009). Production of LVS under current good manufacturing practices yielded a new lot comprised 100% of the blue variant (Pasetti et al., 2008). This lot was recently tested in human phase I clinical trials and shown to be safe and immunogenic (El Sahly et al., 2009). Alternatively, researchers have introduced mutations into LVS to improve its efficacy, typically targeting genes involved in metabolism or virulence (Barry et al., 2009). Deletion of the *purMCD* purine biosynthesis operon in LVS protected mice against lethal LVS challenge (Pechous et al., 2006), but not Schu S4 (Pechous et al., 2008). Similar results were observed with a *guaAB* mutant, lacking critical enzymes in the guanine nucleotide biosynthetic pathway (Santiago et al., 2009). Mutation of virulence genes in LVS yielded more efficacious vaccine candidates. 84% of mice immunized

with an O-antigen polymerase mutant, Ft.LVS::Δ*wzy*, and 40% of mice immunized with the superoxide dismutase mutant, $sodB_{Ft}$, survived Schu S4 challenge (Bakshi et al., 2008; Kim et al., 2012).

LVS mutants may not afford complete protection against Schu S4 challenge due to differences in the protective antigens expressed by each strain (Pechous et al., 2009). Therefore, several Schu S4 mutants have been generated and tested as vaccines. A few of these mutants elicited better protection than LVS against Schu S4 challenge. Approximately 75-80% of mice vaccinated with ΔFTT1103 survived Schu S4 challenge (Qin et al., 2009). FTT1103 encodes a predicted hypothetical protein sharing homology with DsbA proteins that catalyze disulfide bond formation (Qin et al., 2009). Immunization of mice with ΔFTT0918 doubled the median time to death following challenge with a type A *Francisella* strain compared to LVS (Twine et al., 2005). A similar increase in median time to death was observed in Schu S4 Δ*clpB*-vaccinated mice following Schu S4 challenge (Conlan et al., 2010). The *clp*B gene in Schu S4 encodes for a heat shock protein (Conlan et al., 2010), while FTT0918 encodes a hypothetical protein of unknown function (Twine et al., 2005).

1.3.4 Anti-*Francisella* therapies

Since the effectiveness of antibiotics wanes if treatment is delayed, researchers have been working to develop alternative tularemia therapies. One approach that has been successful is non-specific stimulation of the innate immune response. Treatment of mice with aerosolized nontypeable *Haemophilus influenzae* lysate prolonged survival following challenge with a broad

group of pathogens including *F. tularensis* Schu S4 (Evans et al., 2010). Administration of bacterial CpG DNA or a synthetic TLR4 agonist, aminoalkyl glucosaminide phosphate (AGP), protected mice against challenge with lower virulence *F. tularensis* strains, however, their efficacy against Schu S4 is unknown (Elkins et al., 1999b; Lembo et al., 2008). Intranasal administration of cationic liposome-DNA complexes (CDLC) extended the median time to death of mice challenged with Schu S4 by one to two days (Troyer et al., 2009). Similar results were observed when mice were administered the TLR3 agonist, poly (I:C) (Pyles et al., 2010). If poly (I:C) was combined with levofloxacin treatment at day 5, however, 100% of mice were protected against Schu S4 infection (Pyles et al., 2010). Acai polysaccharides and anti-LPS monoclonal antibodies have also been shown to prolong survival following Schu S4 infection (Lu et al., 2012; Skyberg et al., 2012).

1.4 STATEMENT OF THE PROBLEM

F. tularensis possesses multiple strategies to passively and actively avoid recognition and clearance by the host. *F. tularensis* adapts to the host environment by altering its expression of surface carbohydrates, eluding recognition by TLR2 (Zarrella et al., 2011). Moreover, the LPS structure of *F. tularensis* is distinct from other Gram-negative bacteria and poorly immunogenic (Gunn and Ernst, 2007). As a means of actively suppressing the host, *F. tularensis* inhibits NF-κB signaling in macrophages and dendritic cells, resulting in the production of low levels of proinflammatory cytokines (Bosio et al., 2007; Bosio and Dow, 2005; Carlson et al., 2007; Loegering et al., 2006; Russo et al., 2011; Telepnev et al., 2003; Telepnev et al., 2005). *F. tularensis* also inhibits assembly of the NADPH oxidase complex, preventing the production of

reactive oxygen species (McCaffrey and Allen, 2006). Thus, the success of *F. tularensis* as an intracellular pathogen is dependent on its ability to evade the host innate immune response.

Compared to other respiratory pathogens such as *Klebsiella pneumoniae*, the innate immune response to *F. tularensis* is delayed. Typically, innate immune cell recruitment and proinflammatory cytokine production are observed within 24 hours of infection. In the case of *F. tularensis*, neutrophils and monocytes do not increase in number in the lungs until three days post infection. Proinflammatory cytokines are not detected until four days post infection. The role of this inflammatory response in tularemia pathogenesis is not well understood.

We hypothesize that inadequate innate host defenses contribute to mortality in acute *F. tularensis* infection and poor protection in a vaccination model of pneumonic tularemia. First, we performed a comprehensive comparison of the early host response to the virulent type A *F. tularensis* strain Schu S4 and the attenuated type B strain LVS to define unique characteristics associated with type A pathogenesis. Initial characterization identified NK cells as an immune cell population that may contribute to the pathological process in Schu S4-infected mice. Therefore, additional work focused on elucidating the role of NK cells in type A *F. tularensis* infection. We also investigated whether early activation of the innate immune response through stimulation of antigen-presenting cells would improve LVS-mediated protection against Schu S4 challenge. The results of this study expand our knowledge of the innate immune response to *F. tularensis* and its role in tularemia pathogenesis.

2.0 CHARACTERIZATION OF THE HOST RESPONSE TO A VIRULENT *F. TULARENSIS* STRAIN

2.1 ABSTRACT

Tularemia is caused by the intracellular bacterium, *Francisella tularensis*, and varies in clinical presentation and disease severity depending on the infecting strain. Type B *F. tularensis* causes a mild pneumonia, while infection with Type A results in a severe, potentially fatal illness. In mouse models of pneumonic tularemia, infection with a low dose of the attenuated type B strain LVS is effectively controlled and cleared, while the virulent type A strain Schu S4 is lethal. In this study, we sought to identify factors that contribute to the morbidity and mortality associated with type A *F. tularensis* infection. We found the kinetics of Schu S4 growth was more rapid during the earliest stages of infection. One significant immunological difference between these strains was a reduction in the number of viable lung cells, particularly NK cells and T cells, in Schu S4-infected mice. Cell numbers declined in Schu S4-infected mice despite high levels of chemokines in the lung. This decline correlated with lower proinflammatory cytokines and more TUNEL-positive cells. While neutrophils were found within foci containing TUNEL-positive cells, they did not play a role in the induction of cell death. In conclusion, the mortality of Schu S4 infection is associated with early dissemination, cell death, and loss of proinflammatory cytokines.

2.2 INTRODUCTION

Tularemia is caused by the Gram-negative bacterium, *Francisella tularensis*. Inhalation of less than 10 organisms can result in a lethal pneumonia if left untreated (Dennis et al., 2001; McLendon et al., 2006). Due to the high infectivity and mortality associated with *F. tularensis*, the Centers for Disease Control and Prevention has classified this pathogen as a category A bioterrorism agent (Barry et al., 2009). Within *F. tularensis*, there are two clinical relevant subspecies, *tularensis* (type A) and *holarctica* (type B) (Molins et al., 2010). An attenuated type B strain, LVS (live vaccine strain), is commonly used as a model organism to investigate *Francisella* immunology (Metzger et al., 2007). While LVS is avirulent in humans, mice are susceptible to LVS infection through various administration routes (Metzger et al., 2007). Furthermore, murine infection with this strain mimics the course of disease observed in humans (Metzger et al., 2007). To confirm that phenotypes within this model translate to a fully virulent strain, researchers make use of the type A *F. tularensis* strain Schu S4 (Metzger et al., 2007). Comparison of these strains has yielded numerous similarities in pathogenesis.

Although LVS and Schu S4 primarily infect macrophages, these bacteria can also infect dendritic cells, neutrophils, and alveolar epithelial cells (Bosio and Dow, 2005; Elkins et al., 2007; Hall et al., 2007; Hall et al., 2008). Additionally, LVS and Schu S4 possess similar immune evasion strategies including poor stimulation of macrophages and dendritic cells, suppression of TLR signaling, and inhibition of the respiratory burst (Bosio et al., 2007; Bosio and Dow, 2005; Carlson et al., 2007; Loegering et al., 2006; McCaffrey and Allen, 2006; McCaffrey et al., 2010; Russo et al., 2011; Telepnev et al., 2003; Telepnev et al., 2005). *In vivo*, both strains replicate exponentially in the lung and disseminate to the spleen and liver during respiratory infection (Metzger et al., 2007). Furthermore, inflammatory cell infiltrates recruited

to the lung were comparable between LVS and Schu S4. (Hall et al., 2008) Despite these similarities, LVS and Schu S4 exhibit different disease outcomes in mouse models of pneumonic tularemia.

Following low dose respiratory challenge, mice effectively clear LVS two to three weeks post infection (Metzger et al., 2007). Mice infected with the type A strain Schu S4, however, fail to control bacterial replication and succumb within six days (Metzger et al., 2007). To identify mechanisms contributing to the severe mortality associated with Schu S4, a comparative analysis of LVS and Schu S4 infection in mice was performed. Overall, the natural course of disease was similar, although the kinetics of bacterial growth and cytokine and chemokine production were delayed with LVS compared to Schu S4. Moreover, widespread cell death was observed in the lungs of Schu S4-infected mice, correlating with declining levels of proinflammatory cytokines. Together, these results indicate that bacterial and host factors contribute to Schu S4 virulence *in vivo*.

2.3 MATERIALS AND METHODS

2.3.1 *Francisella* strains and growth conditions

F. tularensis subspecies *holarctica* LVS was provided by Dr. Karen Elkins (U.S. Food and Drug Administration). *F. tularensis* subspecies *tularensis* Schu S4 (strain FSC237, catalog number NR-643) was obtained through the National Institutes of Health (NIH) Biodefense and Emerging Infections Research Resources Repository, National Institute of Allergy and Infectious Diseases.

For cultivation of *F. tularensis*, frozen stock cultures were streaked onto chocolate II agar plates and incubated at 37°C, 5% CO_2 for two to three days. These bacteria were then used to inoculate cultures grown in MH broth [Mueller-Hinton broth (Difco) supplemented with 0.1% glucose, 0.025% ferric pyrophosphate (Sigma), and IsoVitaleX (Becton Dickinson)] at 37°C with shaking for 14-18 hours. All work with *F. tularensis* Schu S4 was conducted under BSL-3 conditions at the University of Pittsburgh with approval from the Centers for Disease Control and Prevention Select Agent Program.

2.3.2 Mice

Six- to eight-week old female C57BL/6J and BALB/c mice were purchased from Jackson Laboratories (Bar Harbor, ME). Mice were housed in microisolator cages under specific pathogen-free conditions in a biosafety level-3 animal facility. All research involving animals was conducted in accordance with animal care and use guidelines, and animal protocols were approved by the University of Pittsburgh Animal Care and Use Committee.

2.3.3 Infection of mice with *F. tularensis*

LVS and Schu S4 were grown in MH broth as described above. Mice were infected intratracheally (i.t.) by oropharyngeal instillation as described previously (Horzempa et al., 2010; Russo et al., 2011; Schmitt et al., 2012). Briefly, mice were anesthetized with ketamine (8 mg/kg) and xylazine (80 mg/kg) and suspended by their front incisors in an upright, vertical position. The tongue was extended and 50 μl of LVS or Schu S4 (100 CFU) was deposited at the base of the oropharynx and aspirated by the mouse. To confirm delivery of bacteria to the

respiratory tract, a subset of mice was sacrificed at two hours post infection, and their lungs were homogenized and plated. The actual dose was calculated by plating serial dilutions of the inoculum onto chocolate II agar plates. Mice were monitored twice daily to assess morbidity and mortality following infection.

2.3.4 Generation of tissue homogenates and enumeration of bacteria

Mice were sacrificed at indicated time points to measure CFU in lungs, spleens, and livers. Spleens and livers were homogenized in TSBc [trypticase soy broth (BD Biosciences) supplemented with 0.1% L-cysteine hydrochloride monohydrate (Fisher)]. Lungs were homogenized in RPMI containing 10% fetal bovine serum (FBS). Blood was collected using a heparin-coated needle and syringe by cardiac puncture. A portion of the organ homogenates and blood were serially diluted and plated onto chocolate II agar plates. Plates were incubated at 37°C at 5% CO_2 and individual colonies were enumerated. The remaining lung homogenate was centrifuged at 17,000 x g for three min. to remove cells and tissue debris. The resulting supernatant from the lung homogenate was sterile-filtered through 0.2 µm syringe filters, treated with gentamicin (100 µg/ml), and saved for quantification of cytokines and chemokines.

2.3.5 Isolation of lung cells

Lungs were processed using two different enzymatic digestion techniques. For the initial characterization of cellular infiltrates in the lungs of Schu S4-infected C57BL/6 mice, lungs were minced and incubated in RPMI (Gibco) supplemented with 1% heat-inactivated FBS, 1 mg/ml collagenase D (Roche), 10 µg/ml DNaseI (USB), and 3 mM $CaCl_2$ for 30 min at 37°C with

shaking (170 rpm). For all subsequent experiments, lungs were minced and incubated in RPMI (Gibco) supplemented with 2.4 mg/ml type I collagenase (Gibco), 20 µg/ml DNase I (USB), and 3 mM $CaCl_2$ for 30 min at 37°C with shaking (170 rpm). Similar changes in cellular infiltrates were observed over time in Schu S4-infected lungs with both methods, although the latter enzymatic digestion resulted in a two- to three-fold increase in the total number of cells isolated (Fig. 6). The digested tissue was passed through a 40-µm cell strainer (BD Biosciences) to generate single cell suspensions. Erythrocytes were lysed with ACK Lysis Buffer (Gibco) and remaining cells were washed with RPMI. Total live cells were counted using trypan blue exclusion. Lung cells were resuspended in FACS staining buffer [0.1% bovine serum albumin (BSA) and 0.1% sodium azide in PBS] prior to flow cytometric analysis.

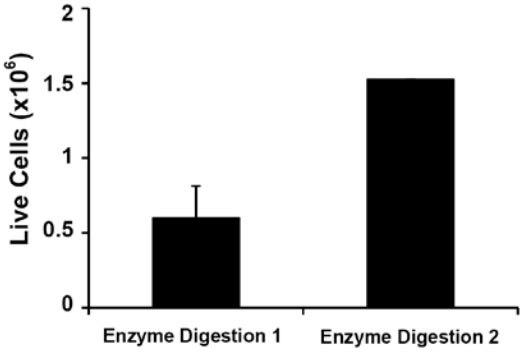

Figure 6. Number of lung cells isolated using different enzymatic digestion techniques.

Lungs were harvested from Schu S4-infected mice (n=2 mice/group) five dpi and processed using two different enzymatic digestion techniques. For enzyme digestion 1, lungs were minced and incubated in RPMI (Gibco) supplemented with 1% heat-inactivated FBS, 1 mg/ml collagenase D (Roche), 10 µg/ml DNaseI (USB), and 3 mM $CaCl_2$ for 30 min at 37°C with shaking (170 rpm). For enzyme digestion 2, lungs were minced and incubated in RPMI (Gibco) supplemented with 2.4 mg/ml type I collagenase (Gibco), 20 µg/ml DNase I (USB), and 3 mM $CaCl_2$ for 30 min at 37°C with shaking (170 rpm). Absolute cell numbers in the lung were enumerated by trypan blue exclusion. Data are expressed as mean ± SD of one independent experiment

2.3.6 Flow cytometry and analysis of lung cells

Individual immune cell populations from the lungs processed above were identified by flow cytometric analysis. Fc receptors were blocked with purified anti-mouse CD16/CD32 (clone 93, eBioscience) for 15 min on ice. Cells were then stained with the following antibodies at 4°C for 25 min: FITC anti-CD49b (clone DX5, eBioscience), FITC anti-TCR-β (clone H57-597, BD Biosciences), PE anti-Ly-6G (clone 1A8, BD Biosciences), APC anti-F4/80 (clone BM8, eBioscience), PerCP-Cy5.5 anti-CD11b (clone M1/70, eBioscience), Pacific Blue® anti-NK1.1 (clone PK136, eBioscience), APC-Alexa Fluor750/eFluor™ 450 anti-CD11c (clone N418, eBioscience), APC-eFluor™ 780 anti-TCR-β (clone H57-597), and PerCP-Cy5.5 anti-CD3 (clone 145-2C11, eBioscience). Isotype control antibodies were included in each experiment to confirm specificity. Dead cells were stained using the LIVE/DEAD® Fixable Blue Dead Cell Stain Kit (Invitrogen). Cells were then washed in PBS and fixed in 4% paraformaldehyde for 30 min at 4°C. After 25 min, cells were washed and fixed in 2% paraformaldehyde. Samples were collected using a LSRII flow cytometer (BD Biosciences) and analysis gates were set on live cells (negative for LIVE/DEAD® Fixable Blue dye) excluding debris based on forward scatter and side scatter. Approximately 100,000 events were collected for each sample. Data was analyzed using FlowJo Software (Tree Star).

2.3.7 Cytokine and chemokine assays

Cytokine and chemokine levels in lung supernatants were determined by using the Milliplex 23-plex Mouse Cytokine/Chemokine Panel (Millipore) on a Bio-Plex 200 system (Bio-Rad Laboratories). Analyte concentrations were calculated against the standards using Bio-Plex Manager 5.0 software (Bio-Rad Laboratories, Inc.).

2.3.8 Immunofluorescence staining of lung tissue sections

Mice were sacrificed and lungs were fixed by inflating with 0.8 ml of 37% formalin for 5 min. Lungs were then harvested and submerged in 37% formalin for 24 hours. Fixed tissues were placed into histology cassettes and transferred to 10% formalin. Tissue sectioning was performed by the University of Pittsburgh, School of Medicine Histology Core in the Department of Pathology Development Laboratory. For immunofluorescence staining, paraffin-embedded sections were deparaffinized in xylene and rehydrated through a series of ethanol washes. The slides were subsequently rinsed with deionized water and incubated in PBS. Sections were blocked with 2.5% BSA in PBS for 30 min and then probed with either rabbit anti-*F. tularensis* (1:500 dilution; BD Biosciences) or rat anti-Ly6G (1:350 dilution; BD Biosciences) overnight at 4°C. As a control, a paired section was probed with normal rabbit IgG (Calbiochem) or rat IgG2a (BD Biosciences). Sections were washed three times in PBS with 0.2% Tween 20 and then probed with a secondary Alexa Fluor 568 goat anti-rabbit antibody (1:1000 dilution, Invitrogen) or Alexa Fluor 555 goat anti-rat antibody (1:1000 dilution, Invitrogen) for at least 1 hour at 25°C. TUNEL analysis was performed by first permeabilizing the tissue sections with permeabilization solution (0.1% Triton X-100, 0.1% sodium citrate) for 8

min on ice. Following permeabilization, the slides were washed three times in PBS and the TUNEL reaction was done using the Fluorescein In Situ Cell Death Detection Kit (Roche) according to the manufacturer's instructions. Following another series of washes in PBS, sections were then stained with 0.5 µg/ml 4′,6-diamidino-2-phenylindole dihydrochloride (DAPI) (Invitrogen) and mounted in ProLong Gold antifade reagent (Invitrogen). Sections were viewed under a Zeiss Axiovert 200 microscope and images were captured at 100x magnification with equal fluorescence exposure times. AxioVision software was used to process the images and make uniform modifications in brightness and contrast.

2.3.9 *In vivo* depletion of neutrophils

Mice were depleted of neutrophils using an anti-Ly6G antibody as described previously with minor modifications (Frazer et al., 2011). Mice were administered 300 µg of rat anti-mouse Ly6G (clone 1A8, BioXCell, West Lebanon, NH) or rat IgG2a control (clone 2A3, BioXCell, West Lebanon, NH) intraperitoneally (i.p.) one day prior to infection with Schu S4 and every three days thereafter until sacrifice. Administration of anti-Ly6G was effective at depleting >95% of neutrophils (Ly-6G$^+$, CD11b$^+$, F4/80$^-$) in the blood (Frazer et al., 2011).

2.3.10 Infection of human NK cells with *F. tularensis* Schu S4

Lymphocytes were purified from human buffy coats from blood donations (Central Blood Bank, Pittsburgh, PA) using Ficoll gradients (Amersham Biosciences) to isolate peripheral blood mononuclear cells and Optiprep gradients (Axis-Shield) to separate out monocytes. NK cells were purified from lymphocytes using a Human NK Cell Isolation Kit (Miltenyi Biotec) per

the manufacturer's instructions. NK cells were washed and resuspended in RPMI supplemented with 10% human serum, 25 mM HEPES, and 1% GlutaMAX. Cells were seeded in 96-well round bottom culture dishes (BD Biosciences) at a density of 2.5 x 10^5 cells/well and infected with Schu S4 at an MOI of 250. After three hours, cells were incubated with Hanks balanced salt solution (Gibco) containing gentamicin (50 µg/ml) for one hour to kill extracellular bacteria. Cultures were then washed three times with warm Hank's balanced salt solution and incubated at 37°C with 5% CO_2 for another 21 hours with fresh culture medium. Actual MOIs were measured by plating serial dilutions of inocula on chocolate II agar plates. At the indicated time points post infection, cells were pelleted and lysed with 0.02% sodium dodecyl sulfate. Serial dilutions of the lysates were plated on chocolate II agar plates for enumeration of viable bacteria.

2.4 RESULTS

2.4.1 Schu S4 reduces the number of immune cells in the lung

In order to directly compare differences in disease progression between LVS and SchuS4, C57BL/6 mice were infected with comparable doses of each *Francisella* strain (approximately 100 CFU). LVS and Schu S4 replicated exponentially in the lungs following pulmonary inoculation (Fig. 7). Both strains grew similarly from one to three days post infection (dpi), but Schu S4 outgrew LVS in the first 24 hours and sustained a higher plateau (Fig. 7). Schu S4 disseminated to the spleen and liver one day earlier than LVS and reached burdens that were three to four logs higher by four dpi (Fig. 7). Similar growth kinetics of Schu S4 were observed in BALB/c mice (Fig. 8). All mice succumbed to Schu S4 infection within five days. In

contrast, LVS growth plateaued three dpi in the lung and five dpi in the spleen and liver, then declined beginning nine dpi (Fig. 9). By 17 dpi, only half of the LVS-infected mice had detectable CFU in the lung (Fig. 9).

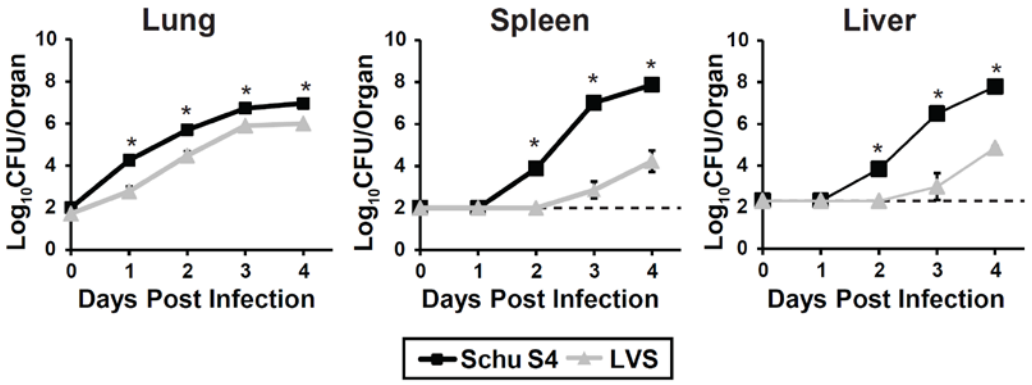

Figure 7. Schu S4 exhibits higher bacterial burdens and earlier dissemination than LVS *in vivo*.

LVS or Schu S4 (~100 CFU) was administered to C57BL/6 mice i.t. (n=4 mice/group). At indicated time points, mice were sacrificed and lungs, spleens, and livers were harvested and homogenized as described in Materials and Methods. Organ homogenates were diluted and plated for CFU enumeration. Data are expressed as mean ± SEM and represent a combination of four independent experiments. For most data points, the error bars are smaller than the symbols. The limit of detection (dashed line) for the spleen and liver was 100 CFU and 200 CFU, respectively. Statistical significance was determined by two-way ANOVA, followed by Bonferroni comparison of means (*, $p<0.05$).

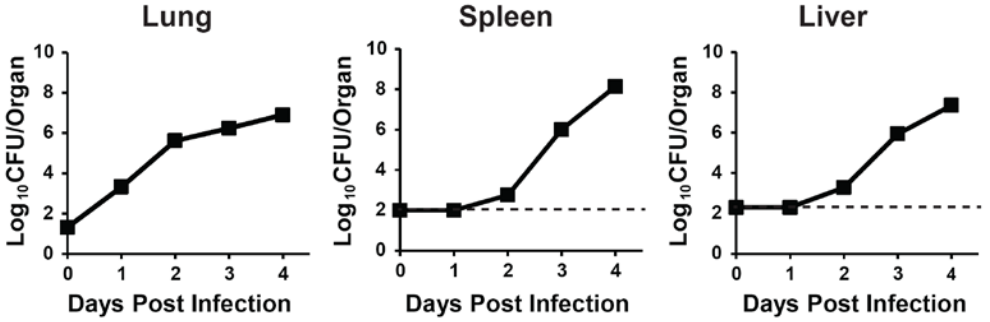

Figure 8. Replication and dissemination of Schu S4 in BALB/c mice.

Schu S4 (~100 CFU) was administered to BALB/c mice i.t. (n=4 mice/group). At indicated time points, mice were sacrificed and lungs, spleens, and livers were harvested and homogenized as described in Materials and Methods. Organ homogenates were diluted and plated for CFU enumeration. Data are expressed as mean ± SEM and represent a combination of two independent experiments. For most data points, the error bars are smaller than the symbols. The limit of detection (dashed line) for the spleen and liver was 100 CFU and 200 CFU, respectively.

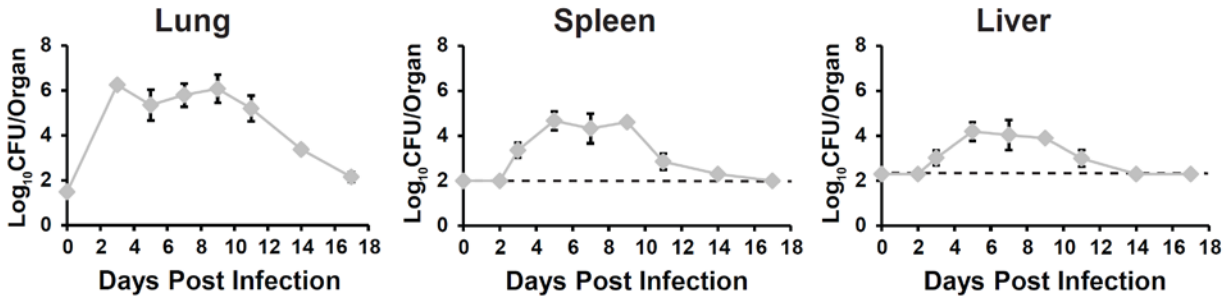

Figure 9. Clearance of LVS from the lung and peripheral organs following infection.

LVS (~100 CFU) was administered to C57BL/6 mice i.t. (n=2-4 mice/group). At indicated time points, mice were sacrificed and lungs, spleens, and livers were harvested and homogenized as described in Materials and Methods. Organ homogenates were diluted and plated for CFU enumeration. Data are expressed as mean ± SD and represent two independent experiments. For most data points, the error bars are smaller than the symbols. The limit of detection (dashed line) for the spleen and liver was 100 CFU and 200 CFU, respectively.

Since the lung is the primary site of *F. tularensis* infection, we first analyzed changes in its cellular composition. As bacterial burden increased over time, the total number of live cells also significantly increased in the lungs of LVS-infected mice compared to PBS controls (Fig. 10). In contrast, the number of viable cells decreased in mice infected with Schu S4, beginning two dpi (Fig. 10). After four days, a significant 60-70% reduction in cell numbers was observed (Fig. 10). A similar decline in viable cells was observed in Schu S4-infected BALB/c mice (Fig. 10). To determine whether the loss in viable cells was attributable to differences in burden, a 100-fold

higher dose of LVS was administered to mice and lung cell numbers were evaluated over time. Similar to low dose LVS challenge, the number of live cells increased four dpi with a high dose of LVS compared to PBS (Fig. 11).

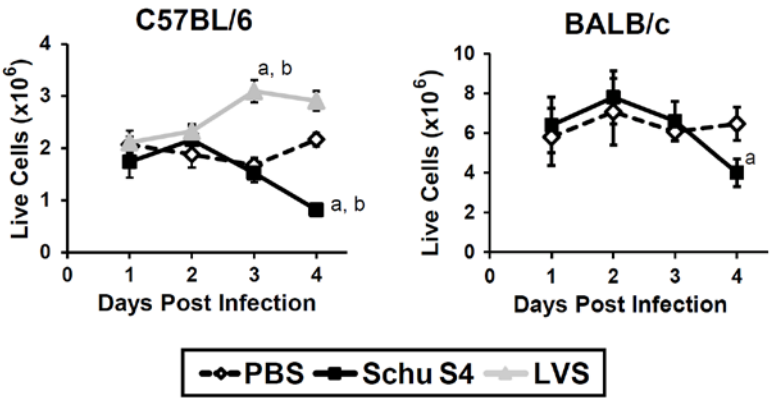

Figure 10. Reduction in viable lung cells in Schu S4-infected mice.

PBS, LVS, or Schu S4 (~100 CFU) was administered to C57BL/6 or BALB/c mice i.t. (n=2-4 mice/group). At indicated time points, mice were sacrificed and lungs were harvested and homogenized as described in Materials and Methods. Absolute cell numbers in the lung were enumerated by trypan blue exclusion. For C57BL/6 mice, data are expressed as mean ± SEM and represent a combination of at least 4 independent experiments. For BALB/c mice, data are expressed as mean ± SD and are representative of two independent experiments. Statistical significance was determined by two-way ANOVA, followed by Bonferroni comparison of means ([a] $p<0.05$ significant compared to PBS; [b] $p<0.05$ significant compared to day1).

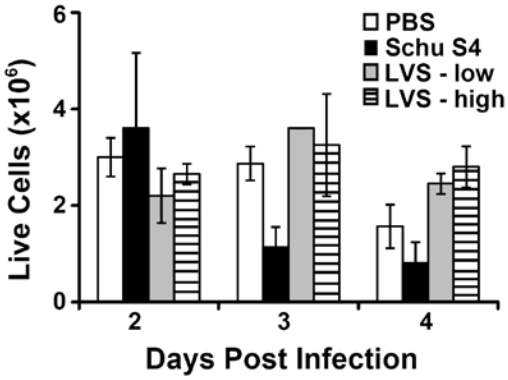

Figure 11. Administration of a higher dose of LVS does not result in reduced numbers of viable cells four dpi.

PBS, LVS (~100 CFU for low or ~10,000 CFU for high), or Schu S4 (~100 CFU) was administered to C57BL/6 mice i.t. (n=2-3 mice/group). At indicated time points, mice were sacrificed and lungs were harvested and homogenized as described in Materials and Methods. Absolute cell numbers in the lung were enumerated by trypan blue exclusion. Data are expressed as mean ± SD of one independent experiment.

To identify which cell populations were being depleted, immune cells were then measured over time by flow cytometry. Neutrophils were the predominant cell population recruited to the lungs after LVS infection (approximately 40% of total cells by day four, Fig. 12A), similar to published results (Hall et al., 2008). The number of macrophages also increased in the lungs of LVS-infected mice (Fig. 12B). No significant differences in the frequency or absolute number of DCs, T cells, or NK cells were observed in LVS-infected mice compared to PBS controls (Fig. 12C-E). Although neutrophil and macrophage numbers increased up to three dpi with Schu S4 (Fig. 12A-B), similar to previous results (Hall et al., 2008), their numbers declined sharply from three to four dpi (Fig. 12A-B). In BALB/c mice, only a significant reduction in macrophages was observed four dpi, while neutrophils continued to increase (Fig 13B-C). In C57BL/6 mice, approximately 90% of the NK cells and T cells were depleted in the lungs four days following

Schu S4 infection (Fig. 12D-E). A similar trend was observed in Schu S4-infected BALB/c mice, with approximately 65% of NK cells and T cells being depleted (Fig. 13D-E). In summary, Schu S4 infection reduced cell viability in the lungs, particularly in the NK cell and T cell populations.

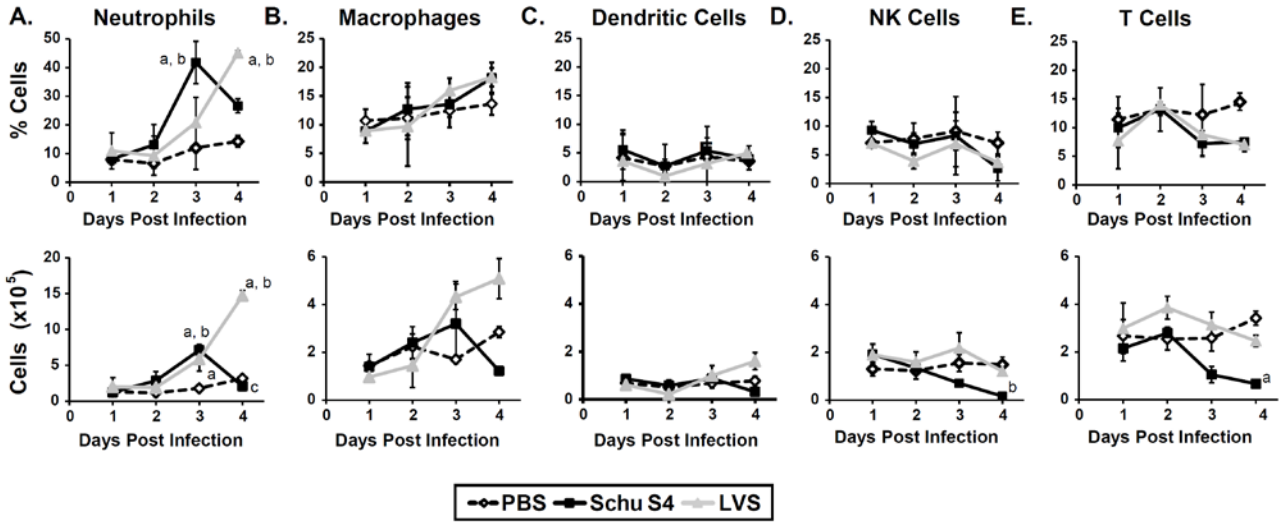

Figure 12. Changes in immune cell populations in the lung over time following Schu S4 infection.

PBS, LVS, or Schu S4 (~100 CFU) was administered to C57BL/6 mice i.t. (n=2-4 mice/group). At indicated time points, mice were sacrificed and lungs were harvested and homogenized as described in Materials and Methods. Different immune cell populations were identified using standard lineage markers by multi-parameter flow cytometry: neutrophils ($Ly6G^{+}$, $F4/80^{low}$), macrophages ($F4/80^{+}$,$Ly\text{-}6G^{-}$), dendritic cells ($CD11c^{high}$,$F4/80^{-}$), NK cells ($DX5^{+}$,$TCR\text{-}\beta^{-}$), and T cells ($DX5^{-}$,$TCR\text{-}\beta^{+}$). Total cell numbers for each population were determined by multiplying the percentages derived for each cell population by the total number of lung cells from each individual mouse. Data are expressed as mean ± SEM and are representative of combination of 2-6 independent experiments. Statistical significance was determined by two-way ANOVA, followed by Bonferroni comparison of means (^{a} $p<0.05$ significant compared to PBS; $^{b}p<0.05$ significant compared to day 1; ^{c} $p<0.05$ significant compared to day 3).

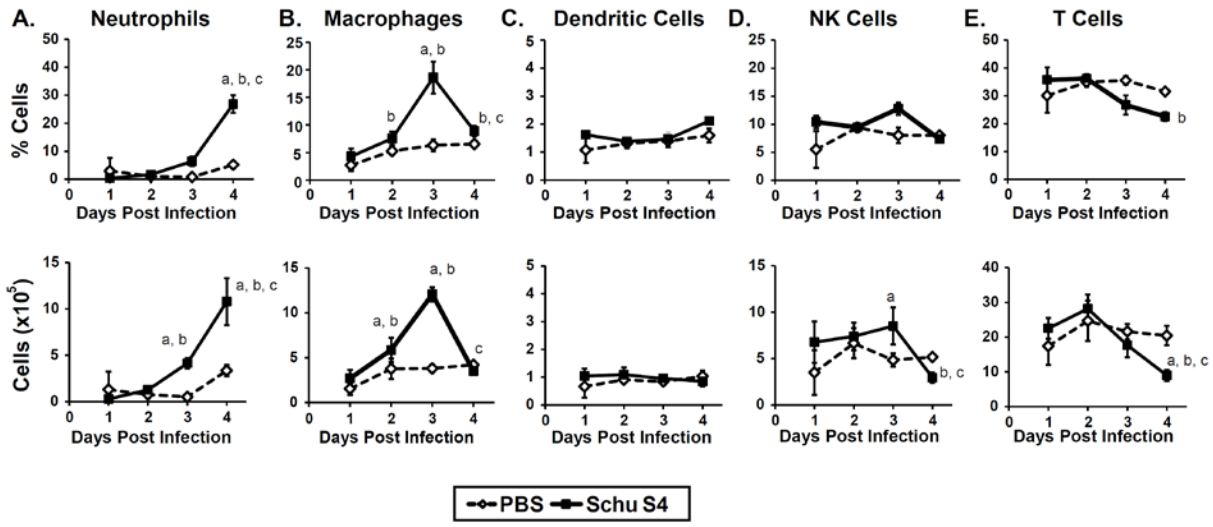

Figure 13. Schu S4 depletion of lymphocytes in BALB/c mice.

PBS or Schu S4 (~100 CFU) was administered to BALB/c mice i.t. (n=4 mice/group). At indicated time points, mice were sacrificed and lungs were harvested and homogenized as described in Materials and Methods. Different immune cell populations were quantified by multi-parameter flow cytometry as described in the legend of Fig. 12. Data are expressed as mean ± SD and are representative of two independent experiments. Statistical significance was determined by two-way ANOVA, followed by Bonferroni comparison of means (^{a} $p<0.05$ significant compared to PBS; $^{b}p<0.05$ significant compared to day1; ^{c} $p<0.05$ significant compared to day 3).

2.4.2 Schu S4 infection modulates cytokine and chemokine production

Since immune cell numbers declined over time in Schu S4-infected mice, we next wanted to evaluate changes in the production of proinflammatory cytokines and chemokines. Most cytokines and chemokines were detected in the lung three dpi with Schu S4, compared to four dpi with LVS (Fig. 14). This delayed response in LVS-infected mice correlated with slower bacterial growth kinetics early following infection compared to Schu S4 (Fig. 7). A number of monocyte, neutrophil, and T cell chemoattractants elicited by Schu S4, including KC, MCP-1,

M-CSF, MIP-2 and RANTES, reached levels 5 to 20-fold higher than LVS four dpi (Fig. 14). IL-13, MIG, MIP-1α, and MIP-1β production in LVS-infected mice was similar to Schu S4, albeit with a slight delay (Fig. 14). In LVS-infected mice, the production of several inflammatory mediators such as IFN-γ, IL-1β, IL-6, and IL-17 continually increased during the first four dpi (Fig. 14). In contrast, these cytokines decreased from three to four dpi with Schu S4 (Fig. 14). As cytokines like IFN-γ and IL-17 are known to play a critical role in control of LVS (Cowley and Elkins, 2011), this decline late during Schu S4 infection may contribute to death of the host. Therefore, we evaluated the effect recombinant adenoviruses expressing IFN-γ (AdIFN-γ) and/or IL-17 (AdIL-17) had on the natural course of disease following infection with Schu S4. In contrast to AdIL-17 (Fig. 15), AdIFN-γ reduced bacterial burdens in the lung and peripheral organs following Schu S4 infection (Fig. 15-16). However, this treatment did not significantly alter the progression of disease in Schu S4-infected mice based on clinical signs and weight loss [14% weight loss in AdIFN-γ treated mice compared to 17% weight loss in mice treated with an empty adenovirus vector (AdY5)]. Therefore, reduced IFN-γ and IL-17 production in Schu S4-infected mice four dpi is not associated with mortality.

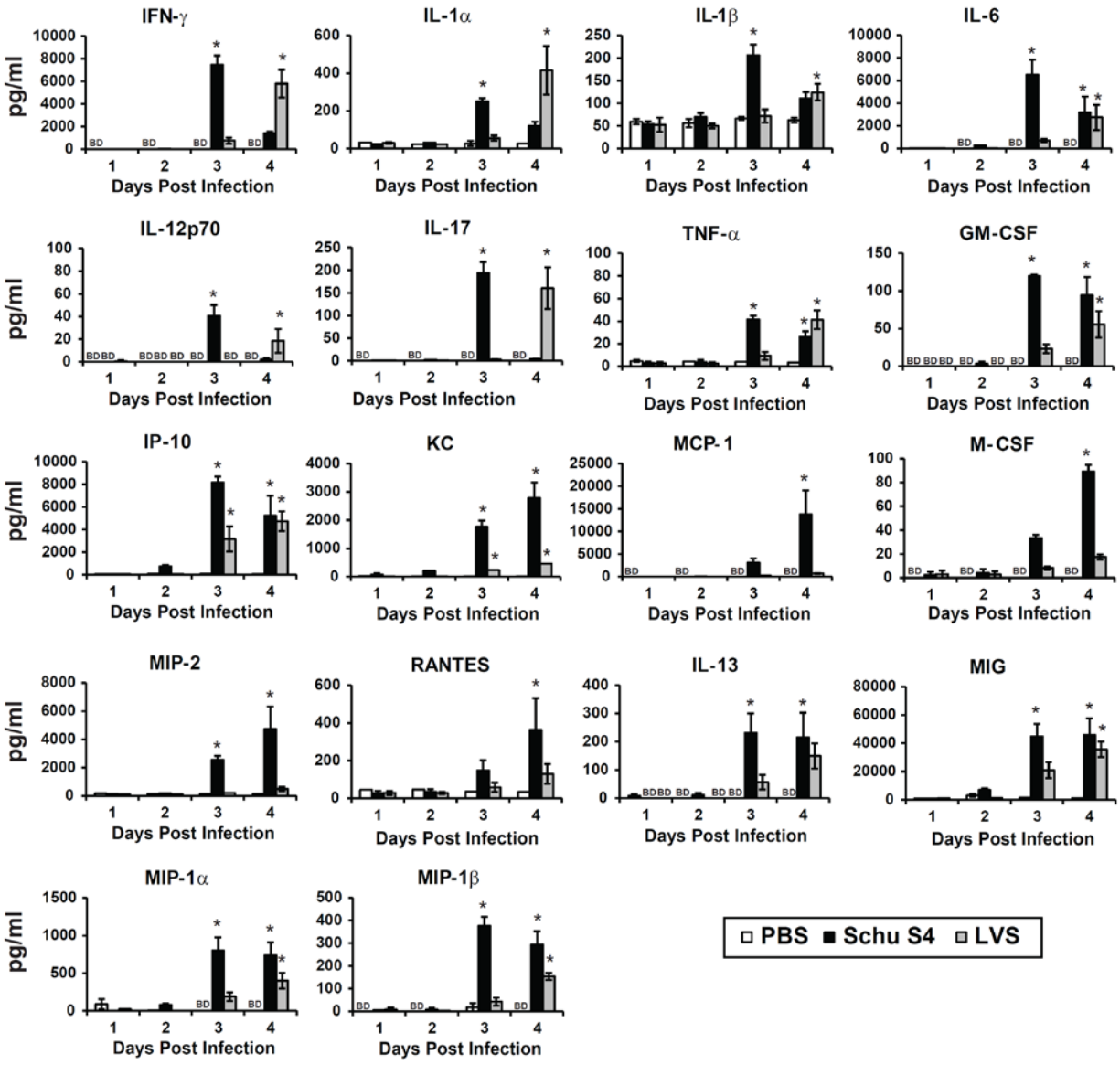

Figure 14. Cytokine and chemokine levels in the lungs of Schu S4-infected mice.

PBS, LVS, or Schu S4 (~100 CFU) was administered to C57BL/6 mice i.t. (n=2-4 mice/group). Supernatants from lung homogenates were assayed for multiple cytokines and chemokines using the Milliplex 23-plex Mouse Cytokine/Chemokine Panel (Millipore) on a Bio-Plex system (Bio-Rad Laboratories, Inc.). Only those cytokines and chemokines reaching detectable levels following infection with Schu S4 or LVS are displayed here. Data are expressed as mean ± SEM (n=2-4 samples/group/timepoint) and are representative of combination of 3 independent experiments. Statistically significant differences in cytokine/chemokine production were determined by a two-way

ANOVA, followed by Bonferroni comparison of means (*, $p<0.05$ compared to PBS). BD = below limits of detection.

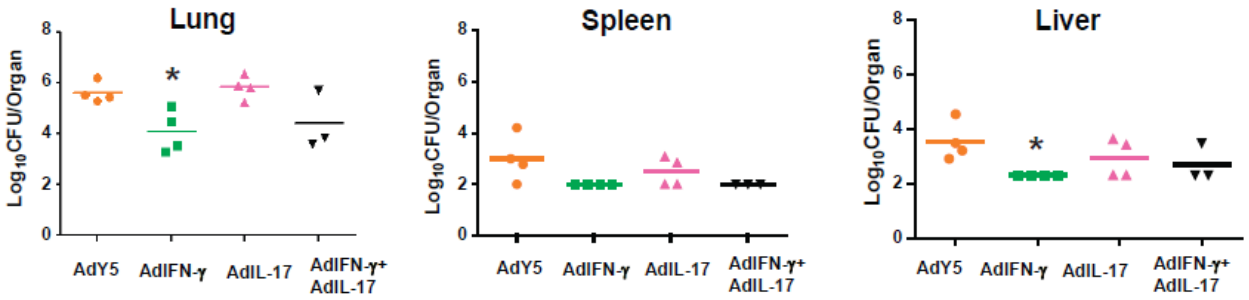

Figure 15. Recombinant adenovirus expressing IFN-γ reduces bacterial burden in Schu S4-infected mice.

BALB/c mice (n=3-4 mice per group) were administered i.t. a recombinant adenovirus expressing IFN-γ (AdIFN-γ, $2x10^8$ PFU) and/or IL-17 (AdIL-17, $2x10^8$ PFU) one day prior to i.t. infection with Schu S4 (100 CFU). An empty adenovirus vector (AdY5) served as a control. Two dpi, mice were sacrificed and lungs, spleens, and livers were harvested and processed as described in the Materials and Methods. Organ homogenates were diluted and plated for CFU enumeration. The limit of detection was 100 CFU per organ, except the liver, which was 200 CFU. Each data point represents an individual mouse with the bar indicating the mean. Statistical significance was determined by two-way ANOVA, followed by Bonferroni comparison of means (*, $p<0.05$ significant compared to AdY5).

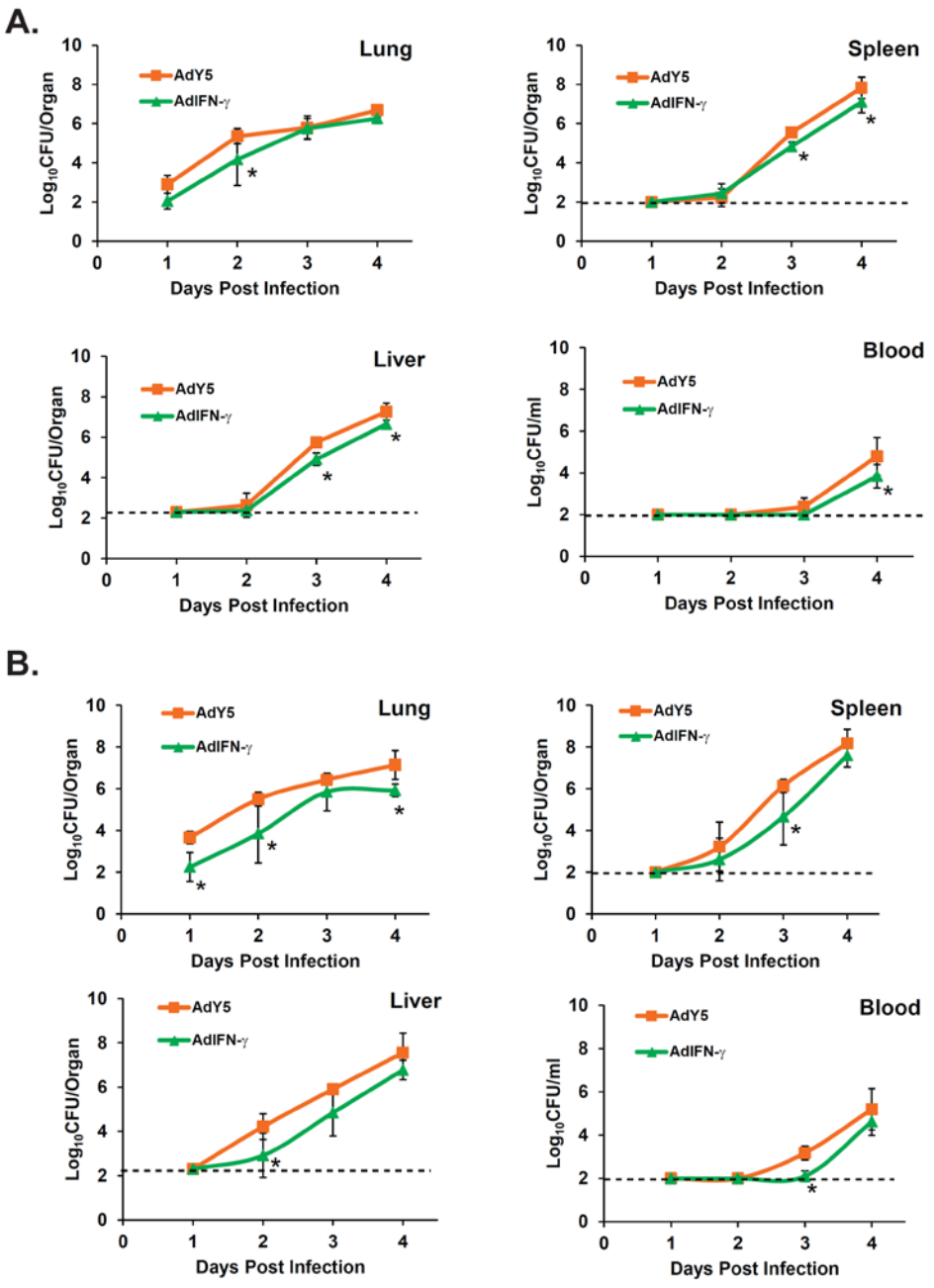

Figure 16. Administration of recombinant adenovirus expressing IFN-γ reduces Schu S4 growth and dissemination in mice.

BALB/c mice (n=4 mice per group) were administered i.t. recombinant adenovirus expressing IFN-γ (AdIFN-γ, $2x10^8$ PFU) either (A) one day prior or (B) one day prior and two days following i.t. infection with Schu S4 (100 CFU). An empty adenovirus vector (AdY5) served as a control. At each timepoint, mice were sacrificed and the designated organs and blood were processed, diluted, and plated for CFU enumeration. The limit of detection was

100 CFU per organ, except the liver, which was 200 CFU. Data are expressed as mean ± SD of one experiment. Statistical significance was determined by two-way ANOVA, followed by Bonferroni comparison of means (*, $p<0.05$ significant compared to AdY5).

2.4.3 Widespread cell death in the lungs of Schu S4-infected mice

To determine if the reduction in immune cells was due to cell death in the lungs of Schu S4-infected mice, TUNEL staining was performed on lung sections from uninfected and infected mice. There was a high frequency of TUNEL-positive cells within Schu S4-infected lungs compared to LVS-infected lungs and uninfected controls at four dpi (Fig. 17). Although TUNEL-positive cells were found near regions where there was a concentration of *Francisella* antigen, no costaining was detected (Fig. 17). We next sought to identify the specific cell populations contained within these infected foci. Only $Ly6G^+$ cells, presumably neutrophils, localized in regions with dense TUNEL staining, although these cells were not TUNEL-positive (Fig. 18).

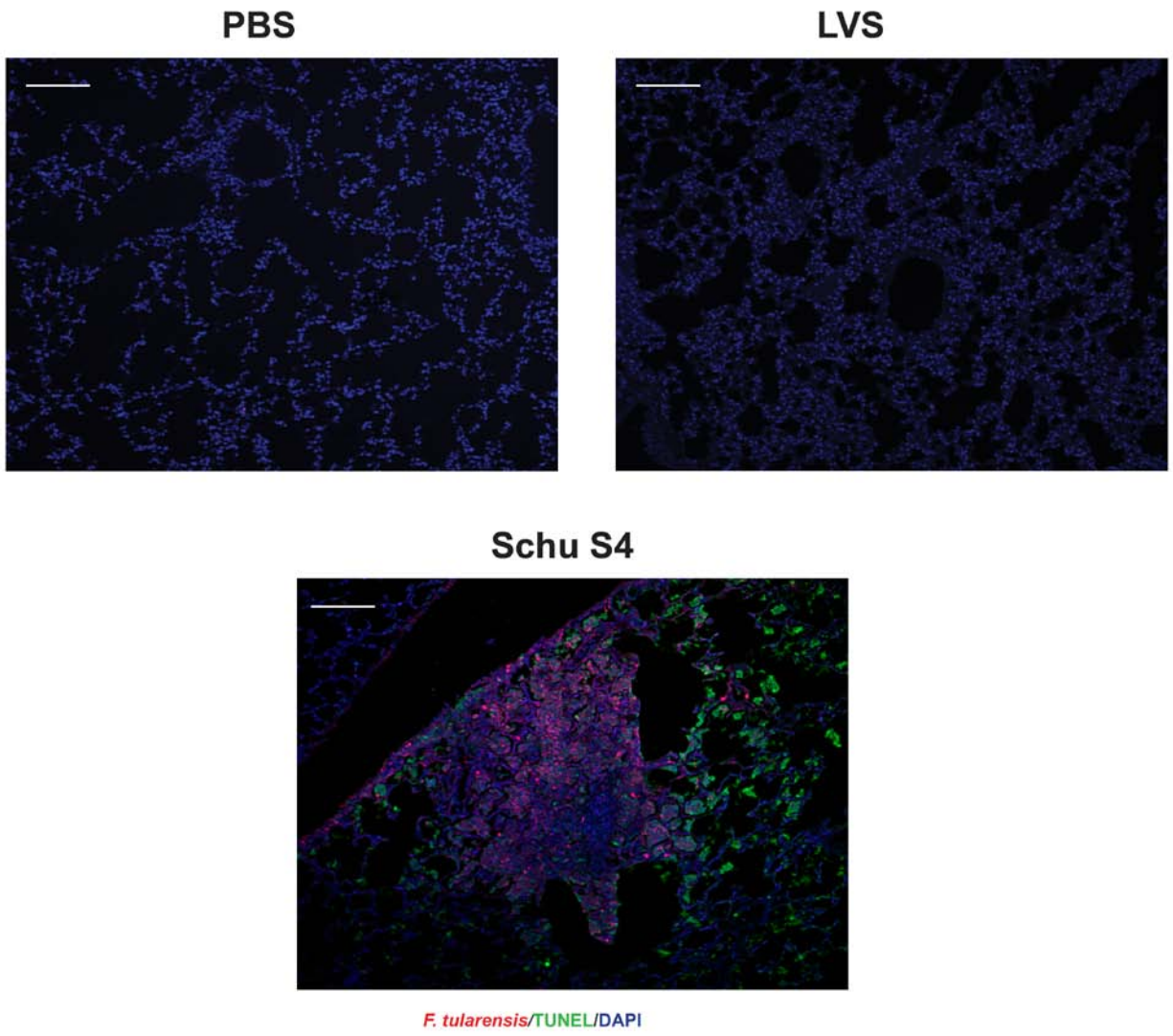

Figure 17. Extensive cell death in the lungs of Schu S4-infected mice.

IT instillation was used to administer PBS, LVS, or Schu S4 (100 CFU) to C57BL/6 mice (n=2-4 mice/group). Four dpi, lungs were harvested, fixed in formalin, and subsequently embedded in paraffin. Deparaffinized lung sections were probed with rabbit anti-*F. tularensis* followed by an Alexa Fluor 568 goat anti-rabbit secondary. A Fluorescein In Situ Cell Death Detection Kit (Roche) was used for the TUNEL assay. DNA was stained with DAPI. Images were captured at 100x magnification with an equal fluorescence exposure time within each channel.

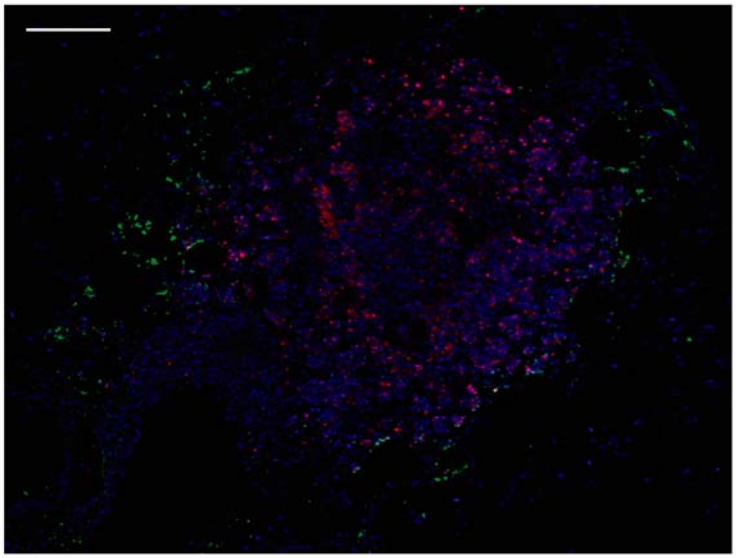

Figure 18. Neutrophils are found within inflammatory foci near TUNEL-positive cells.

Four dpi with Schu S4, lungs were harvested from C57BL/6 mice, fixed in formalin, and subsequently embedded in paraffin. Deparaffinized lung sections were probed with rat anti-mouse Ly6G followed by an Alexa Fluor 555 goat anti-rat secondary. A Fluorescein In Situ Cell Death Detection Kit (Roche) was used for the TUNEL assay. DNA was stained with DAPI. The color merged image (red, Ly-6G; green, TUNEL; blue, DAPI) were captured at 100x magnification with an equal fluorescence exposure time within each channel.

Due to the proximity of TUNEL-positive cells and neutrophils, we hypothesized the recruitment of neutrophils was contributing to the widespread cell death observed in Schu S4-infected mice. Neutrophils were depleted prior to Schu S4 infection using an anti-Ly6G (1A8) antibody and cell death and bacterial burden were evaluated. No significant differences in bacterial burden were observed in neutrophil-depleted mice infected with Schu S4 compared to isotype-treated infected controls (Fig. 19A). In addition, neutrophil depletion did not significantly alter the progression of disease in Schu S4-infected mice based on clinical signs and weight loss (18% for isotype controls and 17% for anti-Ly6G-treated four dpi). Equivalent amounts of TUNEL staining were observed in lung sections from both neutrophil-depleted and isotype-treated Schu S4-infected

mice (Fig. 19B). Therefore, we concluded the cell death observed in the lungs of Schu S4-infected mice was independent of the recruitment of neutrophils.

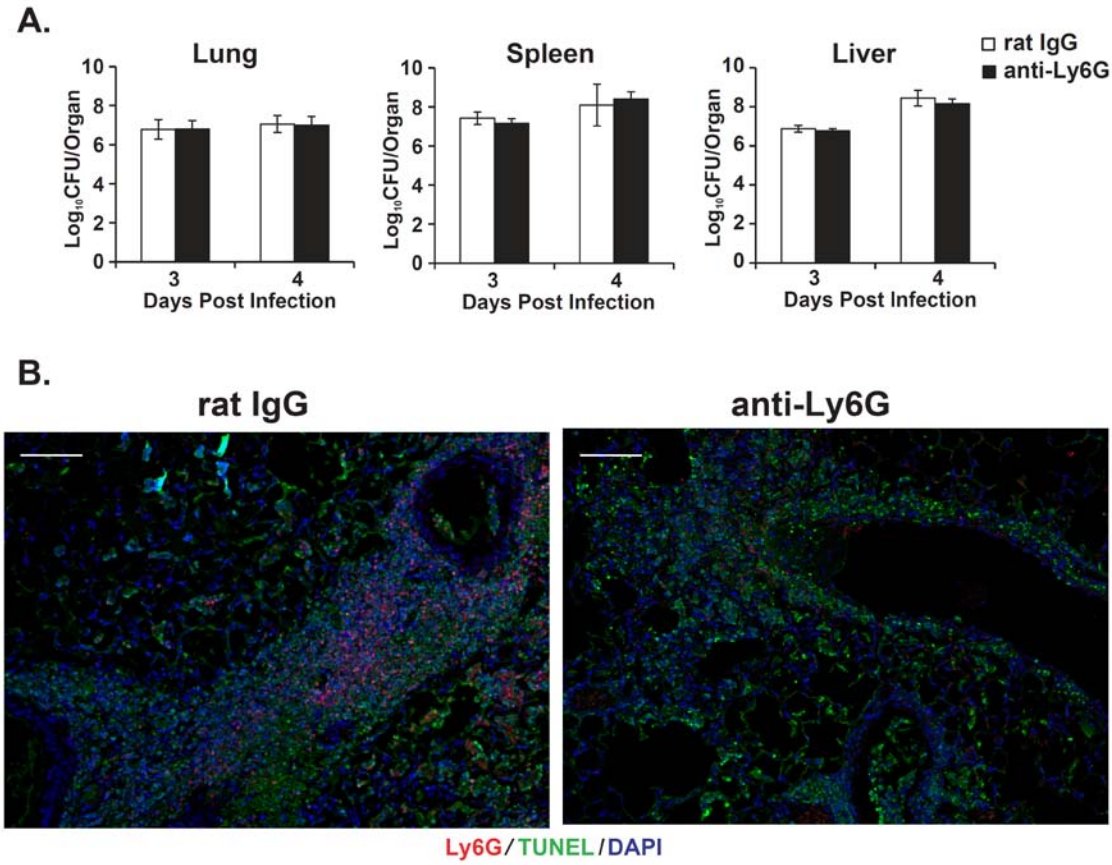

Figure 19. Bacterial burden and TUNEL staining in neutrophil-depleted Schu S4-infected mice.

C57BL/6 mice (n=4 per group) were administered anti-Ly6G or rat IgG2a one day prior to i.t. infection with Schu S4 (100 CFU) and every three days thereafter. (A) Bacterial burdens of neutrophil-depleted Schu S4-infected mice. Four dpi, mice were sacrificed and lungs, spleens, and livers were harvested and processed as described in the Materials and Methods. Organ homogenates were diluted and plated for CFU enumeration. The limit of detection was 100 CFU per organ, except the liver, which was 200 CFU. Data are expressed as mean ± SD and are representative of one independent experiment. (B) Immunofluorescence microscopy of lung sections from Schu S4-infected mice depleted of neutrophils. Four dpi, lungs were harvested, fixed in formalin, and embedded in paraffin. Deparaffinized lung sections were probed with rat anti-mouse Ly6G followed by a secondary Alexa Fluor 555 goat anti-rat antibody. An In Situ Cell Death Detection Kit (Roche) was used for the TUNEL assay. DNA was stained

with DAPI. The color merged images (red, Ly-6G; green, TUNEL; blue, DAPI) were captured at 100x magnification with an equal fluorescence exposure time within each channel.

2.5 DISCUSSION

Pulmonary infection of mice with the type A *F. tularensis* strain Schu S4 is frequently used as a model to investigate tularemia pathogenesis (Metzger et al., 2007). While these studies have elucidated novel pathologic and immunologic features of the infection, it is still not known, however, what contributes to the rapid death of the host. In this study, we compared the course of disease with an attenuated and virulent *F. tularensis* strain to identify factors associated with mortality. Major differences between the two strains included growth rate, cell death, and proinflammatory cytokine production. Thus, we concluded that both bacterial and host factors contribute to type A *F. tularensis* virulence *in vivo*.

In the lung, LVS and Schu S4 exhibit similar growth rates, except during the first 24 hours of infection where Schu S4 demonstrates two logs of growth compared to one log of growth observed with LVS. The enhanced growth of Schu S4 may be attributed to its broader resistance to host defenses compared to LVS. For example, LVS is more susceptible to killing by ROS and RNS compared to Schu S4 (Lindgren et al., 2007). Alternatively, the lower bacterial burdens of LVS may be due to the absence of critical virulence factors, such as *pilA* and FTT0918, in this strain (Salomonsson et al., 2009). Reintroduction of these two genes restored full LVS virulence to wild-type levels of type B strains *in vivo* (Salomonsson et al., 2009). The higher growth plateau reached by Schu S4 may overwhelm the host, resulting in death of the mouse.

Recently, Schu S4 infection has been described to exhibit many hallmarks of sepsis including widespread cell death and hypercytokinemia (Sharma et al., 2011). In this study, we observed a significant reduction in cell viability, particularly in the NK cell and T cell populations, in the lungs of Schu S4-infected mice. Cell numbers declined despite enhanced production of numerous monocyte, neutrophil, and T cell chemoattractants. In other models of sepsis, the loss in lymphocytes is due to the induction of caspase 3-dependent apoptosis (Hotchkiss et al., 2005). It is unlikely, however, that this pathway contributes to NK and T cell death in Schu S4-infected mice because few caspase 3-positive cells are detected in the lung following challenge (Bosio et al., 2007; Parmely et al., 2009). Preliminary *in vitro* studies suggest Schu S4 can invade but not replicate in NK cells (Fig. 20). Therefore, direct cell invasion may contribute to NK cell loss *in vivo*.

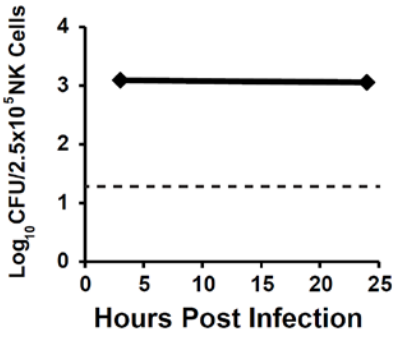

Figure 20. Invasion of human NK cells by *F. tularensis* Schu S4.

NK cells were infected in gentamicin protection assays (MOI = 250) with Schu S4 and lysed at the indicated times post infection as described in Materials and Methods. For both data points, the error bars are smaller than the symbols. Data shown are mean ± SEM from two individual experiments with different donors. The dotted line represents the limits of detection for this assay.

There were also some differences in the influx of various immune cell populations into the lung following Schu S4 infection between C57BL/6 and BALB/c mice. Compared to the gradual decrease in NK cells observed in C57BL/6 mice (Fig. 12D), NK cells numbers remained unchanged during the first three days following Schu S4 infection in BALB/c mice with a dramatic reduction in this population only occuring four dpi (Fig. 13D). In addition, no significant decline in neutrophils was observed in BALB/c mice (Fig. 13A). These differences could not be attributed to differences in bacterial burden since similar growth and dissemination kinetics of Schu S4 were observed in both mouse strains (Fig. 7-8). One possible explanation for these contrasting phenotypes may be differences in the cytokine and chemokine response elicited by Schu S4 in each mouse strain. The distinct cytokine profiles of C57BL/6 and BALB/c mice have been well documented (Gueders et al., 2009; Kuroda et al., 2002; Kuroda and Yamashita, 2003; Mills et al., 2000; Watanabe et al., 2004). These differences in immune cell recruitment, however, did not affect their susceptibility to Schu S4 infection since the median time to death for both mouse strains is 5 days (Conlan et al., 2003).

In addition to the reduced cell numbers in the lung, there was a decrease in cytokines like IFN-γ and IL-17 in Schu S4-infected mice four dpi. In LVS-infected mice, these cytokines continually increase and are essential for control of bacterial replication and clearance (Cowley and Elkins, 2011). While administration of AdIFN-γ reduced bacterial burdens in Schu S4-infected mice (Fig. 15-16), neither this treatment nor AdIL-17 significantly altered morbidity or mortality. These data suggest IFN-γ and IL-17 do not play a beneficial role in tularemia caused by type A strains.

In a recent study involving MMP-9-/- mice, excessive neutrophil recruitment was associated with death following Schu S4 infection (Malik et al., 2007). Depletion of neutrophils,

however, had no significant effect on bacterial burden or disease progression in Schu S4-infected mice. Similar results were observed by KuoLee and colleagues using a different depletion strategy (KuoLee et al., 2011). These data suggest the recruitment of neutrophils does not directly contribute to morbidity or mortality following Schu S4 infection.

3.0 ROLE OF NK CELLS IN HOST DEFENSE AGAINST PULMONARY TYPE A *FRANCISELLA TULARENSIS* INFECTION

An adapted version of this chapter has been submitted:

Schmitt, D.M., D.M. O'Dee, M.J. Brown, J. Horzempa, B.C. Russo, P.A. Morel, and G.J. Nau. 2012. Role of NK cells in host defense against pulmonary type A *Francisella tularensis* infection. *Microbes and Infection*. Submitted.

3.1 ABSTRACT

Pneumonic tularemia is a potentially fatal disease caused by the Category A bioterrorism agent *Francisella tularensis*. Understanding the pulmonary immune response to this bacterium is necessary for developing effective vaccines and therapeutics. In Chapter 2, characterization of immune cell populations in the lungs of mice infected with the type A strain Schu S4 revealed a significant loss in NK cells over time. Since this decline in NK cells correlated with morbidity and mortality, we hypothesized these cells contribute to host defense against Schu S4 infection. Depletion of NK cells prior to Schu S4 challenge significantly reduced IFN-γ and granzyme B in the lung but had no effect on bacterial burden or disease progression. Conversely, increasing NK cell numbers with the anti-apoptotic cytokine IL-15 and soluble receptor IL-15Rα had no

significant impact on Schu S4 growth *in vivo*. A modest decrease in median time to death, however, was observed in LVS-vaccinated mice depleted of $NK1.1^+$ cells and challenged with Schu S4. Therefore, NK cells do not contribute to host defense against acute respiratory infection with type A *F. tularensis in vivo*, but they play a minor role in protection elicited by LVS vaccination.

3.2 INTRODUCTION

The intracellular bacterium *Francisella tularensis* causes the disease tularemia (Oyston, 2008), which can be lethal in 30-60% of untreated individuals after inhalation (Dennis et al., 2001). Among the four different subspecies, only *tularensis* (type A) and *holarctica* (type B) are clinically important (Molins et al., 2010). Type A strains are the most virulent and cause approximately 90% of the tularemia cases detected in North America (Choi, 2002). Furthermore, *F. tularensis* is a potential bioterrorism agent due to its low infectious dose, ease of aerosolization, and high mortality rate (McLendon et al., 2006). The development of effective therapeutics and vaccines against *F. tularensis* depends on a thorough understanding of the pulmonary immune response to this pathogen.

Several studies have characterized the innate immune response elicited following respiratory challenge with the type A *F. tularensis* strain Schu S4 in mice. After inhalation, this bacterium infects and replicates in multiple cell types in the lung, including alveolar macrophages, airway dendritic cells (DCs), and type II alveolar epithelial cells (Bosio and Dow, 2005; Hall et al., 2007; Hall et al., 2008). Although macrophages and DCs typically facilitate clearance of bacterial infections (Lambrecht et al., 2001), *F. tularensis* poorly activates these

cells (Bosio et al., 2007; Carlson et al., 2009; Russo et al., 2011). *F. tularensis*-infected macrophages and DCs secrete low levels of proinflammatory cytokines, do not upregulate costimulatory molecules, and are unresponsive to stimulation with TLR ligands (Bosio et al., 2007; Carlson et al., 2009; Russo et al., 2011). Consequently, *F. tularensis* replicates exponentially in the lung and disseminates to the spleen and liver two to three days following infection (Metzger et al., 2007). Inflammatory cell infiltrates comprised predominantly of monocytes and neutrophils are observed in the lung three days post infection (Conlan et al., 2003; Hall et al., 2008; Metzger et al., 2007). *F. tularensis* infects neutrophils and inhibits the NADPH oxidase complex, blocking the production of reactive oxygen species (Hall et al., 2008; McCaffrey et al., 2010). Depleting or enhancing the recruitment of neutrophils has no impact on Schu S4 infection suggesting these cells are not major contributors to host defense (KuoLee et al., 2011). The role of other innate immune cells in type A *Francisella* infection *in vivo* has not been investigated.

NK cells serve two primary functions in combating bacterial infections: perforin-mediated cytolysis and secretion of IFN-γ. While perforin contributes to control of LVS growth *in vitro*, *prf*$^{-/-}$ mice remain equally susceptible to *F. tularensis* (Sanapala et al., 2012). Early during infection, NK cells are recruited to the lung and are the primary source of IFN-γ (Bokhari et al., 2008; Lopez et al., 2004). Depletion of NK cells results in lower IFN-γ production and shortened mouse survival from lethal pulmonary challenge with LVS (Bokhari et al., 2008; Lopez et al., 2004; Metzger et al., 2007). In addition, a number of therapies that reduce mortality associated with pneumonic tularemia are dependent on NK cells. For example, protection mediated by acai polysaccharides and CpG DNA was attributed to inhibition of *F. tularensis* intramacrophage replication by NK cells (Elkins et al., 2009; Elkins et al., 1999b; Skyberg et al.,

2012). NK cells are also required to prolong survival after treatment with recombinant IL-12 and cationic liposome DNA-complexes (Duckett et al., 2005; Troyer et al., 2009). While these studies suggest NK cells play a beneficial role in *Francisella* immunity, the contribution of NK cells during type A pneumonic tularemia has not been directly investigated.

Previously, we demonstrated NK cell numbers significantly declined over time in the lungs of type A *F.tularensis*-infected mice (Fig. 12D and 13D), correlating with morbidity and mortality. To assess the role of NK cells in type A *Francisella* infection, we used two different strategies to modulate NK cell numbers: antibody-mediated depletion and treatment with IL-15 and its receptor (IL-15Rα). Our results indicate that NK cells do not play a major role in host defense against acute respiratory infection with type A *F. tularensis*, but make a limited contribution in a vaccinated animal.

3.3 MATERIALS AND METHODS

3.3.1 *Francisella* strains and growth conditions

F. tularensis subspecies *holarctica* LVS was provided by Dr. Karen Elkins (U.S. Food and Drug Administration). *F. tularensis* subspecies *tularensis* Schu S4 (strain FSC237, catalog number NR-643) was obtained through the National Institutes of Health (NIH) Biodefense and Emerging Infections Research Resources Repository, National Institute of Allergy and Infectious Diseases. Frozen stock cultures were streaked onto chocolate II agar plates and incubated at 37°C with 5% CO_2 for two to three days. These bacteria were then used to inoculate cultures grown in MH broth [Mueller-Hinton broth (Difco) supplemented with 0.1% glucose, 0.025% ferric

pyrophosphate (Sigma), and IsoVitaleX (Becton Dickinson)] at 37°C with shaking. All work with Schu S4 was conducted under BSL-3 conditions at the University of Pittsburgh with approval from the CDC Select Agent Program.

3.3.2 Infection and immunization of mice

Six- to eight-week old female C57BL/6J mice purchased from Jackson Laboratories (Bar Harbor, ME) were housed in microisolator cages under specific pathogen-free conditions in a biosafety level-3 animal facility. Mice were infected intratracheally [~100 colony forming units (CFU)] by oropharyngeal instillation as described previously (Horzempa et al., 2010; Russo et al., 2011; Schmitt et al., 2012). For LVS vaccinations, mice were administered ~1000 CFU intranasally (Schmitt et al., 2012). Mice were challenged with Schu S4 five weeks following LVS vaccination. All research involving animals was conducted in accordance with animal care and use guidelines, and animal protocols were approved by the Institutional Animal Care and Use Committee.

3.3.3 Generation of tissue homogenates and enumeration of bacteria

Mice were sacrificed at indicated time points to measure CFU in lungs, spleens, and livers (Horzempa et al., 2010; Russo et al., 2011; Schmitt et al., 2012). Spleens and livers were homogenized in TSBc [trypticase soy broth (BD Biosciences) supplemented with 0.1% L-cysteine hydrochloride monohydrate (Fisher)]. Lungs were homogenized in RPMI containing 10% fetal bovine serum (FBS). Blood was collected using a heparin-coated needle and syringe by cardiac puncture. A portion of the organ homogenates and blood were serially diluted and

plated onto chocolate II agar plates. Plates were incubated at 37°C at 5% CO_2 and individual colonies were enumerated. The limit of detection was 100 CFU per organ (or per ml blood), except the liver, which was 200 CFU. The remaining lung homogenate and blood was centrifuged at 17,000 x g for three min. to remove cells and tissue debris. The resulting supernatant from the lung homogenate was sterile-filtered through 0.2 μm syringe filters, treated with gentamicin (100 μg/ml), and saved for quantification of cytokines and chemokines. Plasma was treated with gentamicin (300 μg/ml) and ciprofloxacin (25 μg/ml) and also saved for quantification of cytokines and chemokines.

3.3.4 Isolation of lung cells

Lungs were minced and incubated in RPMI (Gibco) supplemented with 2.4 mg/ml type I collagenase (Gibco), 20 μg/ml DNase I (USB), and 3 mM $CaCl_2$ for 30 min. at 37°C with shaking (170 rpm). The digested tissue was passed through a 40-μm cell strainer (BD Biosciences) to generate single cell suspensions. Erythrocytes were lysed with ACK Lysis Buffer (Gibco) and remaining cells were washed with RPMI. Total live cells were counted using trypan blue exclusion. Lung cells were resuspended in FACS staining buffer [0.1% bovine serum albumin (BSA) and 0.1% sodium azide in PBS] prior to flow cytometric analysis.

3.3.5 Flow cytometry and analysis of lung cells

Individual immune cell populations from the lungs processed above were identified by flow cytometric analysis. Fc receptors were blocked with purified anti-mouse CD16/CD32 (clone 93, eBioscience) for 15 min. on ice. Cells were then stained with the following antibodies at 4°C for

25 min.: FITC anti-CD49b (clone DX5, eBioscience), FITC anti-TCR-β (clone H57-597, BD Biosciences), PE anti-Ly-6G (clone 1A8, BD Biosciences), APC anti-F4/80 (clone BM8, eBioscience), PerCP-Cy5.5 anti-CD11b (clone M1/70, eBioscience), Pacific Blue® anti-NK1.1 (clone PK136, eBioscience), APC-Alexa Fluor750/eFluor™ 450 anti-CD11c (clone N418, eBioscience), APC-eFluor™ 780 anti-TCR-β (clone H57-597), eFluor™ 450 anti-CD4 (clone RM4-5, eBioscience), APC-eFluor™ 780 anti-CD8 (clone 53-6.7, eBioscience) and PerCP-Cy5.5 anti-CD3 (clone 145-2C11, eBioscience). Isotype control antibodies were included in each experiment to confirm specificity. Dead cells were stained using the LIVE/DEAD® Fixable Blue Dead Cell Stain Kit (Invitrogen). Cells were then washed in PBS and fixed in 4% paraformaldehyde for 30 min. at 4°C. For intracellular staining of granzyme B, fixed cells were washed, permeabilized with 0.1% saponin in FACS buffer, and stained with PE-conjugated anti-granzyme B (clone GB11, Invitrogen). After 25 min., cells were washed and fixed in 2% paraformaldehyde. Samples were collected using a LSRII flow cytometer (BD Biosciences) and analysis gates were set on live cells (negative for LIVE/DEAD® Fixable Blue dye) excluding debris based on forward scatter and side scatter. Approximately 100,000 events were collected for each sample. Data was analyzed using FlowJo Software (Tree Star).

3.3.6 Cytokine and chemokine assays

Cytokine and chemokine levels in lung supernatants and plasma were determined by ELISA (mouse IFN-γ, R&D Systems) or using the Milliplex 23-plex or 32-plex Mouse Cytokine/Chemokine Panel (Millipore) on a Bio-Plex 200 system (Bio-Rad Laboratories). Analyte concentrations were calculated against the standards using Bio-Plex Manager 5.0 software (Bio-Rad Laboratories, Inc.). Granzyme B levels were measured in lung supernatants

by ELISA (eBioscience). The limits of detection were 31 pg/ml for IFN-γ and 39 pg/ml for granzyme B.

3.3.7 *In vivo* depletion of NK cells

Mice were depleted of NK cells using either an anti-asialo GM1 (Lopez et al., 2004) or anti-NK1.1 (Thatte et al., 2011) antibody as described previously with minor modifications. Mice were administered 20 µl of anti-asialo GM1 (Cedarlane) or normal rabbit IgG control (Alpha Diagnostic International Inc.) intranasally (i.n.) and intraperitoneally (i.p.) three days prior to infection with Schu S4 and every three days thereafter until sacrifice. For depletion with anti-NK1.1, mice were administered 200 µg of antibody (Bio X Cell) or mouse IgG2a control (Bio X Cell) i.n. and i.p. three days prior to infection with Schu S4 and every seven days thereafter until sacrifice. Administration of either anti-asialo GM1 or anti-NK1.1 was effective at depleting >90% of the NK cells (DX5/NK1.1^{+} CD3/TCR-β^{-}) (Lopez et al., 2004; Thatte et al., 2011).

3.3.8 Administration of IL-15 and IL-15Rα to mice

Mice were treated with a combination of recombinant mouse IL-15 (eBioscience) and mouse IL-15Rα subunit Fc chimera (R&D Systems) as described previously with some modifications (Inoue et al., 2010). Briefly, IL-15+IL-15Rα complexes were formed by incubating 300 µg of IL-15 and 1.4 mg of IL-15Rα-Fc together in PBS (total volume of 1 ml) at 37°C for 20 min. Samples were then diluted 10-fold in PBS. Each mouse was then administered 50 µl of the IL-15+IL-15Rα (1.5 µg IL-15 and 7 µg IL-15Rα) solution intratracheally (i.t.) one day prior, on the

same day, and two days following Schu S4 infection. For experiments where IL-15+IL-15Rα was administered intratracheally with recombinant IFN-γ (eBioscience), mice were treated with IL-15+IL-15Rα two days prior, on the same day, and one day following Schu S4 infection. IFN-γ (10 μg) was given on the same day as Schu S4 infection and one day later.

3.3.9 Immunofluorescence staining of lung tissue sections

Lungs were inflated, harvested, and processed as described previously (Horzempa et al., 2010). Deparaffinized tissue sections were blocked with 2.5% BSA in PBS for 30 min. and then probed with rabbit anti-*F. tularensis* (1:500 dilution; BD Biosciences) overnight at 4°C. As a control, a paired section was probed with normal rabbit IgG (Calbiochem). Sections were washed three times in PBS with 0.2% Tween 20 and then probed with a secondary Alexa Fluor 568 goat anti-rabbit antibody (1:1000 dilution, Invitrogen) for at least 1 hour at 25°C. TUNEL analysis was performed by first permeabilizing the tissue sections with permeabilization solution (0.1% Triton X-100, 0.1% sodium citrate) for 8 min. on ice. Following permeabilization, the slides were washed three times in PBS and the TUNEL reaction was done using the Fluorescein In Situ Cell Death Detection Kit (Roche). After three PBS washes, sections were then mounted in ProLong Gold antifade reagent containing ′,6 -diamidino-2-phenylindole dihydrochloride (DAPI) (Invitrogen). Sections were viewed under a Zeiss Axiovert 200 microscope and images were captured at 100x magnification with an equal exposure times within each channel. AxioVision software was used to adjust brightness and contrast uniformly across all images.

3.4 RESULTS

3.4.1 Schu S4 infection modulates secretion of NK cell effectors IFN-γ and granzyme B

The loss of NK cells during Schu S4 infection (Fig. 12D and 13D) suggested there would be immunological consequences. In LVS infection, NK cells are the major producers of IFN-γ (Lopez et al., 2004). Mice depleted of NK cells are more susceptible to pulmonary challenge with a sublethal dose of LVS (Lopez et al., 2004). To evaluate the function of NK cells in Schu S4 infection, both cytokines and extracellular granzyme B levels were measured in the lungs of infected mice. In LVS-infected mice, IFN-γ was detected at three dpi in the lung and continued to increase until seven dpi (Fig. 21A-B). In contrast, IFN-γ levels peaked three dpi with Schu S4 and declined four dpi (Fig. 21A). No IFN-γ was detected in PBS controls at any of the time points (Fig. 21A).

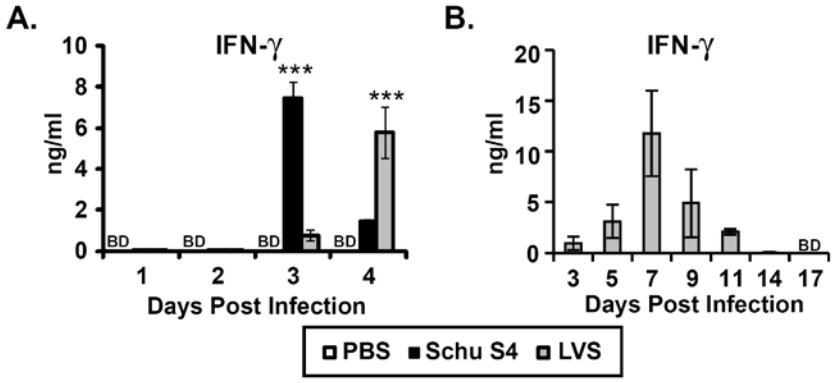

Figure 21. Increase in IFN-γ in the lungs of LVS- and Schu S4-infected mice.

At the indicated time points, IFN-γ was measured in lung supernatants from mice treated i.t. with either PBS, LVS, or Schu S4 (100 CFU) using the Milliplex 23-plex Mouse Cytokine/Chemokine Panel (Millipore) on a Bio-Plex system (Bio-Rad Laboratories, Inc.) (n=2-4 mice/group). (A) Data are expressed as mean ± SEM of at least 2 independent experiments. Statistical significance was determined by two-way ANOVA, followed by Bonferroni

comparison of means (*** $p<0.001$ significant compared to PBS). (B) For the LVS timecourse, data are expressed as mean ± SD of one experiment. BD = below limits of detection.

The lytic activity of NK cells was measured by the release of extracellular granzyme B in the lung. Granzyme B was only modestly elevated in the lungs of LVS-infected mice at four dpi compared to PBS controls (Fig. 22A). In contrast, granzyme B levels in Schu S4-infected mice were higher than PBS controls beginning three dpi; and by four dpi (Fig. 22A), approximately three- to four-fold more granzyme B was detected compared to LVS-infected mice (Fig. 22A). Since the accumulation of granzyme B in the lung of Schu S4-infected mice correlated with a decline in NK cells, we were interested in identifying the granzyme B-positive cell populations present in the lung. Lung cells were isolated three dpi from Schu S4-infected mice and stained for intracellular granzyme B. Approximately 78% of the granzyme B-positive cells in the lung were NK cells (Fig. 22C). The remaining granzyme B-positive populations were primarily T cells and $DX5^-$ TCR-β^- cells (Fig. 22C). Therefore, reduced NK cell numbers in Schu S4-infected mice inversely correlated with the release and accumulation of granzyme B in the lung. IFN-γ levels, however, did not have a clear correlation with loss of NK cells since IFN-γ peaked three dpi when NK cell numbers were beginning to decline.

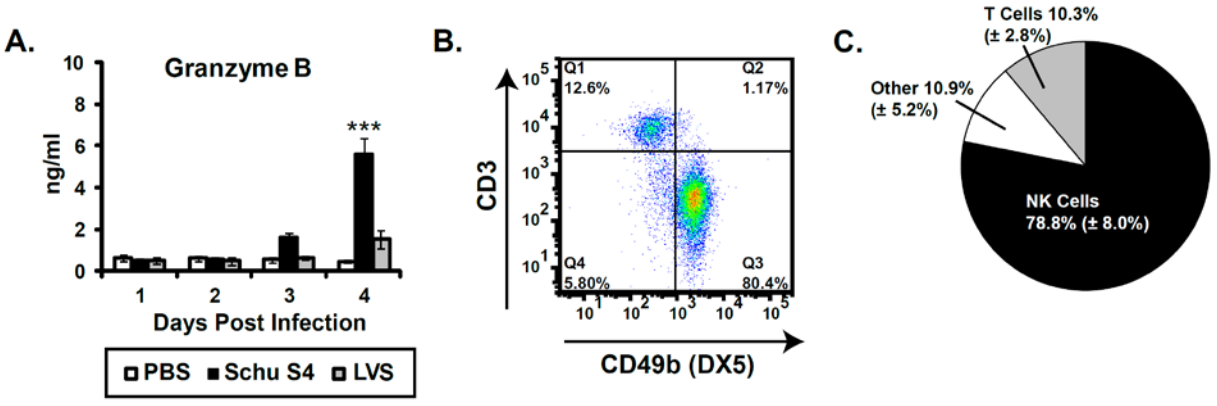

Figure 22. Increase in extracellular granzyme B levels in the lung of Schu S4-infected mice.

(A) At the indicated time points, granzyme B was measured in lung supernatants from mice treated i.t. with either PBS, LVS, or Schu S4 (100 CFU) using an ELISA kit (n=2-4 mice/group). Data are expressed as mean ± SEM of at least 2 independent experiments. Statistical significance was determined by two-way ANOVA, followed by Bonferroni comparison of means (*** $p<0.001$ significant compared to PBS). BD = below limits of detection. (B) Representative dot plot illustrating the percentage of granzyme B-positive cells in the lung of Schu-S4 infected mice that are expressing surface markers specific for NK cells (CD49b/DX5) and T cells (TCR-β) three dpi. (C) Cumulative data from two independent experiments representing the mean percentage (± SEM) of each cell population that is granzyme B-positive. Cells that were negative for both DX5 and TCR-β were defined as "other".

3.4.2 Depletion of NK cells in Schu S4-infected mice reduces IFN-γ and granzyme B levels in the lung but does not change bacterial burden

Widespread tissue damage and cell death is observed in the lungs of Schu S4-infected mice four dpi (Sharma et al., 2011). Concomitantly, there was a significant decline in lung NK cells (Fig. 12D and 13D) corresponding with reduced IFN-γ and high levels of granzyme B (Fig. 21A and 22A). To determine whether NK cells have a beneficial or pathologic role in acute Schu S4 infection, NK cells were depleted with an anti-asialo GM1 antibody prior to and during infection. Approximately 10-fold less IFN-γ and granzyme B was detected in the lungs of Schu S4-infected mice receiving anti-asialo GM1 compared to an isotype control four dpi (Fig. 23A-B), whereas the treatments had no appreciable effect in mice given PBS (Fig. 23A-B). Based on these data, NK cells were the primary source of IFN-γ and granzyme B in the lung following Schu S4 infection.

We next investigated the effect of NK cell depletion on the course of Schu S4 infection. Despite substantial effects on IFN-γ and granzyme B (Fig. 23A-B), no differences in bacterial burdens were seen in Schu S4-infected mice treated with the anti-asialo GM1 antibody compared

to isotype controls four dpi (Fig. 23C). In addition, Schu S4-infected mice depleted of NK cells exhibited similar clinical signs of illness and weight loss (14% for isotype and 16% for anti-asialo GM1 four dpi) compared to infected controls. Furthermore, perforin-deficient mice, which lack NK cell lytic function, were equally susceptible to Schu S4 infection as wild-type mice (median time to death of 5 days). Therefore, NK cells did not have a demonstrable impact on host defense against acute Schu S4 infection.

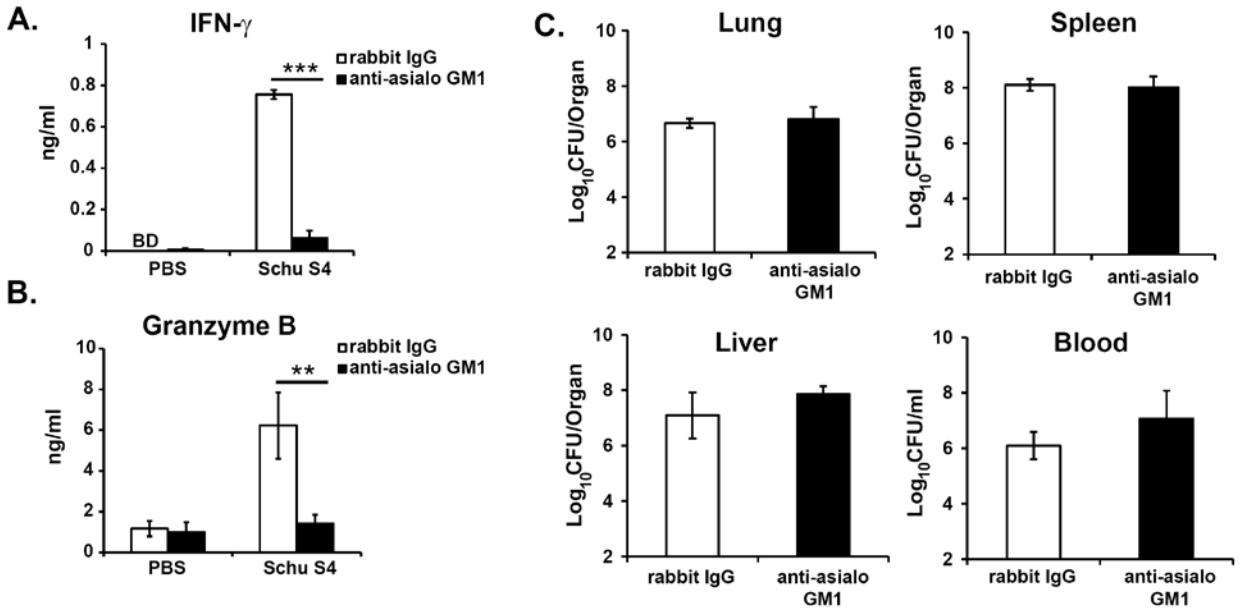

Figure 23. Depletion of NK cells in Schu S4-infected mice reduces IFN-γ and granzyme B in the lung but does not change bacterial burdens.

Mice (n=4 per group) were administered anti-asialo GM1 or normal rabbit IgG i.n. and i.p three days prior to i.t. infection with Schu S4 (100 CFU) and every three days thereafter. PBS-treated mice (n=4 per group) administered either anti-asialo GM1 or rabbit IgG served as controls. Four dpi, mice were sacrificed and lungs, spleens, livers, and blood were harvested and processed as described in the Materials and Methods. (A-B) IFN-γ and granzyme B were measured in lung supernatants by ELISA. (C) Organ homogenates and blood were diluted and plated for CFU enumeration. Data are expressed as mean ± SEM of 3 independent experiments. Statistical significance was determined by two-way ANOVA, followed by Bonferroni comparison of means ($^{**}p<0.01$, $^{***}p<0.001$ significant compared to rabbit IgG). BD = below limits of detection.

3.4.3 Contribution of NK cells in host resistance to Schu S4 challenge in LVS-vaccinated mice

In addition to their role in innate immunity, NK cells also influence adaptive immune responses (Hall et al., 2010). Though NK cell depletion had little effect on acute infection, we considered the possibility that NK cells might contribute to host resistance to Schu S4 infection in LVS-vaccinated mice. To assess the role of NK cells in protection elicited by LVS, NK cells were depleted from vaccinated mice with antibodies prior to Schu S4 infection. Four dpi, a 0.5-1.5 log increase in Schu S4 burden was measured in all organs of vaccinated mice that received anti-asialo GM1 compared to vaccinated mice treated with control rabbit IgG (Fig. 24A). We hypothesized that greater Schu S4 burdens would translate to reduced survival after NK cell depletion. Anti-asialo GM1 treatment caused a significant reduction in survival of LVS-vaccinated mice compared to controls, where the median time to death (MTD) shifted from 10 to 6 days (Fig. 24B). These data demonstrate that anti-asialo GM1 treatment increased infection severity and reduces survival of LVS-vaccinated mice following Schu S4 challenge.

Although asialo-GM1 is predominantly expressed on NK cells, this marker is also expressed on a subset of other immune cell populations such as $CD8^+$ T cells and basophils (Lee et al., 1996; Nishikado et al., 2011). To test the specificity of the results obtained with anti-asialo GM1, we used an alternative depletion strategy with a different antibody, anti-NK1.1, prior to challenge with Schu S4. Compared to the four day difference in survival observed with anti-asialo GM-treated vaccinated mice and isotype controls, vaccinated mice treated with anti-NK1.1 succumbed to Schu S4 challenge only one to two days earlier than mouse IgG controls

(Fig. 24C). This difference in survival between the two depletion strategies suggested NK cells had a minor role in LVS-mediated protective immunity to Schu S4 challenge.

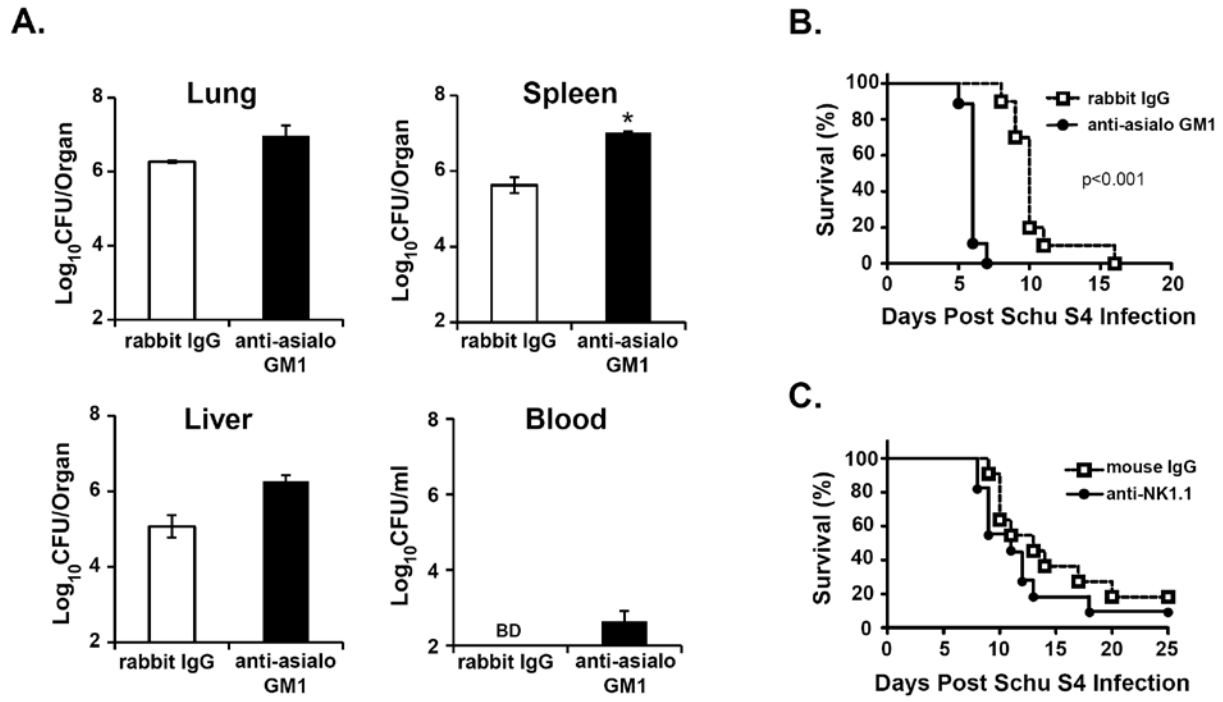

Figure 24. Contribution of NK cells in LVS-mediated immunity to Schu S4 challenge.

Mice were vaccinated intranasally with LVS (1000 CFU). Five weeks later, mice were challenged i.t with Schu S4 (100 CFU). (A) Treatment of vaccinated mice with anti-asialo GM1 increases bacterial burdens in the organs and blood following Schu S4 infection. LVS-vaccinated mice (n=4-5 mice per group) were administered anti-asialo GM1 or normal rabbit IgG prior to infection with Schu S4 as described in the Materials and Methods. Four days post Schu S4 infection, mice were sacrificed and the designated organs and blood were processed, diluted, and plated for CFU enumeration. Data are expressed as mean ± SEM of two independent experiments. Statistical significance was determined by two-way ANOVA, followed by Bonferroni comparison of means (* $p<0.05$ significant compared to rabbit IgG). BD = below limits of detection. (B) Reduced survival of LVS-vaccinated mice treated with anti-asialo GM1and infected with Schu S4. The data are combined from two independent experiments (n=5 mice per group). $p<0.001$, log-rank test. (C) NK cells play a minor role in immunity to Schu S4 infection in LVS vaccinated mice. LVS-vaccinated mice (n=5-6 mice per group) were administered anti-NK1.1 or mouse IgG prior to infection with Schu S4 as described in the Materials and Methods. Survival was monitored over time. The

data are combined from two independent experiments. Statistical significance was reached in only one experiment ($p<0.05$, log-rank test).

3.4.4 Enhanced survival of lymphocytes and reduced systemic cytokine production induced by IL-15+IL-15Rα does not improve host resistance to acute Schu S4 infection

Depletion of NK cells failed to exacerbate or ameliorate acute Schu S4 infection. Augmenting NK cell numbers and activation, however, may improve host defenses since these cells are major producers of IFN-γ (Lopez et al., 2004). The anti-apoptotic cytokine IL-15 plays a critical role in the development, homeostasis, and function of NK cells and enhances the proliferation of NK cells *in vivo* when given with a soluble form of its receptor (IL-15Rα) (Bulfone-Paus et al., 1997; Oh et al., 2008; Rubinstein et al., 2006; Stonier and Schluns, 2010). IL-15+IL-15Rα treatment reduces NK cell apoptosis, increases expression of IFN-γ, and improves survival in two murine models of sepsis (Inoue et al., 2010). Since Schu S4 infection also has features of sepsis, we tested the effects of IL-15+IL-15Rα in this model.

Four dpi, intratracheal IL-15+IL-15Rα treatment increased viable lung cells of Schu S4-infected mice by two-fold compared to Schu S4-infected controls treated with PBS (Fig. 25A). A similar increase in lung cells was observed in uninfected mice receiving IL-15+IL-15Rα (Fig. 25A). Among the lung immune cells evaluated, no significant differences in the frequency or absolute number of macrophages and neutrophils were observed in Schu S4-infected mice after IL-15+IL-15Rα treatment (Fig 25B-C). Although IL-15+IL-15Rα significantly increased the frequency of DCs in the lung of uninfected controls, there was no effect on DCs in Schu S4-

infected mice (Fig. 25D). More importantly, IL-15+IL-15Rα treatment significantly increased the frequency of NK cells and T cells in the lungs of both uninfected and Schu S4-infected mice by 70-80% (Fig. 25E-F). Therefore, IL-15+IL-15Rα treatment enhanced the number of viable cells during Schu S4 infection.

We next tested whether IL-15+IL-15Rα treatment altered systemic cytokines and chemokines after Schu S4 infection. In other models of sepsis, IL-15+IL-15Rα modulated the levels of circulating IFN-γ, IL-6, and TNF-α. Analyzing plasma by Luminex, there was a statistically significant reduction in IFN-γ and IL-6 in Schu S4-infected mice treated with IL-15+IL-15Rα compared to PBS-treated controls (Fig. 25G). TNF-α levels in Schu S4-infected mice remained unchanged in response to IL-15+IL-15Rα treatment (Fig. 25G). In addition to IFN-γ and IL-6, ten other cytokines and chemokines were significantly downregulated in Schu S4-infected mice treated with IL-15+IL-15Rα compared to PBS (Table 3). No statistically significant differences in chemokine and cytokine concentrations were detected in uninfected mice treated with IL-15+IL-15Rα and PBS (Table 3). Therefore, IL-15+IL-15Rα reduced inflammatory mediators in the bloodstream of Schu S4-infected mice.

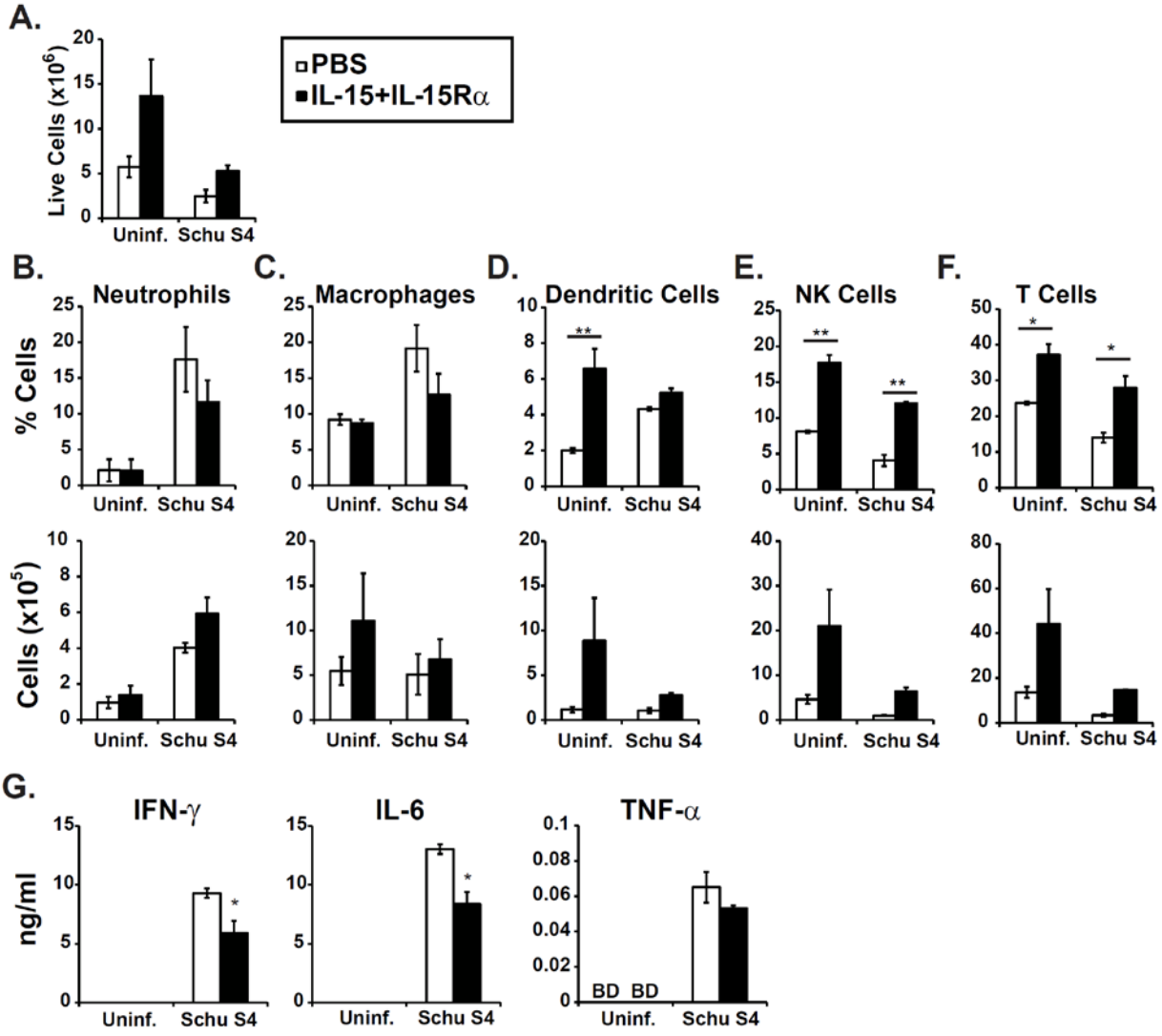

Figure 25. Changes in lung immune cell populations and systemic cytokine and chemokine production following IL-15+IL-15Rα treatment of Schu S4-infected mice.

Mice (n=4 per group) were administered PBS or IL-15+IL-15Rα i.t. one day prior, on the same day, and two days following i.t. Schu S4 infection (100 CFU). Uninfected (Uninf.) mice (PBS-treated, n=4 per group) administered PBS or IL-15+IL-15Rα served as controls. Mice were sacrificed four dpi and lungs were processed as described in Materials and Methods. (A) Absolute cell numbers in the lungs were enumerated by trypan blue exclusion. (B-F) Changes in individual immune cell populations were evaluated by flow cytometric analysis: neutrophils ($Ly6G^{+}$, $F4/80^{low}$), macrophages ($F4/80^{+}$, $Ly\text{-}6G^{-}$), dendritic cells ($CD11c^{high}$, $F4/80^{-}$), NK cells ($DX5^{+}$, TCR-β^{-}), and T cells ($DX5^{-}$, TCR-β^{+}). (G) Lung supernatants were assessed for multiple cytokines and chemokines using the Milliplex

32-plex Mouse Cytokine/Chemokine Panel (Millipore) on a Bio-Plex system (Bio-Rad Laboratories, Inc.). The cytokines shown here were previously demonstrated to be modulated by IL-15+IL-15Rα in other models of sepsis (Inoue et al., 2010). All other cytokine and chemokine values can be found in Table 3. Data are expressed as mean ± SEM of two independent experiments. Statistical significance was determined by two-way ANOVA for each cell type and analyte comparing the effects of infection and treatment, followed by Bonferroni comparison of means ($^{*}p<0.05$, $^{**}p<0.01$, significant compared to PBS treatment). BD = below limits of detection.

Table 3. Plasma cytokine and chemokine levels following IL-15+IL-15Rα treatment of Schu S4-infected mice.

Infection	**Uninfected**		**Schu S4**	
Treatment	**PBS**	**IL-15+IL-15Rα**	**PBS**	**IL-15+IL-15Rα**
Analytes (pg/ml)				
Eotaxin	295.12 (± 25.31)	268.20 (± 9.31)	1528.34 (± 223.28)	1465.66 (± 171.11)
G-CSF	89.20 (± 18.13)	269.21 (± 17.76)	46192.76 (± 135.93)[b]	46680.28 (± 1089.98)[b]
GM-CSF	6.31 (± 1.04)	12.99 (± 3.18)	85.10 (± 3.28)	70.61 (± 2.03)[c]
IFN-γ	3.55 (± 0.40)	5.08 (± 2.29)	9282.53 (± 406.68)[b]	5926.99 (± 1014.94)[b, c]
IL-1α	14.51 (± 5.06)	18.65 (± 4.03)	371.64 (± 11.49)	358.42 (± 8.03)
IL-1β	BD	BD	44.54 (± 4.35)	58.70 (± 3.26)[c]
IL-2	BD	BD	3.66 (± 0.27)	4.05 (± 0.60)
IL-3	BD	BD	BD	BD
IL-4	BD	BD	BD	BD
IL-5	5.16 (± 1.31)	9.18 (± 1.86)	20.75 (± 1.12)	14.24 (± 2.86)
IL-6	3.35 (± 0.17)	8.34 (± 2.74)	13024.09 (± 684.81)[b]	8362.11 (± 383.54)[b, c]
IL-7	BD	BD	4.27 (± 0.84)	4.47 (± 1.27)
IL-9	63.47 (± 21.59)	82.35 (± 38.69)	41.66 (± 3.17)	27.14 (± 2.81)
IL-10	BD	BD	145.97 (± 10.16)	138.54 (± 8.12)

IL-12 (p40)	4.05 (± 0.37)	5.99 (± 1.23)	20.03 (± 1.30)	14.50 (± 2.48)
IL-12 (p70)	4.72 (± 0.04)	5.19 (± 1.99)	69.98 (± 4.85)	51.29 (± 0.50)[c]
IL-13	35.60 (± 8.79)	45.60 (± 10.24)	938.27 (± 80.52)	808.23 (± 67.79)
IL-15	15.45 (± 4.37)	372.53 (± 360.23)	83.00 (± 16.27)	46.50 (± 2.49)
IL-17	BD	BD	12.16 (± 0.08)	7.49 (± 1.15)[c]
IP-10	55.54 (± 6.81)	159.24 (± 30.09)	3331.32 (± 260.90)	3376.18 (± 451.18)
KC	23.31 (± 6.43)	65.60 (± 15.99)	9457.03 (± 1158.09)[b]	5992.04 (± 894.92)[b]
LIF	BD	3.62 (± 0.42)	44.50 (± 16.71)	12.07 (± 3.88)
MCP-1	3.44 (± 0.24)	9.31 (± 3.85)	7245.75 (± 129.83)[b]	3255.51 (± 1195.59)[b, c]
M-CSF	BD	3.47 (± 0.27)	72.37 (± 4.46)	32.26 (± 11.16)[c]
MIG	19.35 (± 0.07)	60.91 (± 17.05)	12814.46 (± 592.76)[b]	12348.07 (± 425.51)[b]
MIP-1α	8.71 (± 0.36)	13.24 (± 4.18)	192.20 (± 17.89)	122.22 (± 19.49)[c]
MIP-1β	14.18 (± 7.05)	16.33 (± 4.32)	727.24 (± 36.14)	326.06 (± 59.94)[c]
MIP-2	BD	10.87 (± 1.31)	1671.68 (± 107.40)	598.28 (± 127.01)[c]
RANTES	5.61 (± 0.40)	7.73 (± 1.48)	169.30 (± 8.98)	99.54 (± 6.73)[c]
TNF-α	BD	BD	65.08 (± 8.67)	53.24 (± 1.51)
VEGF	BD	BD	3.42 (± 0.10)	BD
LIX	620.82 (±426.10)	469.70 (± 145.79)	913.93 (± 46.49)	616.62 (± 192.55)

[a]BD = below limits of detection.
[b]Values were extrapolated from the standard curve for a subset of samples.
[c]$p<0.05$ by two-way ANOVA comparing the effects of treatment and infection and Bonferroni comparison of means, significant compared to PBS treatment

The effect of IL-15+IL-15Rα on bacterial burdens in Schu S4-infected mice was then measured. Despite changes in immune cells and modulation of cytokines, IL-15+IL-15Rα had no impact on bacterial numbers measured four dpi (Fig. 26). In addition, IL-15+IL-15Rα did not

significantly alter the progression of disease in Schu S4-infected mice based on clinical signs and weight loss (17% for PBS-treated and 16% for IL-15+IL-15Rα-treated four dpi). Administration of IL-15+IL-15Rα by different routes, either intraperitoneally or both intraperitoneally and intratracheally, did not affect bacterial burdens following Schu S4 infection (Fig. 27). Therefore, IL-15+IL-15Rα treatment did not improve host resistance to pulmonary Schu S4 infection.

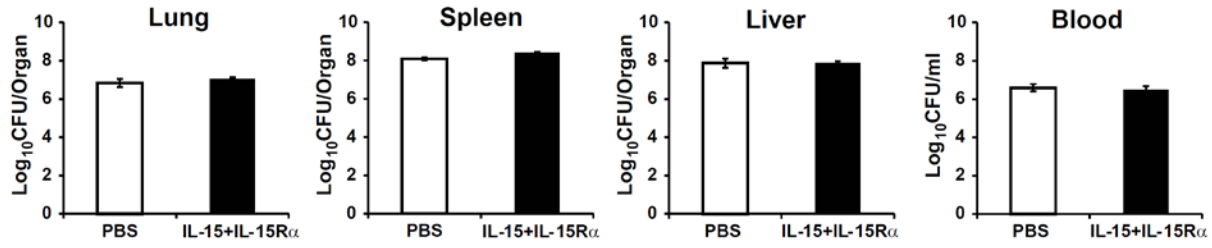

Figure 26. Bacterial burden following IL-15+IL-15Rα treatment of Schu S4-infected mice.

Mice were administered PBS or IL-15+IL-15Rα and infected with Schu S4 as described in the legend to Fig. 26. Bacterial burdens in the organs and blood of Schu S4-infected mice treated with IL-15+IL-15Rα four dpi (n=4 mice per group). Data are expressed as mean ± SEM and are representative of two independent experiments.

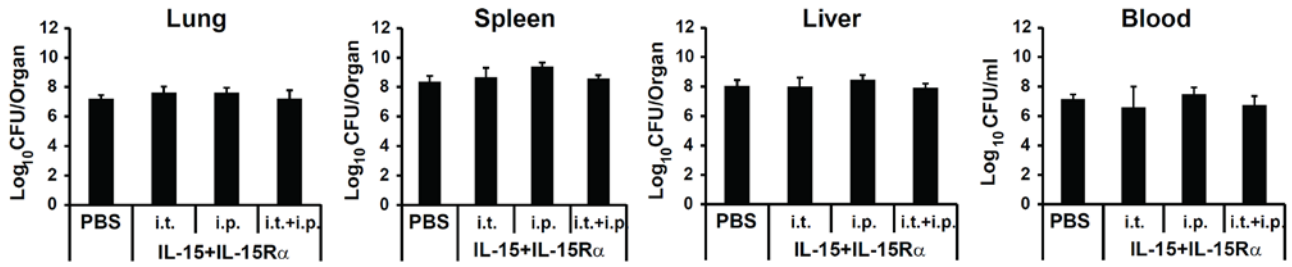

Figure 27. Bacterial burden following pulmonary and/or systemic administration of IL-15+IL-15Rα to Schu S4-infected mice.

Mice (n=4 per group) were administered PBS i.t. or IL-15+IL-15Rα i.t., i.p., or i.t. and i.p. one day prior, on the same day, and two days following i.t. Schu S4 infection (100 CFU). Four dpi, mice were sacrificed and the designated organs and blood were processed, diluted, and plated for CFU enumeration. Data are expressed as mean ± SD of one independent experiment.

Although IL-15+IL-15Rα improved the absolute number of viable cells present in the lungs of Schu S4-infected mice, there was still a 60-70% loss in viable lung cells after Schu S4 infection irrespective of treatment group (Fig. 25A). This suggested IL-15+IL-15Rα was not limiting the widespread cell death that occurred in the lungs of Schu S4-infected mice. To investigate this further, lung sections from treated and untreated Schu S4-infected mice were probed for apoptotic cells. As observed previously (Sharma et al., 2011), robust TUNEL staining was localized around regions of infection in the lung of Schu S4-infected mice four dpi (Fig. 28). A similar pattern of TUNEL staining was observed in Schu S4-infected mice that were treated with IL-15+IL-15Rα (Fig. 28). In regions with no bacterial antigen staining, a low frequency of $TUNEL^{+}$ cells was detected (Fig. 28). Limited TUNEL staining was also seen in uninfected mice (Fig. 28). These results corroborated the loss in lung cells observed by flow cytometric analysis and suggest that the inability of IL-15+IL-15Rα to limit cell death in the lung may contribute to its poor effectiveness as a treatment for type A *F. tularensis*.

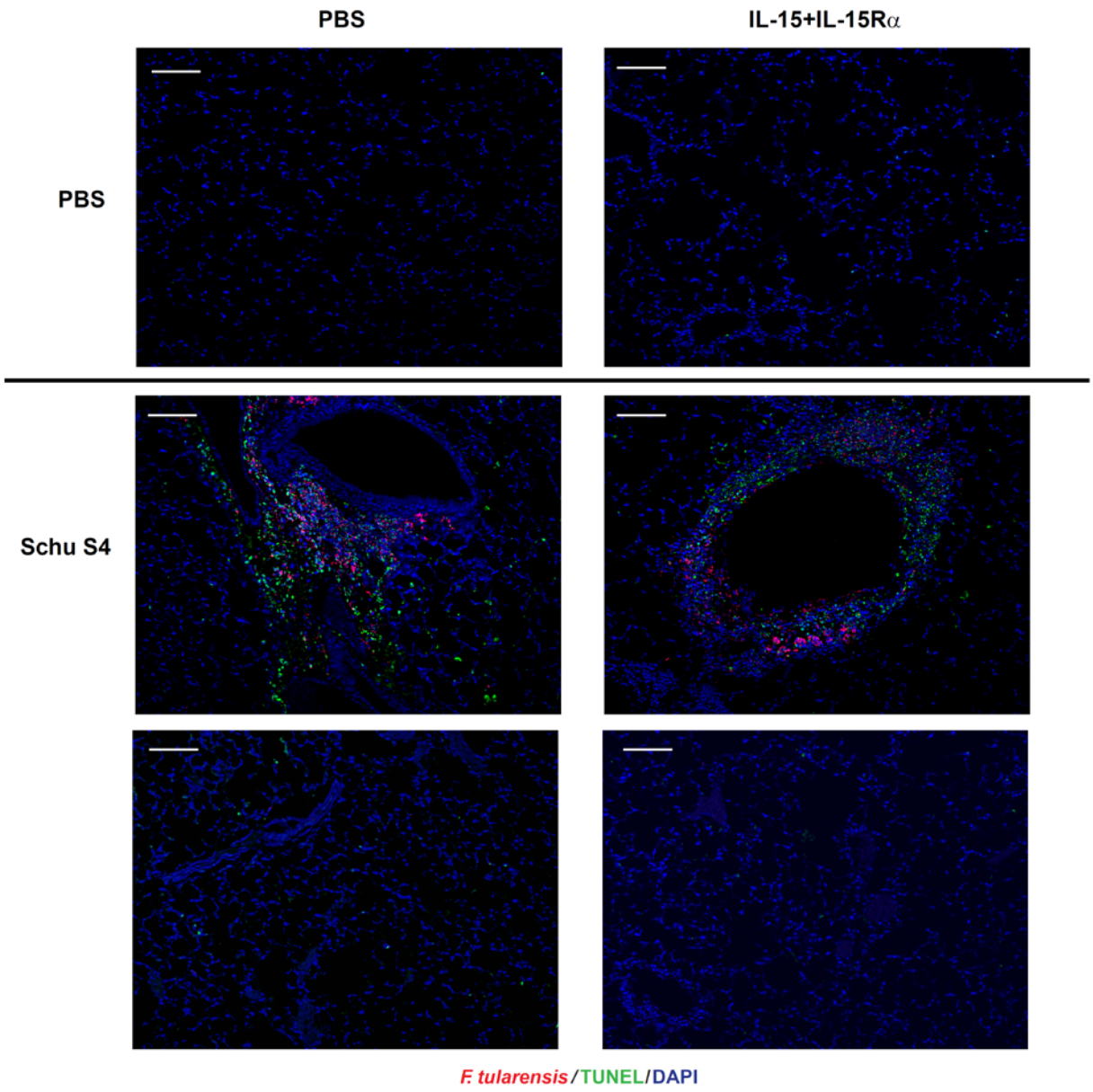

Figure 28. TUNEL staining following IL-15+IL-15Rα treatment of Schu S4-infected mice.

Immunofluorescence microscopy of lung sections from uninfected and Schu S4-infected mice treated with IL-15+IL-15Rα. Four dpi, lungs were harvested, fixed in formalin, and embedded in paraffin. Deparaffinized lung sections were probed with rabbit anti-*F. tularensis* followed by a secondary Alexa Fluor 568 goat anti-rabbit antibody. An In Situ Cell Death Detection Kit (Roche) was used for the TUNEL assay. DNA was stained with DAPI. The color merged images (red, *F. tularensis*; green, TUNEL; blue, DAPI) were captured with an equal fluorescence exposure time within each channel and are representative of two independent experiments with a total

of 3-4 mice per group. The scale bars in the upper left hand corners of the images represent a length of 100 μm. The top panel of images from Schu S4-infected mice represents areas with dense *F. tularensis* antigen staining while the bottom panel of images represents areas with little to no *F. tularensis* antigen staining.

3.5 DISCUSSION

NK cells can promote or antagonize host resistance to bacterial pathogens (Badgwell et al., 2002; Feng et al., 2006; Le-Barillec et al., 2005; Sherwood et al., 2004). In studies with LVS, NK cells are important for the early control of infection through the secretion of IFN-γ (Bokhari et al., 2008; Lopez et al., 2004; Metzger et al., 2007). We began investigating NK cells in Schu S4 infection because of their role in LVS immunity and because of the marked changes observed after pulmonary challenge (Fig. 12D and 13D). Similar to neutrophils (Fig. 17) (KuoLee et al., 2011), modulation of NK cells did not have a demonstrable effect on Schu S4 infection *in vivo*. Neither depletion with antibodies nor enhanced NK cell numbers via treatment with IL-15+IL-15Rα had an impact on bacterial burden or the progression of disease following Schu S4 challenge. Our results suggest NK cells are dispensable for host resistance to acute type A *Francisella* infection.

Different results were observed when NK cells were depleted with anti-asialo GM1 or anti-NK1.1 in the vaccination/challenge model (Fig. 24B-C). Anti-asialo GM1 treatment reduced survival of LVS-vaccinated mice challenged with Schu S4. An explanation for this effect is a partial loss in $CD8^+$ T cells in anti-asialo GM1-treated mice. Although asialo GM1 is expressed predominantly on NK cells, it is also detected on a subpopulation of NK T cells, activated $CD8^+$ T cells, gamma-delta T cells, and basophils (Nishikado et al., 2011; Trambley et al., 1999).

While no off-target effects of anti-asialo GM1 were observed in naive mice, there was a 60% reduction in the number of $CD8^+$ T cells in vaccinated mice treated with anti-asialo GM1 compared to isotype controls four days post Schu S4 infection (Fig. 29). Previous work by Conlan *et al.* demonstrated that depletion of $CD8^+$ T cells significantly reduces survival from secondary challenge with type A *Francisella* (Wayne Conlan et al., 2005). Anti-asialo GM1, therefore, may have depleted *Francisella*-immune $CD8^+$ T cells making mice more susceptible to challenge with Schu S4. Additionally, the biological impact of anti-NK1.1 treatment, which does not affect $CD8^+$ T cells, was small (Fig. 24C). Together, these results suggest NK cells minimally contribute to LVS-mediated protective immunity.

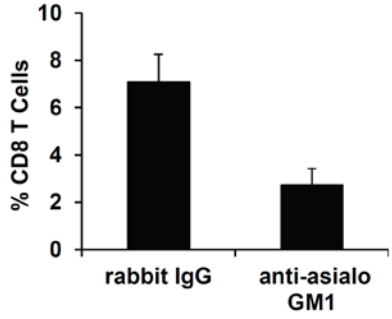

Figure 29. Reduction in $CD8^+$ T cells following anti-asialo GM1 treatment of LVS-vaccinated mice challenged with Schu S4.

Four days post Schu S4 infection, single cell suspensions from the lungs of LVS-vaccinated mice (n=4-5 mice per group) administered either anti-asialo GM1 or normal rabbit IgG were stained with fluorescently conjugated antibodies against CD3, CD4, CD8, and CD49b (DX5). The frequency of $CD8^+$ T cells was measured by gating on those cells that were $CD3^+DX5^-CD8^+CD4^-$. Data are expressed as mean ± SD of one independent experiment.

While NK cell depletion failed to alter acute Schu S4 infection, we also tested the effect of increasing NK cell numbers. IL-15+IL-15Rα treatment had a significant effect on survival in a mouse model of cecal ligation and puncture (CLP) and *Pseudomonas aeruginosa* pneumonia

(Inoue et al., 2010). However, no difference in bacterial burden or disease severity was observed between IL-15+IL-15Rα-treated and PBS-treated mice infected with Schu S4 (Fig. 26-27). There are several possible explanations for the effects of IL-15+IL-15Rα in these different sepsis models. Although serum IFN-γ levels increased with IL-15+IL-15Rα in CLP mice (Inoue et al., 2010), IFN-γ decreased following IL-15+IL-15Rα treatment in Schu S4-infected mice (Fig. 25G). This decrease in IFN-γ inversely correlated with an increase in total cells, specifically NK cells and T cells, following IL-15+IL-15Rα treatment. The presence of more cells in the lung may have resulted in the enhanced consumption of IFN-γ and the detection of lower levels by Luminex. To compensate for the reduced availability of IFN-γ, we treated Schu S4-infected mice with recombinant IFN-γ along with IL-15+IL-15Rα. However, no significant difference in bacterial burden or disease progression was observed in Schu S4-infected mice treated with IFN-γ+IL-15+IL-15Rα compared to PBS controls (Fig. 30).

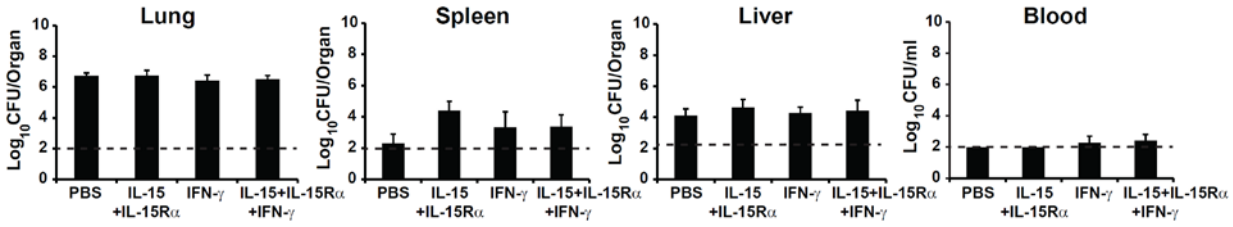

Figure 30. Bacterial burden following IL-15+IL-15Rα+IFN-γ treatment of Schu S4-infected mice.

Mice (n=4 per group) were administered IL-15+IL-15Rα and/or IFN-γ to Schu S4-infected mice (100 CFU) as described in Materials and Methods. Two dpi, mice were sacrificed and the designated organs and blood were processed, diluted, and plated for CFU enumeration. Data are expressed as mean ± SD of one experiment.

Other cytokines may also contribute to the limited effect of IL-15+IL-15Rα in pneumonic tularemia. Systemic levels of TNF-α and IL-6 were significantly lower in CLP mice treated with

IL-15+IL-15Rα, but only IL-6 was significantly reduced in IL-15+IL-15Rα-treated Schu S4-infected mice (Fig. 25G and Table 3). The differential regulation of TNF-α and IL-6 has been observed in other treatment models and was hypothesized to be due to different cellular origins of these two cytokines (Di Santo et al., 1997). The persistently elevated TNF-α levels in Schu S4-infected mice may worsen disease despite IL-15+IL-15Rα therapy, since high circulating levels of TNF-α are associated with mortality in some models of sepsis (Hotchkiss and Karl, 2003).

IL-15+IL-15Rα also prevents the apoptotic depletion of lymphocytes and DCs in CLP mice (Inoue et al., 2010). However, a 60-70% loss in viable lung cells was still observed in IL-15+IL-15Rα-treated mice infected with Schu S4 compared to uninfected controls (Fig. 25A). The absolute number of DCs, T cells, and NK cells also declined at a similar rate (Fig. 25D-F). TUNEL staining of lung tissue sections from both PBS and IL-15+IL-15Rα-treated mice infected with Schu S4 confirmed that cell death was not limited by cytokine treatment (Fig. 28). These results suggest the mechanism of cell death in Schu S4-infected mice may differ from the Bim and PUMA-dependent apoptosis in CLP mice (Inoue et al., 2010). In summary, IL-15+IL-15Rα has different effects on systemic cytokine production and cell death in two independent sepsis models: CLP and pneumonic tularemia. This suggests IL-15+IL-15Rα may not be generally applicable to treat sepsis of different etiologies.

4.0 A *FRANCISELLA TULARENSIS* STRAIN THAT IMPROVES STIMULATION OF ANTIGEN-PRESENTING CELLS DOES NOT ENHANCE VACCINE EFFICACY

This chapter is adapted from the original publication:

Schmitt, D.M., D.M. O'Dee, J. Horzempa, P.E. Carlson, Jr., B.C. Russo, J.M. Bales, M.J. Brown, and G.J. Nau. 2012. A *Francisella tularensis* Live Vaccine Strain That Improves Stimulation of Antigen-Presenting Cells Does Not Enhance Vaccine Efficacy. *PLoS One*. 7: e31172.

4.1 ABSTRACT

Vaccination is a proven strategy to mitigate morbidity and mortality of infectious diseases. The methodology of identifying and testing new vaccine candidates could be improved with rational design and *in vitro* testing prior to animal experimentation. The tularemia vaccine, *Francisella tularensis* live vaccine strain (LVS), does not elicit complete protection against lethal challenge with a virulent type A *Francisella* strain. One factor that may contribute to this

poor performance is limited stimulation of antigen-presenting cells. In this study, we examined whether the interaction of genetically modified LVS strains with human antigen-presenting cells correlated with effectiveness as tularemia vaccine candidates. Human dendritic cells infected with wild-type LVS secrete low levels of proinflammatory cytokines, fail to upregulate costimulatory molecules, and activate human T cells poorly *in vitro*. One LVS mutant, strain 13B47, stimulated higher levels of proinflammatory cytokines from dendritic cells and macrophages and increased costimulatory molecule expression on dendritic cells compared to wild-type. Additionally, 13B47-infected dendritic cells activated T cells more efficiently than LVS-infected cells. A deletion allele of the same gene in LVS displayed similar *in vitro* characteristics, but vaccination with this strain did not improve survival after challenge with a virulent *Francisella* strain. *In vivo*, this mutant was attenuated for growth and did not stimulate T cell responses in the lung comparable to wild-type. Therefore, stimulation of antigen-presenting cells *in vitro* was improved by genetic modification of LVS, but did not correlate with efficacy against challenge *in vivo* within this model system.

4.2 INTRODUCTION

The development of vaccines is essential to combat harmful infectious diseases (Hinman, 1998). Obtaining licensure after discovery of a vaccine, however, can take up to 20 years due to the stringent testing required to confirm the safety and efficacy of the vaccine (Barrett and Beasley, 2009). To expedite this process, *in vitro* tests could be developed to define correlates of protection and identify more promising vaccine candidates. These assays would be particularly beneficial with vaccine candidates for highly pathogenic organisms, such as the bacterium

Francisella tularensis, when challenge studies cannot be performed in humans because of contemporary regulations that govern clinical trials (Quill and Giovanni, 2004).

F. tularensis is the causative agent of tularemia (Oyston, 2008). This zoonotic disease is endemic in North America and parts of Europe and Asia, and outbreaks in these regions are frequently associated with the handling of infected animals or transmission by arthropod vectors (Oyston, 2008; Sjostedt, 2007). *F. tularensis* is also classified by the Centers for Disease Control and Prevention as a Category A bioterrorism agent (McLendon et al., 2006). When inhaled, less than 10 organisms can cause an acute pneumonia that is lethal in up to 60% of infected individuals if left untreated (Dennis et al., 2001). The World Health Organization predicted that if virulent *F. tularensis* was aerosolized over a metropolitan area of five million people, more than 19,000 people would die and 250,000 individuals would be incapacitated (McLendon et al., 2006). An effective vaccine would be useful to reduce the number of naturally occurring tularemia cases and to protect against a possible intentional release.

To date, two different types of tularemia vaccines have been studied in humans. The Foshay vaccine consisted of chemically killed *F. tularensis* and was effective at reducing the incidence of laboratory-acquired tularemia cases from approximately 100% to 30% in the 1950s (Foshay, 1950; Kadull et al., 1950). However, killed *F. tularensis* provided only minimal protection from aerosol type A *Francisella* challenge in a vaccine trial (Saslaw et al., 1961). Researchers in the former Soviet Union took a different approach and developed a range of live attenuated *Francisella* strains to immunize people against tularemia (Titball and Oyston, 2003). One of these strains, a live attenuated strain of *F. tularensis* subsp. *holarctica*, live vaccine strain (LVS), was superior to the Foshay-type vaccines at providing protection (Burke, 1977; McCrumb, 1961; Saslaw et al., 1961). While two clinical studies involving small numbers of

human vaccinees demonstrated effectiveness of LVS against aerosol challenge by virulent type A *Francisella* (McCrumb, 1961; Saslaw et al., 1961), a later study showed variable efficacy that diminished over time (Hornick and Eigelsbach, 1966). Vaccination of individuals by aerosol improved the efficacy of LVS but this required a high dose of 10^6 to 10^8 organisms which frequently resulted in severe adverse side effects (Hornick and Eigelsbach, 1966).

Currently, LVS is not approved by the Food and Drug Administration (FDA) due to concerns about its undefined attenuation, mechanism of protection, and reversion frequency (Wayne Conlan and Oyston, 2007). In order to obtain FDA approval, several groups are working to address these issues. Recent work by Salomonsson *et al.* identified two regions of difference, RD18 and RD19, which are deleted in LVS and account for its attenuation (Salomonsson et al., 2009). Additional studies improved the manufacturing process of LVS in compliance with good manufacturing practice guidelines (Pasetti et al., 2008). This new lot of LVS was further characterized in human phase I clinical trials (El Sahly et al., 2009). Researchers are also introducing mutations into LVS in order to improve its efficacy and bolster attenuation. One example is an LVS mutant deficient in iron superoxide dismutase (*sodB*$_{Ft}$). Compared to LVS, *sodB*$_{Ft}$ increases median time to death and percent survival of C57BL/6 mice from pulmonary type A *Francisella* challenge (Bakshi et al., 2008). As work toward the licensing of LVS continues, attempts have been made to replace LVS with a genetically defined, attenuated type A *Francisella* strain. For example, Schu S4 ΔFTT_1103 and Schu S4 Δ*clpB*, provide 75% and 60% protection, respectively, from virulent type A *Francisella* challenge in BALB/c mice (Conlan et al., 2009; Qin et al., 2009). Nevertheless, LVS remains the only tularemia vaccine to date that has been shown to be effective in humans (McCrumb, 1961; Saslaw et al., 1961).

A potential limitation of LVS as a vaccine is its relative stimulation of antigen-presenting cells (APCs). Published work has shown LVS stimulates murine and human DCs (Ben Nasr et al., 2006; Katz et al., 2006), though it is now known that culture conditions influence stimulation of innate immunity (Carlson et al., 2007; Carlson et al., 2009; Hazlett et al., 2008; Loegering et al., 2006; Zarrella et al., 2011). In contrast, other studies have shown that LVS suppresses the activation of murine macrophages (Bosio and Dow, 2005; Loegering et al., 2006; Parsa et al., 2008; Telepnev et al., 2003; Telepnev et al., 2005) and dendritic cells (DCs) (Bosio and Dow, 2005). Murine macrophages and DCs cultured with LVS produce little to no proinflammatory cytokines *in vitro* compared to DCs cultured with other bacteria or TLR ligands (Bosio and Dow, 2005; Loegering et al., 2006; Telepnev et al., 2003; Telepnev et al., 2005). Stimulation with TLR ligands such as *Escherichia coli* LPS fails to restore cytokine secretion by these cells suggesting that LVS is actively suppressing TLR signaling (Bosio and Dow, 2005; Carlson et al., 2007; Loegering et al., 2006; Telepnev et al., 2003). Another study showed that this suppression is due to downregulation of critical inflammatory signaling pathways involved in MAPK and NF-κB activation (Telepnev et al., 2005).

In this study, we tested whether *in vitro* screening of potential tularemia vaccine candidates for enhanced stimulation of APCs would improve a candidate's immunogenicity, and ultimately protection after challenge. After initial testing of several LVS strains, we evaluated one genetic locus in detail with mutant strains that showed desirable vaccine characteristics *in vitro*, including attenuation in macrophages and enhanced DC stimulation. Despite these traits, they did not predict better protection against virulent type A *Francisella* challenge.

4.3 MATERIALS AND METHODS

4.3.1 *Francisella* strains and growth conditions

For cultivation of *F. tularensis* LVS strains and Schu S4, frozen stock cultures were streaked onto chocolate II agar plates and incubated at 37°C, 5% CO_2 for 2-3 days. LVS strains were grown in Chamberlain's chemically defined broth medium (CDM) (Chamberlain, 1965) or MH broth [Mueller-Hinton broth (Difco) supplemented with 0.1% glucose, 0.025% ferric pyrophosphate (Sigma), and IsoVitaleX (Becton Dickinson)] for *in vitro* infections. For mouse vaccinations, MH broth or TSBc [trypticase soy broth (BD Biosciences) supplemented with 0.1% L-cysteine hydrochloride monohydrate (Fisher)] was used for culturing of LVS strains. Schu S4 was grown in MH broth for infections of vaccinated mice. Broth cultures were grown at 37°C with shaking for 14-18 hours. When required, antibiotics were added to the media at the following concentrations: kanamycin at 10 μg/ml, chloramphenicol at 5 μg/ml, and hygromycin at 200 μg/ml.

4.3.2 Generation of formalin-fixed *F. tularensis* Schu S4 (ffSchu S4)

Schu S4 was grown in MH broth as described above. Following overnight culture, bacteria were washed, resuspended in PBS (Gibco), and adjusted to an OD_{600} of 0.3. Bacteria were then resuspended in 10% buffered formalin (Fisher) and incubated at 25°C for 10 min with shaking (200 rpm). Bacteria were washed five times and resuspended in PBS for an approximate concentration of $1 - 3 \times 10^8$ CFU/ml. Bacterial killing was confirmed by plating of formalin-fixed Schu S4 on chocolate II agar plates in which no colonies were observed following

extensive incubation (data not shown). Prior to formalin fixation, an aliquot of the bacterial suspension was removed and tested for viable CFU by plating serial dilutions on chocolate II agar.

4.3.3 Construction of LVS mutants

Construction of LVS strain 1664d was described previously (Horzempa et al., 2008a). The *F. tularensis* LVS ΔcapC mutant was generated using homologous recombination with a suicide plasmid. This plasmid contained two segments homologous to regions flanking FTL_1415 and one third of the 5' and 3' ends of this ORF, surrounding a chloramphenicol acetyltransferase gene (*cat*) under the control of the *F. tularensis groE* promoter (Table 4). Linearized plasmid was electroporated into LVS (Baron et al., 1995) and double cross-over events were selected on cysteine heart agar with 5% defibrillated rabbit blood containing 2.5 μg/ml chloramphenicol. Recombination was confirmed by PCR.

Table 4. Bacterial strains, plasmids, and primers used in this study.

Strain, plasmid, or primer	Description	Source or Reference
***F. tularensis* Strains**		
LVS	*F. tularensis* subsp. *holarctica* live vaccine strain	Karen Elkins
13B47	LVS with the Tn from pSD26 disrupting FTL_0883 in base pair 115 of 842 from the 5′ end	This study
1664d	LVS *deoB* (FTL_1664) disruption mutant	(Horzempa et al., 2008a)
ΔcapC	LVS containing *cat* replacing the central one third of *capC* (FTL_1415)	This study
ΔFTL_0883	LVS FTL_0883 in-frame deletion mutant	(Russo et al., 2011)
ΔFTL_0883::pJH1-FTL-0883	LVS ΔFTL_0883 cis-complement	(Russo et al., 2011)
***E. coli* Strains**		
sd-4	Streptomycin-dependent *E. coli* mutant (ATCC 11143)	ATCC 11143
Plasmids		

pSD26	*E. coli* shuttle plasmid (colE1, Ap^R) encoding the C9 transposase and *himar* transposon (Km^R)	Simon Dillon and Eric Rubin
Primers		
capC-1	5'–CCGCGGAAGCGACACATGGACTTTTGA–3'	This study
capC-2	5'–GAATTCAATATGATAATAGTTACTATAACT–3'	This study
capC-3	5'–ATGCATTTATATTATCCCTGGACTTAT–3'	This study
capC-4	5'–ACTAGTTTAGATTTTTTATTATCGTTA–3'	This study

To generate strain 13B47, plasmid pSD26 (a gift from Eric Rubin and Simon Dillon) was electroporated into LVS as previously described (Horzempa et al., 2008b). pSD26 is an *E. coli* plasmid delivery vector (*colE1*, Ap^R) that encodes a *Himar1* transposase (Rubin et al., 1999) and a transposon containing a kanamycin resistance cassette under the control of the *F. tularensis groE* promoter (Table 4). Following recovery in trypticase soy broth supplemented with 0.1% cysteine, bacteria were plated on cysteine heart broth with 5% defibrinated rabbit blood containing kanamycin (5 μg/ml). Colonies that emerged in the presence of kanamycin were isolated and screened for lack of response to extracellular spermine (Russo et al., 2011). The selection phenotype was lack of growth in CDM plus an inhibitor of endogenous polyamine biosynthesis, dicyclohexylamine (Russo et al., 2011). Transposon mutants that failed to grow were then tested for their ability to stimulate cytokines (Russo et al., 2011). Strain 13B47 elicited high concentrations of TNF-α from human macrophages and had a transposon insertion in FTL_0883 (Russo et al., 2011). DNA sequencing showed that the precise location of this transposon was in base pair 115 of 842 from the 5′ end of FTL_0883. Construction of an in-frame deletion mutant, ΔFTL_0883, and a cis-complement strain was described previously (Russo et al., 2011).

4.3.4 Infection of macrophages and DCs with *F. tularensis* LVS strains

Human monocytes were differentiated into macrophages and DCs by *in vitro* culture as described previously (Horzempa et al., 2008a). Briefly, monocytes were purified from human buffy coats from blood donations (Central Blood Bank, Pittsburgh, PA) using Ficoll gradients (Amersham Biosciences) to isolate peripheral blood mononuclear cells, Optiprep gradients (Axis-Shield) to enrich for monocytes, and panning on plastic to further purify monocytes (final purity, >95% based on microscopy). For macrophages, cells were cultured in 60-mm-diameter culture dishes for 7 days at 37°C with 5% CO2 in 5 ml of Dulbecco's modified Eagle's medium (Invitrogen) supplemented with 20% fetal bovine serum (Invitrogen), 10% human serum (Gemini Biosciences), 25 mM HEPES (Gibco), and 1% GlutaMAX (Invitrogen). Beginning on day 4 of culture, 0.5 ml of fresh media was added daily. On day 7, macrophages were removed from the culture dish by using a lidocaine-EDTA solution (5 mM EDTA and 4 mg of lidocaine/ml in PBS, pH 7.2). For DCs, human monocytes were seeded at a density of 1×10^6 cells/ml in 24 well plates (Costar) in complete RPMI [10% FCS, 25 mM HEPES, 1% non-essential amino acids, 1% sodium pyruvate, 1% Glutamax and 0.1% 2-mercaptoethanol (all from Gibco)] supplemented with 1000 U/ml GM-CSF and 1000 U/ml IL-4 (both from eBioscience) and incubated at 37°C with 5% CO2. On day 3 of culture, 10% of the media was replaced with fresh complete RPMI supplemented with GM-CSF and IL-4 and non-adherent cells were harvested at day 5.

For generation of murine DCs, bone marrow was flushed from femurs and tibias of C57BL/6J mice with complete DC medium [DMEM supplemented with 10% heat-inactivated FBS, 25 mM HEPES, 1% non-essential amino acids, 1% sodium pyruvate, 1% GlutaMAX and 0.1% 2-mercaptoethanol (all from Gibco)]. Freshly isolated cells were washed and red blood

cells were lysed with ACK Lysis Buffer (Gibco). After washing and counting, cells were resuspended in complete DC media supplemented with 500 U/ml GM-CSF (eBioscience) and seeded into T75 flasks or 24-well plates at a concentration of 20-30 million cells per flask or 1 x 10^6 cells/well, respectively. Cells were incubated at 37°C, 5% CO_2 for 5-6 days and fresh complete DC media with 500 U/ml GM-CSF was added every 2 days. Bone marrow DCs (BMDCs) were purified using CD11c magnetic beads (Miltenyi Biotec) per the manufacturer's instructions. The resulting cells were greater than 90% $CD11c^+$ as assessed by flow cytometry.

For cytokine and flow cytometry experiments, human cells were washed and resuspended in DMEM supplemented with 1% human serum, 25 mM HEPES, and 1% GlutaMAX. Murine BMDCs were washed and resuspended in DMEM supplemented with 10% FBS, 25 mM HEPES, 1% non-essential amino acids, 1% sodium pyruvate, 1% GlutaMAX and 0.1% 2-mercaptoethanol (all from Gibco). DCs and macrophages were seeded into 24-well plates (Costar) at 5 x 10^5 cells/well and 1.5 x 10^5 cells/well, respectively. Infections were conducted using two different methods with the goal of maintaining eukaryotic cell viability. A multiplicity of infection (MOI) of 10 was used for 24-hour co-cultures at 37°C with 5% CO_2, allowing cultures to proceed without washing. In other experiments, DCs were cultured with bacteria at an MOI of 500 for two hours as described below, which results in a high infection rate but with minimal effects on cell viability (Carlson et al., 2007; Horzempa et al., 2008a). As a positive control, macrophages and DCs were stimulated with *E. coli* strain sd-4 (ATCC 11143) (Nau et al., 1997). Supernatants were collected at various times post infection (6, 12, 24, and 48 hours) and DCs were prepared for flow cytometric analysis.

Gentamicin protection assays were used to assess intracellular growth (Small et al., 1987). Here, macrophages and DCs were seeded in Primaria 96-well culture dishes (BD

Biosciences) at a density of 5 x 10^4 cells/well and infected with bacteria at an MOI of 500. After two hours, cells were incubated with Hanks balanced salt solution (Gibco) containing gentamicin (20 µg/ml) for 20 min to kill extracellular bacteria. Cultures were then washed three times with warm Hank's balanced salt solution and incubated at 37°C with 5% CO_2 for another 22 hours with fresh culture medium. Actual MOIs were measured by plating serial dilutions of inocula on chocolate II agar plates. At the indicated time points post infection, viable CFU were measured as described previously (Horzempa et al., 2008a; Horzempa et al., 2010). Bacterial growth was compared using Student's *t*-test.

For DC-T cell co-culture assays, DCs were resuspended in complete T cell medium [DMEM supplemented with 10% heat-inactivated FBS, 25 mM HEPES, 1% non-essential amino acids, 1% sodium pyruvate, 1% GlutaMAX and 0.1% 2-mercaptoethanol (all from Gibco)] and seeded in 96-well round bottom plates (BD Biosciences) at a density of 2 x 10^4 cells/well. DCs were cultured with different *F. tularensis* LVS strains at an MOI of 10 for 24 hours prior to co-culture with T cells (see "Human DC-$CD4^+$ T cell co-culture").

4.3.5 Flow cytometry and analysis of human monocyte-derived DCs

Surface markers on *F. tularensis*-infected human monocyte-derived DCs were evaluated by flow cytometric analysis. Following infection, DCs were removed from 24-well plates using a 2 mM EDTA solution. Cells were washed once and resuspended in FACS staining buffer [0.1% bovine serum albumin and 0.1% sodium azide in PBS]. Nonspecific antibody binding was blocked with human FcR Blocking Reagent (Miltenyi Biotec). Cells were stained with fluorescein isothiocyanate (FITC)-conjugated anti-CD1b (clone MT-101, AbD Serotec), phycoerythrin (PE)-conjugated anti-CD86 (clone IT2.2, eBioscience), PE-Cy5-conjugated anti-

CD80 (clone 2D10.4, eBioscience), and PE-Cy7-conjugated anti-HLA-DR (clone LN3, eBioscience) at 4°C for 30 min. Isotype control antibodies were included in each experiment to confirm specificity of staining. After washing and fixing in 2% paraformaldehyde for 30 min at 4°C, cells were analyzed using a LSRII flow cytometer (BD Biosciences) and FlowJo Software (Tree Star). Statistically significant differences in CD80, CD86, and HLA-DR expression by infected DCs were determined by one-way ANOVA, followed by Bonferroni comparison of means.

4.3.6 Human DC-CD4$^+$ T cell co-culture

DC-T cell co-cultures were performed similarly to previous studies (Le Nouen et al., 2010; Munir et al., 2011; Torres et al., 2007). CD4$^+$ T cells were purified from human peripheral blood mononuclear cells that passed through the Optiprep gradient by positive selection using the Dynal CD4 Positive Isolation Kit (Invitrogen) per the manufacturer's instructions. These cells were > 95% CD3$^+$CD4$^+$ T cells as assessed by flow cytometry. Purified CD4$^+$ T cells were then stained with 2.5 μM CFSE for 10 min at 37°C, washed, and resuspended in complete T cell medium. CFSE-labeled T cells from a single donor were then added to DCs from a different donor that had been exposed to bacteria. DC-T cell co-cultures were performed in a 96-well round bottom plate at a ratio of 10:1 (2 x 10^5 T cells/2 x 10^4 DCs/well) for a period of 5 days at 37°C with 5% CO_2. After harvesting supernatants, cells were washed once and resuspended in FACS staining buffer, treated with human FcR Blocking Reagent (Miltenyi Biotec), and stained with APC-conjugated anti-CD4 (clone OKT4, eBioscience) at 4°C for 30 min. After washing and fixing in 2% paraformaldehyde for 30 min at 4°C, fluorescence was measured using a FACSCalibur flow cytometer (BD Biosciences) and analyzed with FlowJo Software (Tree Star).

For T cell proliferation, $CFSE^{low}$ cells were measured in the $CD4^+$ gate. Statistically significant differences in the percentage of proliferating T cells following co-culture with infected DCs were determined by one-way ANOVA, followed by Bonferroni comparison of means.

4.3.7 Mice

Six- to eight-week old female C57BL/6J mice were purchased from Jackson Laboratories (Bar Harbor, ME). Mice were housed in microisolator cages under specific pathogen-free conditions in a biosafety level-3 animal facility. All research involving animals was conducted in accordance with animal care and use guidelines, and animal protocols were approved by the University of Pittsburgh Animal Care and Use Committee.

4.3.8 Immunization of mice

LVS and ΔFTL_0883 were cultured in MH broth or TSBc as described above. Mice were immunized subcutaneously (s.c.) or intratracheally (i.t.). Vaccinations were performed i.t. by oropharyngeal instillation as described previously (Horzempa et al., 2010). A subset of mice was sacrificed at 2 hours post infection, and their lungs were homogenized and plated to confirm delivery of bacteria to the respiratory tract. Actual administered doses were determined by plating serial dilutions of the inocula onto chocolate II agar plates.

4.3.9 Infection of mice with *F. tularensis* Schu S4

Schu S4 was grown in MH broth as described above. Mice were infected i.t. with 100 CFU of Schu S4 six weeks following LVS or ΔFTL_0883 vaccination. The actual dose was calculated by plating serial dilutions of the inoculum onto chocolate II agar plates. Following infection, mice were monitored daily for survival.

4.3.10 Measurements of bacterial burden *in vivo*

Bacterial burdens in the organs of mice vaccinated with LVS strains were measured as previously described (Horzempa et al., 2010; Russo et al., 2011). Mice were sacrificed at the indicated time points and lungs, spleens, and livers were removed and homogenized in 1 ml (lungs, spleens) or 2 ml (livers) of TSBc. A portion of the organ homogenates were serially diluted and plated onto chocolate II agar plates. Plates were incubated at 37°C at 5% CO_2 and individual colonies were enumerated.

4.3.11 *In vitro* stimulation of lung cells from vaccinated mice

Six weeks following vaccination with LVS or ΔFTL_0883, lungs were excised, minced, and incubated in RPMI (Gibco) supplemented with 12 mg type I collagenase (Gibco), 100 µg DNase I (USB), and 3 mM $CaCl_2$ for 30 min at 37°C with shaking (170 rpm). The digested tissue was passed through a 40 µm cell strainer (BD Biosciences) to generate single cell suspensions. Erythrocytes were lysed with ACK Lysis Buffer (Gibco) and remaining cells were washed with RPMI. Viable cells were counted using trypan blue exclusion. Cells were

resuspended in complete RPMI [RPMI supplemented with 10% heat-inactivated FBS, 25 mM HEPES, 1% non-essential amino acids, 1% sodium pyruvate, 1% GlutaMAX and 0.1% 2-mercaptoethanol (all from Gibco)] and seeded into 96-well round bottom plates at 1.5 x 10^6 cells/well. Lung cells from naïve mice served as controls. BMDCs were generated as described above without CD11c magnetic bead purification. BMDCs were resuspended in complete RPMI and added at a 1:10 ratio (1.5 x 10^5 BMDCs/1.5 x 10^6 lung cells) to lung cells. Cells were incubated at 37 °C with either media alone or ffSchu S4 at dose of 10 CFU per cell. After 48 hour co-culture, supernatants were collected for analysis of cytokines and chemokines.

4.3.12 Cytokine and chemokine assays

DCs and macrophage supernatants were tested by ELISA using commercially available kits to measure TNF-α (R&D Systems), IL-12p40 (human, R&D Systems; mouse, eBioscience), and IL-6 (human, R&D Systems) according to the manufacturer's instructions. IFN-γ in supernatants from human DC-$CD4^+$ T cell co-cultures was also measured by ELISA (human, R&D Systems). The limits of detection for the ELISAs were: human TNF-α – 15.6 pg/ml, human and mouse IL-12p40 – 31.2 pg/ml, human IL-6 – 9.7 pg/ml, and human IFN-γ – 15.6 pg/ml. Cytokine and chemokine levels in lung supernatants from *in vitro* re-stimulation assays were determined by ELISA (mouse IFN-γ, R&D Systems; mouse IL-17A, Biolegend) or by using the Milliplex 32-plex Mouse Cytokine/Chemokine Panel (Millipore) on a Bio-Plex 200 system (Bio-Rad Laboratories). Analyte concentrations were calculated against the standards using Milliplex Analyst software (version 3.5; Millipore). The limits of detection for the ELISAs were 31.2 pg/ml for mouse IFN-γ and 15.6 pg/ml for mouse IL-17A. Statistically significant differences in

cytokine production were identified by one- or two-way ANOVA followed by Bonferroni comparison of means.

4.4 RESULTS

4.4.1 Limited inflammatory response of human DCs to LVS

We have shown previously that human macrophages have a limited capacity to produce proinflammatory cytokines following infection with LVS (Carlson et al., 2007). We hypothesized that human DCs would also be hyporesponsive to LVS stimulation. To test this, human macrophages and DCs were co-cultured with LVS, and then supernatants were harvested and analyzed for the proinflammatory cytokines TNF-α, IL-6, and IL-12p40. Similar to our findings with macrophages (Fig. 31A), LVS elicited little to no proinflammatory cytokines from human DCs (Fig. 31B). As a positive control, human DCs were stimulated with *E. coli* (Nau et al., 1997). *E. coli*-stimulated DCs produced significantly higher levels of all cytokines measured compared to untreated DCs or DCs cultured with LVS (Fig. 31B).

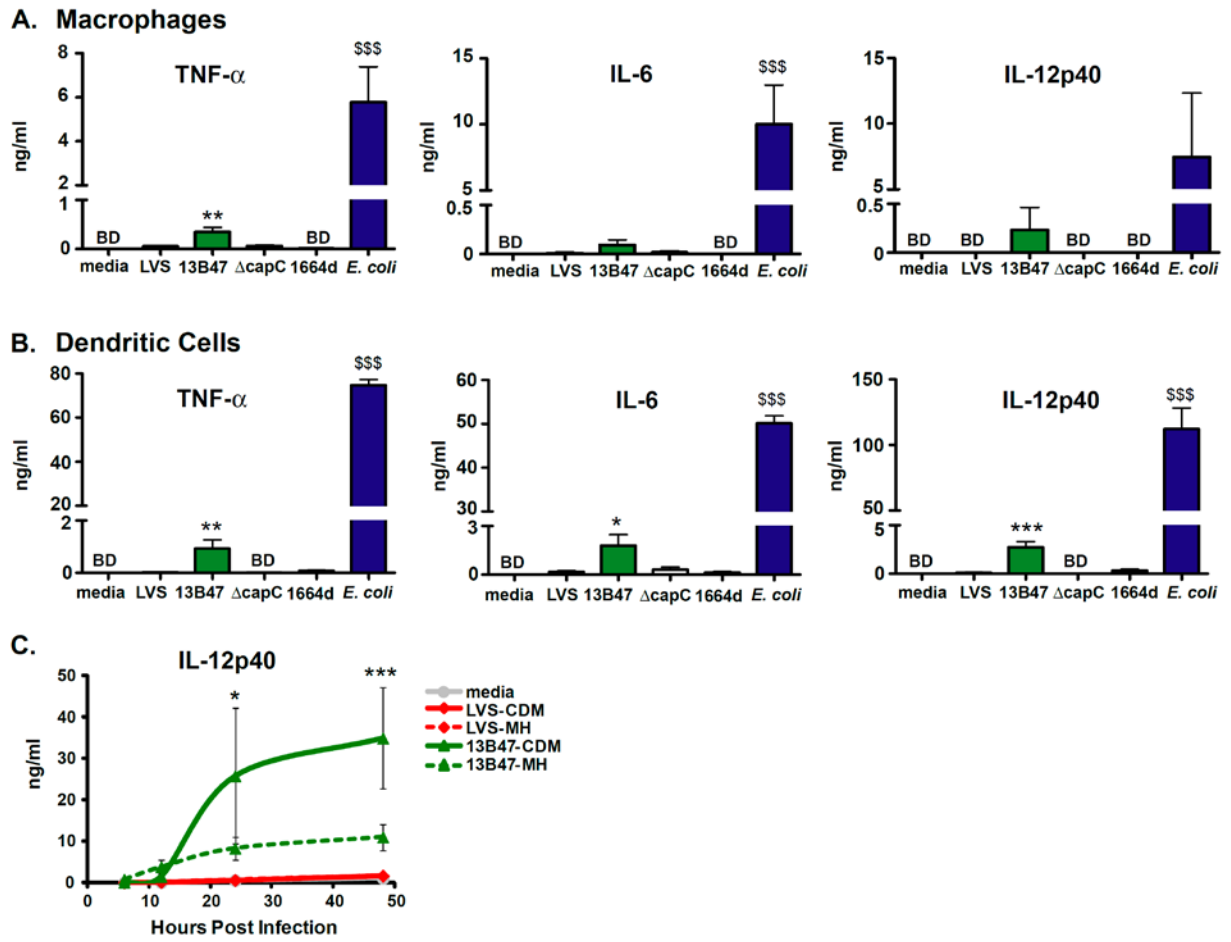

Figure 31. ***F. tularensis*** **LVS strain 13B47 stimulates human monocyte-derived DCs and macrophages to produce proinflammatory cytokines.**

LVS and LVS mutants, 13B47, ΔcapC, and 1664d, were cultured overnight in a chemically defined media (CDM) or Mueller-Hinton (MH) broth. The four bacterial cultures were used to inoculate macrophages (A, 1.5 x 10^5 cells/well) and DCs (B and C, 5 x 10^5 cells/well) at an MOI of 10. As a positive control, DCs and macrophages were cultured with *E. coli* strain sd-4 (MOI=10). Supernatants were harvested after 24 hours (A-B) or at indicated times (C), and TNF-α, IL-6, and IL-12p40 were measured by ELISA. Data are expressed as the mean ± SEM of three individual experiments with different donors. The level of cytokine production from each group was compared by a one (A-B) or two-way ANOVA (C), followed by the Bonferroni comparison of means. ($$$, $p<0.001$ for *E. coli* vs. all other groups). When comparing only the DCs infected with the *F. tularensis* strains, 13B47 elicited higher cytokine production than the uninfected group (A-B) or LVS cultured in the same media (C). *, $p<0.05$; **, $p<0.01$; ***, $p<0.001$. BD = below limits of detection of the ELISA.

4.4.2 Identification of an immunostimulatory *F. tularensis* LVS strain

We hypothesized that a LVS mutant inducing a stronger proinflammatory response from APCs *in vitro* would be a more effective tularemia vaccine candidate. Surveying pre-existing LVS mutants generated in our laboratory, we tested several for their ability to stimulate cytokine production from human DCs and macrophages (Table 4). Human DCs and macrophages were co-cultured with each of the mutants in parallel with wild-type LVS, and supernatants were analyzed for cytokines. Cytokine production by DCs and macrophages infected with either ΔcapC or 1664dwas similar to LVS-infected cells at 24 hours post infection (Fig. 31A-B). In contrast, DCs and macrophages infected with the 13B47 strain produced elevated levels of all cytokines measured (Fig. 31A-B). Although the cytokine levels elicited by 13B47 were lower than those produced by cells stimulated with *E. coli* (Fig. 31A-B), each was readily detected. Among the LVS strains tested, therefore, 13B47 stimulated the most proinflammatory cytokines from human APCs.

We next assessed whether the medium used to grow the bacteria would influence stimulation of DCs. LVS grown in media containing high levels of polyamines such as CDM stimulates low levels of proinflammatory cytokines from macrophages (Carlson et al., 2007; Carlson et al., 2009; Russo et al., 2011). To address the effect culture conditions may have on the DC phenotypes observed here, LVS and 13B47 were cultured in CDM or MH broth prior to co-culture with human DCs. At various time points post infection, supernatants were harvested and analyzed for detection of IL-12p40. At 24 and 48 hours post infection, greater than 10-fold higher levels of IL-12p40 were produced by human DCs cultured with 13B47 compared to wild-

type LVS (Fig. 31C). IL-12p40 production by DCs was higher regardless of whether 13B47 was cultured in CDM or MH broth (Fig. 31C). This result indicated that induction of cytokine production by 13B47 was not dependent on the growth medium used to culture this strain.

4.4.3 Maturation of DCs infected with *F. tularensis* strain 13B47

In addition to the secretion of cytokines, DCs must undergo a process called maturation in order to efficiently prime T cells and initiate the adaptive immune response . Among these alterations, the expression of MHC and costimulatory molecules increases. Since 13B47 stimulated cytokine production from human DCs, we next evaluated whether these cells also changed their surface phenotype in response to this mutant. The expression of CD80, CD86, and HLA-DR was measured on DCs following culture with either wild-type *F. tularensis* LVS, 13B47, ΔcapC, 1664d, or *E. coli* as a positive control for maturation. LVS elicited little to no change in expression of maturation markers on the surface of human DCs (Fig. 32A-C). Similar results were observed with the LVS mutants ΔcapC and 1664d (Fig. 32B-C). In contrast, the percentage of high-expressing cells and/or geometric mean fluorescence intensity increased after culture with 13B47 for CD80 and CD86 (Fig. 32). A similar trend of heightened expression of HLA-DR was also observed with 13B47-infected DCs (Fig. 32). Likewise, *E. coli*-stimulated DCs increased expression of costimulatory molecules and MHC (Fig. 32). These data suggest that DCs undergo maturation after exposure to *F. tularensis* strain 13B47 and, therefore, may be better suited to initiate an adaptive immune response.

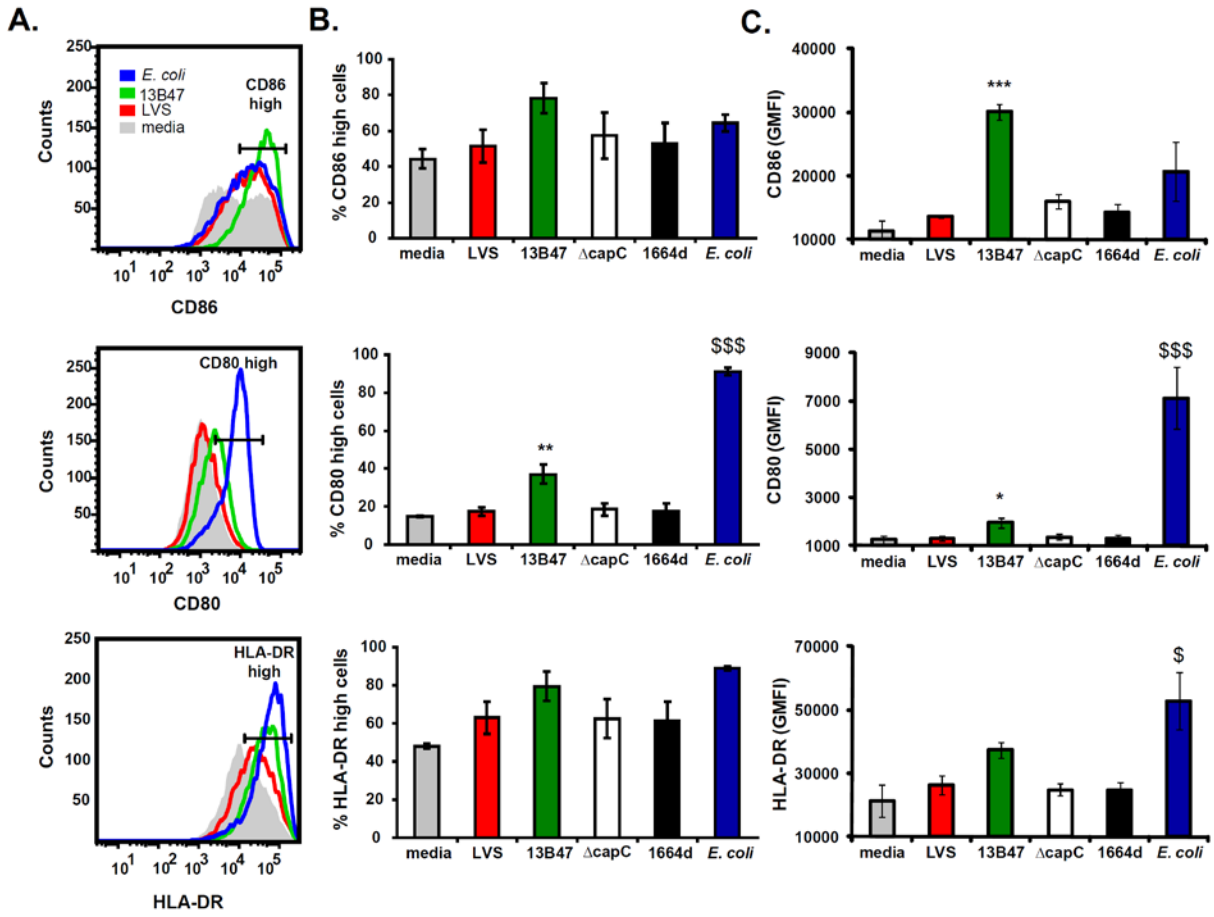

Figure 32. Human monocyte-derived DCs mature following exposure to LVS strain 13B47.

DCs were stimulated with either LVS, 13B47, ΔcapC, 1664d, or *E. coli* for 24 hours (MOI=10). Cells were harvested and analyzed for changes in surface expression of CD86, CD80, and HLA-DR. Cells were gated on CD1b-positive population. (A) Representative histograms for CD86, CD80, and HLA-DR expression on LVS-, 13B47-, and *E. coli*-treated DCs from one experiment. Histograms for ΔcapC- and 1664d-infected DCs were similar to LVS (data not shown). (B) Mean percentages of DCs with high CD86, CD80, and HLA-DR expression (± SEM) from three individual experiments with different donors. (C) Geometric mean fluorescence intensities (GMFI) of CD86, CD80, and HLA-DR (± SEM) on DCs from three individual experiments with different donors. Statistically significant differences in CD86, CD80, and HLA-DR expression by infected DCs were determined by one-way ANOVA, followed by Bonferroni comparison of means (*, $p<0.05$; **, $p<0.01$; ***, $p<0.001$).

4.4.4 Growth of 13B47 in human macrophages and DCs

Intracellular growth is a hallmark of pathogenic *Francisella* strains. Although 13B47 stimulated APCs to secrete cytokines and upregulate costimulatory molecules, it was unclear if its intracellular growth was altered. To test this, human DCs and macrophages were infected with either wild-type LVS or strain 13B47, and lysed at various times post infection to enumerate intracellular bacteria. 13B47 was attenuated for growth at 24 hours post infection in human macrophages (Fig. 33). Surprisingly, 13B47 was still capable of replicating in human DCs (Fig. 33), albeit with a slightly slower rate compared to wild-type LVS (estimated generation time of 783 minutes versus 275 minutes for wild-type). These data suggest that, while the cytokine response to 13B47 is similar between macrophages and DCs, these cells differ in their ability to control growth of this mutant.

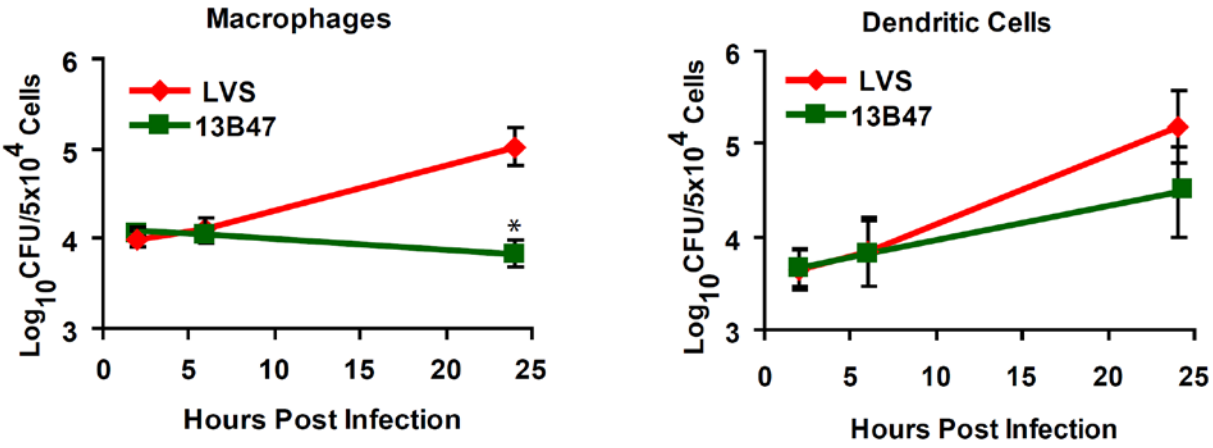

Figure 33. LVS strain 13B47 is attenuated for growth in human macrophages and replicates slowly in DCs. DCs or macrophages were infected in gentamicin protection assays (MOI = 500) with LVS or 13B47 and lysed at the indicated times post infection. Data shown are mean ± SEM from three individual experiments with different donors. Statistically significant differences in growth at 24 hours post infection were determined by Student's t-test (*, $p<0.05$).

4.4.5 Enhanced activation of $CD4^+$ T cells by *F. tularensis* strain 13B47-infected DCs

Enhanced maturation of human DCs by 13B47 led us to hypothesize the resulting DCs would stimulate T cells more effectively. This was tested by measuring human $CD4^+$ T cell proliferation and cytokine production following co-culture with allogeneic DCs pre-treated with LVS, 13B47, or *E. coli*. T cell proliferation was measured by CFSE dilution after co-culture with infected DCs for 5 days as described previously (Le Nouen et al., 2010; Munir et al., 2011; Torres et al., 2007). An increase in the percentage of proliferating $CD4^+$ T cells was observed following co-culture with 13B47-infected DCs compared to unstimulated $CD4^+$ T cells (Fig. 34A and B). This increased percentage of proliferating $CD4^+$ T cells was comparable to the level of proliferating T cells observed following co-culture with *E. coli*-infected DCs (Fig. 34A and B). In contrast, the percentage of proliferating $CD4^+$ T cells following co-culture with LVS-treated DCs was not significantly different from the baseline level of proliferation observed with unstimulated DCs (Fig. 34B). Culturing T cells with bacteria alone in the absence of DCs also did not induce high levels of proliferation (7.52% proliferating $CD4^+$ T cells for LVS, 8.22% proliferating $CD4^+$ T cells for 13B47).

T cell activation following co-culture with infected DCs was also assessed by cytokine production. IFN-γ concentrations in the supernatants of the DC-T cell co-cultures described above showed a similar trend to the proliferation data. $CD4^+$ T cells cultured with 13B47-infected DCs produced higher levels of IFN-γ compared to those stimulated with LVS-infected DCs (Fig. 34C). T cells stimulated with bacteria alone in the absence of DCs did not produce measurable levels of IFN-γ (< 15.6 pg/ml). The proliferation and cytokine production data together suggest DC maturation induced by 13B47 had measurable consequences on T cells *in vitro*.

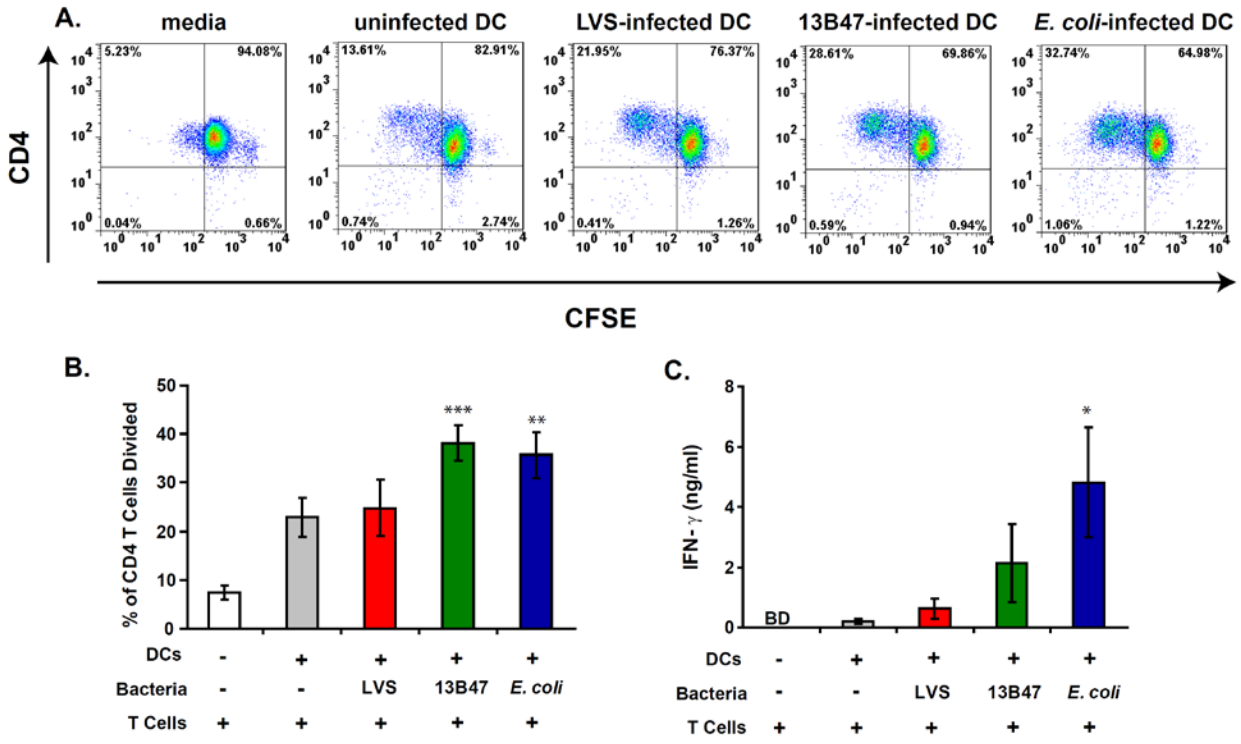

Figure 34. Enhanced proliferation and IFN-γ production by CD4$^+$ T cells stimulated with LVS strain 13B47-infected DCs.

Purified CFSE-labeled CD4$^+$ T cells from a single donor were co-cultured with either *E. coli*-infected, *F. tularensis* LVS-infected, or 13B47-infected DCs from a different donor at a ratio of 10:1 (2 x 10^5 T cells/2 x 10^4 DCs/well) for 5 days. (A) Representative dot plots showing loss of CFSE fluorescence versus CD4 staining on day 5 for each group from one experiment. (B) The mean percentages of proliferating CD4$^+$ T cells were calculated (± SEM) from five individual experiments with different donors. (C) IFN-γ levels were measured in day 5 supernatants by ELISA. Data are presented as the mean ± SEM from four individual experiments with different donors that were represented in Figure 4B. BLD = below limits of detection of the ELISA. Statistically significant differences in mean percentages and GMFI for all groups were determined by one-way ANOVA, followed by Bonferroni comparison of means (*, $p<0.05$; **, $p<0.01$; ***, $p<0.001$).

4.4.6 Evaluation of the LVS FTL_0883 mutant as a tularemia vaccine

Protection from virulent type A *Francisella* infection is largely dependent on the development of robust T cell-mediated immunity (Elkins et al., 2007). Based on the data obtained with human cells *in vitro*, we hypothesized that vaccination with 13B47 would prolong survival and improve T cell responses compared to LVS in mice challenged with virulent *Francisella*. However, 13B47 is not optimal since it contains a transposon that could be unstable. To generate a more suitable vaccine candidate, an in-frame deletion mutant was created in LVS, ΔFTL_0883, that does not incorporate an antibiotic resistance marker (Russo et al., 2011). Similar to human macrophages (Russo et al., 2011), more IL-12p40 and TNF-α was produced by human DCs cultured with ΔFTL_0883 than wild-type LVS (Fig. 35A-B). These cytokine levels were similar to, or greater than, that produced by DCs cultured with 13B47 (Fig. 35A-B). Moreover, IL-12p40 and TNF-α levels continued to rise from 24-48 hours when DCs were cultured with ΔFTL_0883 (Fig. 35B). To confirm the heightened stimulation of macrophages and DCs was due to deletion of FTL_0883, an in cis-complementing construct (pJH1-FTL_0883) was generated and introduced into ΔFTL_0883 (Russo et al., 2011). Complementation of ΔFTL_0883 with the wild-type copy of the gene significantly reduced IL-12p40 and TNF-α production by human macrophages (Russo et al., 2011) and DCs (Fig. 35B). Differential induction of IL-12p40 from human DCs by FTL_0883 mutants and wild-type LVS was also observed at a higher MOI of 500 (Fig. 35C).

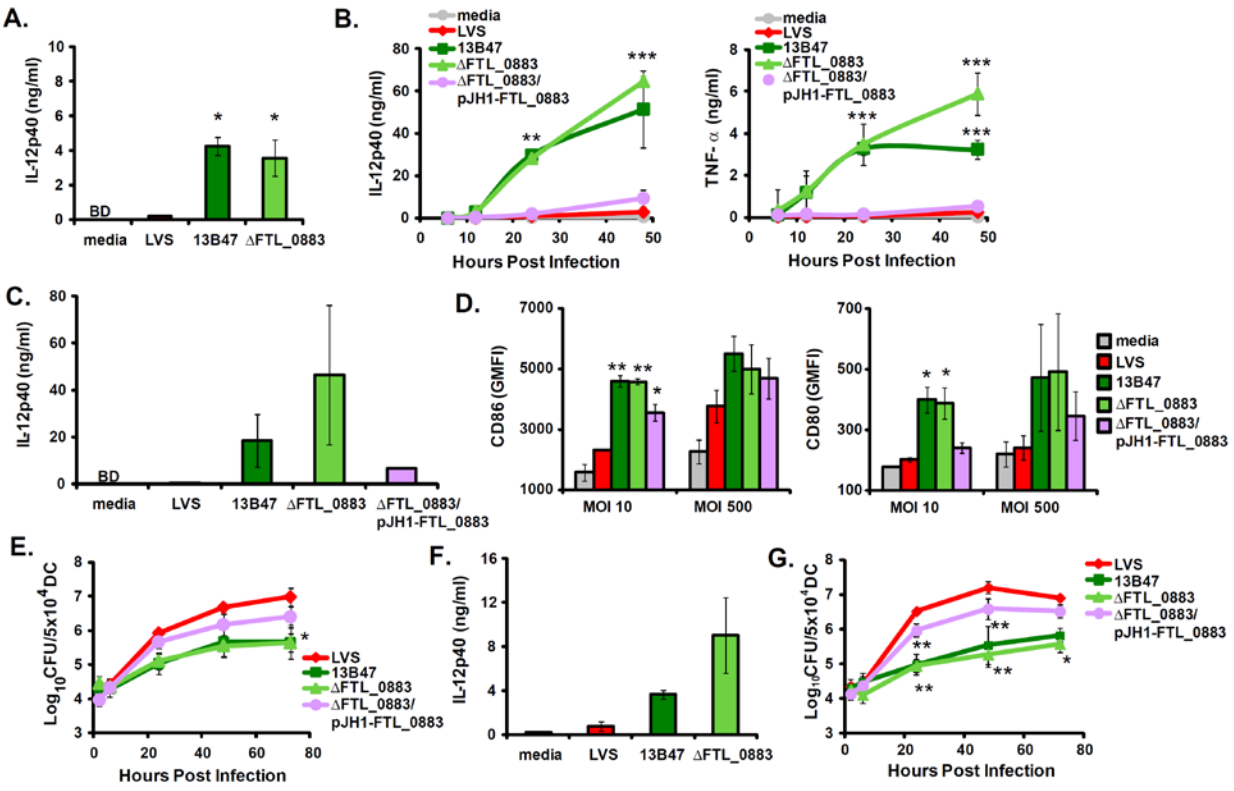

Figure 35. FTL_0883 deletion mutant, ΔFTL_0883, elicits maturation of DCs and is attenuated for growth similar to 13B47.

Human (A-E) and murine DCs (F-G) were cultured with either LVS, 13B47, ΔFTL_0883, or ΔFTL_0883::pJH1-FTL_0883 at an MOI of 10 (A-B, D, and F) or 500 followed by gentamicin treatment (C-E, and G). For cytokines, supernatants were harvested at 24 hours (A, C, and F) or the indicated time points (B), and IL-12p40 and TNF-α were measured by ELISA. For flow cytometry experiments (D), DCs were harvested 24 hours post infection and GMFIs for CD80 and CD86 were measured. For gentamicin protection assays (E, G), DCs were infected with LVS strains at an MOI of 500 and then lysed at indicated time points to enumerate intracellular bacteria. Data are presented as the mean ± SEM from at least two independent experiments. Statistically significant differences between groups were determined by one (A, C, D, and F) or two-way ANOVA (B, E, and G), followed by Bonferroni comparison of means (*, $p<0.05$; **, $p<0.01$; ***, $p<0.001$). BLD = below limits of detection of the ELISA.

Changes in CD80 and CD86 expression were also evaluated in human DCs cultured with either wild-type LVS or FTL_0883 mutants. As demonstrated previously in Fig. 32, expression of CD80 and CD86 was not altered on human DCs cultured with wild-type LVS at a low MOI (Fig. 35D). Culturing of human DCs with 13B47 or ΔFTL_0883, however, caused a statistically significant increase in expression of both costimulatory molecules on the surface (Fig. 35D). CD80 and CD86 expression were also higher on DCs cultured with 13B47 or ΔFTL_0883 than on LVS-infected DCs using a higher MOI (Fig. 35D). Lower levels of CD80 and CD86 were also measured on human DCs cultured with the ΔFTL_0883 strain complemented with a wild-type copy of the gene compared to DCs cultured with ΔFTL_0883 (Fig. 35D).

Deletion of FTL_0883 in LVS reduces its ability to replicate in human and murine macrophages (Russo et al., 2011). Additionally, the LVS mutant containing a transposon insertion in the FTL_0883 gene, 13B47, was attenuated for growth in human macrophages and replicated slowly in human DCs (Fig. 33). To measure ΔFTL_0883 replication in human DCs, DCs were infected with either wild-type LVS, 13B47, ΔFTL_0883, or the complemented strain, and lysed at various times post infection to enumerate intracellular bacteria. ΔFTL_0883 replicated more slowly in human DCs than wild-type LVS, exhibiting at least 5-fold less growth 24 hours post infection (Fig. 35E). Similar results were observed 48 and 72 hours post infection with up to a 20-fold difference in growth between ΔFTL_0883 and LVS measured 72 hours post infection (Fig. 35E). The growth kinetics for ΔFTL_0883 and 13B47 in human DCs over the 72 hour period were indistinguishable (Fig. 35E). Complementation of ΔFTL_0883 with a wild-type copy of the gene restored growth of the mutant to near wild-type levels (Fig. 35E). In summary, 13B47 and ΔFTL_0883 were similar with 1) reduced growth in human DCs, 2)

increased expression of CD80 and CD86, and 3) stimulation of IL-12p40 and TNF-α production by human DCs.

To test whether the phenotypes observed in human DCs were species-specific, murine DCs were also tested with these LVS strains. IL-12p40 levels were higher in supernatants from murine DCs cultured with either 13B47 or ΔFTL_0883 compared to LVS (Fig. 35F). Growth of strains with mutations in FTL_0883 was also less than wild-type in murine DCs (Fig. 35G). Similar to published work (Bosio and Dow, 2005), LVS replicated approximately 100-fold over 24 hours in murine DCs (Fig. 35G). Both 13B47 and ΔFTL_0883 grew less robustly in murine DCs, which was less than wild-type at 24, 48, and 72 hours post infection (Fig. 35G). Growth of the ΔFTL_0883 was nearly restored to wild-type levels by the complementing construct containing a wild-type copy of the gene (Fig. 35G). These results showed that human and murine DCs responded similarly to 13B47 and ΔFTL_0883.

Having established the *in vitro* phenotypes of the ΔFTL_0883 strain, we next assessed its ability to stimulate adaptive immune responses *in vivo*. C57BL/6J mice were vaccinated by either subcutaneous (s.c.) or respiratory (i.t.) routes with LVS or ΔFTL_0883. Mice were challenged six weeks later i.t. with the type A *F. tularensis* strain Schu S4. Vaccination of C57BL/6J mice with LVS prolongs survival but does not completely protect against a secondary challenge with a type A *Francisella* strain (Chen et al., 2003; Wu et al., 2005). This experimental design allowed us to determine whether ΔFTL_0883 vaccination conferred better protection than LVS. All mice that received a sham vaccination with PBS succumbed to the Schu S4 infection within 5 days following challenge (Table 5). Although mice vaccinated s.c. with LVS and ΔFTL_0883 survived longer than sham-vaccinated controls, they still required

euthanasia within 7 days of Schu S4 infection (Table 5). No survival differences were observed between animals vaccinated s.c. with LVS and ΔFTL_0883 (Table 5).

Vaccination by a respiratory route, however, showed statistically significant differences in protective efficacy. The median time to death of mice vaccinated i.t. with LVS was approximately 10-12 days following Schu S4 challenge (Table 5). This median time to death was double the median time to death for sham-vaccinated controls (5 days, Table 5) and was similar to previous work (Wu et al., 2005). In contrast, mice vaccinated with ΔFTL_0883 survived for a median of 6 days (Table 5). Therefore, vaccination with ΔFTL_0883 by a respiratory route provided less protection than that elicited by wild-type LVS.

Table 5. Survival of immunized mice following intratracheal Schu S4 challenge

Route	Vaccine	Vaccination Dose	Time to Death of Individual Mice (days)	Median Time to Death (days)
Control	PBS	N/A	5, 5, 5, 5, 5	5
Subcutaneous	LVS	1×10^4	6, 7, 7, 7, 7	7
	ΔFTL_0883	1×10^4	6, 6, 7, 7, 7	7
Intratracheal	Experiment 1			
	LVS	1×10^3	10,12,12, >33, >33	12[b]
	ΔFTL_0883	1×10^3	5, 6, 6, 7, 7	6
	Experiment 2			
	LVS	2×10^3	9, 9, 10, 11, 12	10[b]
	ΔFTL_0883	2×10^3	6, 6, 6, 7, 7	6

[a]Mice were immunized with either LVS or ΔFTL_0883 at the indicated dose and then challenged with 100 CFU of Schu S4 i.t.
[b]Significant difference $p < 0.005$ by log rank test.

To investigate the differences in the protection elicited by the two strains, we evaluated bacterial burdens in the lung and peripheral organs following respiratory vaccination. LVS replicated exponentially in the lung for the first three days following i.t. immunization (Fig. 36). The lung bacterial burden remained steady until day 6 post immunization and then slowly began

to decline up to day 10 (Fig. 36). Dissemination to the spleen and liver occurred at day 3 with LVS burden peaking at day 6 and being cleared by day 10 (Fig. 36). Despite comparable doses of bacteria used in the vaccinations, lower levels of ΔFTL_0883 were detected at all time points in the lung and beginning at day 3 in peripheral organs post immunization (Fig. 36). While clearance of LVS from the lung does not occur until 22 days post infection (Jia et al., 2010), ΔFTL_0883 was cleared more rapidly at approximately 10 days post infection (Fig. 36). Viable ΔFTL_0883 were measured in the spleens and livers of seven of eight mice by day 6, but none were detected in these organs at day 10 (Fig. 36). Therefore, LVS achieved higher numbers for a longer period of time in the lung and periphery following vaccination.

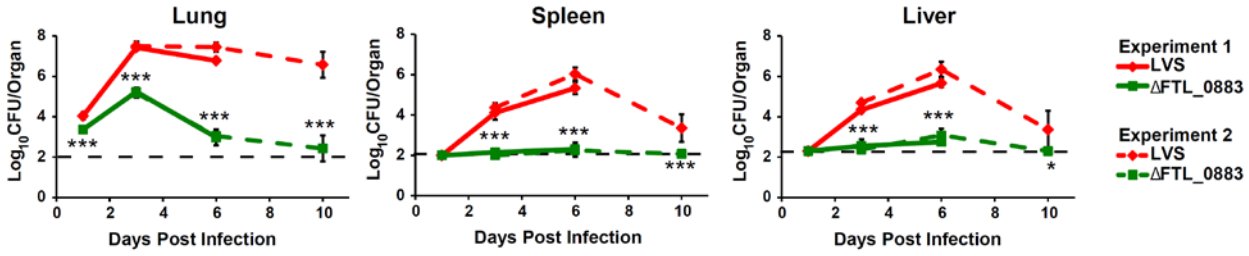

Figure 36. ΔFTL_0883-vaccinated mice have reduced bacterial burdens.

Mice were vaccinated i.t. (1.5×10^3 CFU) with either LVS or ΔFTL_0883 (n=4 mice/group/time point). At indicated time points (days 1, 3, and 6 for experiment 1; days 3, 6, and 10 for experiment 2), mice were sacrificed and the CFU/organ was determined as described in Materials and Methods. The limits of detection for the lung, spleen, and liver are depicted by the black dashed lines and were 100, 100, and 200 CFU, respectively. Data are presented as mean ± SD for each individual experiment. Statistically significant differences between groups in each experiment were determined by two-way ANOVA, followed by Bonferroni comparison of means (*, $p<0.05$; ***, $p<0.001$).

We next sought an immunological explanation for the performance of ΔFTL_0883 vaccination. We hypothesized wild-type LVS induced superior T cell responses than

ΔFTL_0883, and measured cytokine and chemokine responses by lung cells after i.t. vaccination. Cells were harvested from the lungs of LVS- and ΔFTL_0883-vaccinated mice and were re-stimulated *in vitro* with ffSchu S4. Cells from mice vaccinated with LVS produced higher amounts of IFN-γ with re-stimulation than cells from naïve mice or those that received ΔFTL_0883 (Fig. 37A). IFN-γ production by lung cells from mice vaccinated with ΔFTL_0883, however, was not statistically significantly different than naïve controls (Fig. 37). Increasing the vaccination dose of ΔFTL_0883 by three-fold failed to improve IFN-γ responses by the lung cells (Fig. 37). Consistent with the IFN-γ results, the IFN-γ inducible chemokine MIG was also higher in cultures from mice vaccinated with LVS (Table 6). In contrast to IFN-γ, cells from both vaccination groups produced comparable amounts of IL-17 after re-stimulation. A 2-3 fold increase in IL-17 production was observed in lung cells from mice vaccinated with ΔFTL_0883 and LVS compared to naïve controls (Fig. 37). No other statistically significant differences were consistently detected in the other cytokines and chemokines that were tested (Table 6). Therefore, the protection elicited by LVS against Schu S4 challenge correlated with IFN-γ production by lung cells after re-stimulation with antigen.

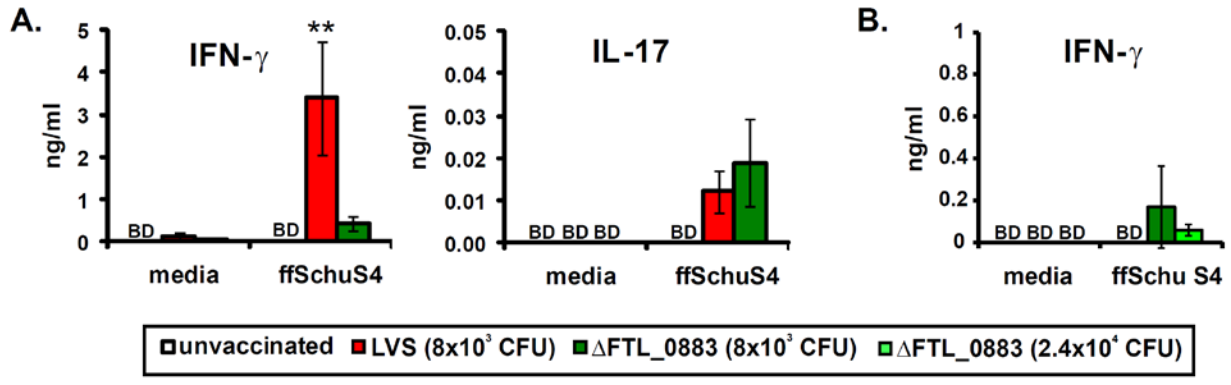

Figure 37. Cells from mice vaccinated with LVS produce more IFN-γ after re-stimulation.

Mice were vaccinated i.t. with either LVS or ΔFTL_0883 (n=3-4 mice/group). Age-matched naïve mice (n=3) served as negative controls. Lung cells were isolated from vaccinated and unvaccinated mice 30 days post

vaccination and incubated with formalin-fixed SchuS4 (ffSchu S4) and BMDCs for 48 hours. (A) Culture supernatants were collected and assessed for multiple cytokines and chemokines using the Milliplex 32-plex Mouse Cytokine/Chemokine Panel (Millipore) on a Bio-Plex system (Bio-Rad Laboratories, Inc.). Baseline levels of cytokine/chemokine production were established by the culturing of lung cells in media alone (no antigen). Data are presented as the mean ± SD of triplicate wells from one individual experiment. Another experiment of similar design was performed with a vaccination dose of 500 CFU i.t., and IL-17 and IFN-γ levels were measured by ELISA. Similar results were observed in both experiments. (B) IFN-γ production by lung cells isolated from mice vaccinated with two different doses of ΔFTL_0883 as measured by ELISA. Statistically significant differences in cytokine/chemokine production were determined by one-way ANOVA, followed by Bonferroni comparison of means. (**, $p<0.01$ for LVS v. ΔFTL_0883 following ffSchu S4 re-stimulation). BD = below levels of detection.

Table 6. Cytokine and chemokine levels following re-stimulation of lung cells from LVS- and ΔFTL_0883-vaccinated mice.

Cytokines	media			ffSchu S4		
	unvaccinated	LVS	ΔFTL_0883	unvaccinated	LVS	ΔFTL_0883
Eotaxin	36.22 (± 36.64)	6.54 (± 5.79)	17.56 (± 20.90)	21.49 (± 17.00)	BD	8.52 (± 6.32)
G-CSF	747.33 (± 762.62)	574.67 (±140.20)	499.33 (± 252.75)	729.33 (± 436.38)	1172.33 (± 246.67)	847.67 (± 352.55)
GM-CSF	17.67 (± 17.37)	10.15 (± 5.41)	15.70 (± 8.72)	19.10 (± 13.67)	37.10 (± 10.66)	39.03 (± 3.21)
IFN-γ	3.58 (± 0.65)	136.98 (± 102.23)	5.67 (± 2.96)	3.13 (± 0.13)	3393.33[a] (± 1326.94)	437.00 (± 177.60)
IL-1α	54.11 (± 36.80)	48.71 (± 9.74)	43.33 (± 14.64)	50.19 (± 23.69)	86.74 (± 14.39)	61.49 (± 11.33)
IL-1β	5.64 (± 4.22)	4.21 (± 1.01)	4.21 (± 1.02)	7.02 (± 4.23)	10.50 (± 3.81)	7.16 (± 2.50)
IL-2	15.29 (± 1.50)	5.73 (± 2.37)	14.77 (± 2.14)	10.67 (± 3.05)	10.19 (± 2.91)	30.35 (± 16.48)
IL-3	5.91 (± 1.48)	3.14 (± 0.10)	8.55 (± 3.61)	3.79 (± 1.38)	BD	5.71 (± 4.34)
IL-4	BD	BD	BD	BD	BD	BD
IL-5	2490.33 (± 1492.86)	846.00 (± 602.44)	2929.00 (± 313.23)	2053.00 (± 1079.36)	1394.67 (± 986.09)	2786.33 (± 178.77)
IL-6	7068.67 (± 5028.98)	6212.67 (± 3448.59)	7974.33 (± 2762.77)	7267.33 (± 4588.33)	7729.33 (± 1940.69)	8717.00 (± 1750.64)
IL-7	BD	BD	BD	BD	BD	BD
IL-9	4.66 (± 2.53)	BD	14.20 (± 19.05)	BD	BD	BD
IL-10	13.96 (± 9.98)	14.93 (± 8.76)	14.35 (± 4.05)	12.30 (± 4.39)	16.98 (± 7.53)	16.36 (± 4.06)
IL-12p40	BD	BD	BD	BD	BD	BD
IL-12p70	6.27 (± 2.87)	3.92 (± 1.59)	4.88 (± 1.67)	5.55 (± 3.17)	5.85 (± 0.95)	5.78 (± 0.12)
IL-13	31.02 (± 20.80)	18.97 (± 11.75)	24.41 (± 10.22)	25.57 (± 17.67)	36.73 (± 7.69)	28.62 (± 7.96)
IL-15	3.79 (± 0.51)	BD	BD	3.30 (± 0.18)	BD	BD
IL-17	BD	3.67 (± 0.81)	3.33 (± 0.22)	BD	12.21 (± 5.08)	19.00 (± 10.26)
IP-10	1189.00 (± 862.87)	800.67 (± 334.83)	828.67 (± 202.02)	1055.33 (± 490.12)	704.00 (± 52.26)	1459.33 (± 511.86)
KC	2202.00 (± 2584.55)	1089.00 (± 415.29)	1037.33 (± 661.61)	2144.67 (± 2085.64)	2183.33 (± 706.93)	1809.00 (± 671.22)
LIF	79.60 (± 65.33)	32.50 (± 19.64)	54.34 (± 22.58)	60.52 (± 46.15)	32.90 (± 11.02)	53.54 (± 13.34)
MCP-1	3227.33 (± 2018.19)	1303.67 (± 786.34)	1685.00 (± 909.16)	2808.67 (± 1153.49)	872.67 (± 180.59)	1772.00 (± 218.63)

M-CSF	BD	BD	BD	BD	BD	BD
MIG	124.30 (± 78.80)	1982.00 (± 484.81)	297.00 (± 45.92)	99.85 (± 39.88)	7559.00[b] (± 1019.65)	1732.67 (± 980.18)
MIP-1α	34.19 (± 9.90)	18.20 (± 11.15)	24.37 (± 8.64)	34.85 (± 7.74)	16.07 (± 3.41)	29.39 (± 4.31)
MIP-1β	94.45 (± 26.82)	32.42 (± 15.69)	53.45 (± 25.14)	90.73 (± 11.05)	29.66 (± 16.52)	69.52 (± 11.99)
MIP-2	278.67 (± 155.00)	422.00 (± 134.97)	180.72 (± 87.05)	427.67 (± 206.73)	1462.67 (± 582.14)	686.00 (± 476.43)
RANTES	82.34 (± 52.90)	73.95 (± 24.44)	84.49 (± 23.50)	93.70 (± 50.31)	111.68 (± 26.61)	146.33 (± 18.34)
TNF-α	17.36 (± 4.21)	26.54 (± 1.71)	18.09 (± 3.31)	20.99 (± 5.56)	41.39[b] (± 4.48)	27.05 (± 1.92)
VEGF	294.67 (± 280.23)	258.00 (± 83.21)	260.00 (± 93.82)	253.33 (± 188.23)	516.00 (± 122.26)	340.67 (± 163.93)
LIX	579.72 (± 692.87)	195.88 (± 153.91)	291.00 (±193.12)	504.70 (± 514.62)	222.00 (± 48.54)	315.00 (± 86.56)

[a]$p<0.05$ by one-way ANOVA followed by Bonferroni comparison of means, significant compared to ΔFTL_0883 following ffSchu S4 re-stimulation by both Luminex and ELISA
[b]$p<0.05$ by one-way ANOVA followed by Bonferroni comparison of means, significant compared to ΔFTL_0883 following ffSchu S4 re-stimulation by Luminex only
[c]BD = below levels of detection

4.5 DISCUSSION

Several studies, including this one, indicate LVS poorly stimulates innate immune cells (Bosio and Dow, 2005; Carlson et al., 2007; Carlson et al., 2009; Loegering et al., 2006; Telepnev et al., 2003; Telepnev et al., 2005). This suggests insufficient activation of DCs could contribute to incomplete protection engendered by LVS. In this study, we sought to improve vaccine efficacy with a LVS strain that stimulated APCs better than wild-type LVS. The LVS mutants used in this study (Table 4) were selected based on specific characteristics. All three of these genes (FTL_1415, FTL_1664, and FTL_0883) have been identified in negative selection screens in *F. novicida* and/or LVS to be necessary for growth and/or survival in mice (Su et al., 2007; Weiss et al., 2007). The ΔcapC mutant was of interest because another LVS mutant in the capBCA operon, ΔcapB, afforded protection in BALB/c mice against challenge with the virulent

Francisella strain Schu S4 (Jia et al., 2010). Mutation of FTL_1664 in LVS resulted in diminished uptake by human DCs (Horzempa et al., 2008a), which may affect DC activation. Recently, our laboratory has shown that LVS FTL_0883 mutants like 13B47 stimulate innate immune cells and are attenuated *in vitro* and *in vivo,* making this mutant a possible vaccine candidate (Russo et al., 2011).

Strains with mutations in the FTL_0883 locus of LVS showed promise based on *in vitro* results. The 13B47 and ΔFTL_0883 derivatives of LVS stimulated human DCs and macrophages (Fig. 31, 32, and 35), which was associated with better stimulation of T cells *in vitro* (Fig. 34). Contrary to our hypothesis, however, improving APC stimulation *in vitro* with the ΔFTL_0883 strain did not enhance protection *in vivo*. The median time to death doubled in mice vaccinated in the respiratory tract with LVS compared to naïve animals. In contrast, the median time to death of mice vaccinated with ΔFTL_0883 was similar to naïve animals (Table 5). Enhancing DC stimulation with ΔFTL_0883, therefore, failed to establish a protective immune response.

The poor performance of ΔFTL_0883 as a vaccine may be due directly to its attenuation. Mutation of the FTL_0883 locus in LVS attenuates growth in macrophages and DCs (Russo et al., 2011). In addition, bacterial burdens in the lung and periphery of ΔFTL_0883-vaccinated mice are less than animals that received wild-type (Fig. 36). Based on these findings, the attenuation and accelerated clearance of ΔFTL_0883 *in vivo* may prevent a sufficient adaptive immune response from being established. Consistent with this model, restimulation of lung cells isolated from ΔFTL_0883-vaccinated mice produced less IFN-γ than mice receiving wild-type (Fig. 37A). Since IFN-γ is a critical mediator of protective immunity against tularemia (Chen et al., 2003; Elkins et al., 2010; Wayne Conlan et al., 2005), the diminished IFN-γ response we

observed following restimulation likely contributed to the lack of protection after vaccination with ΔFTL_0883.

Additional factors may also contribute to the vaccination results seen in this study. Though the molecular function of the protein encoded by FTL_0883 is unknown, it is possible that protective antigens may not be expressed since spermine responsiveness and transcription are altered after mutation of FTL_0883 (Russo et al., 2011). Alternatively, different cytokine profiles stimulated in the host by the ΔFTL_0883 mutant may influence the vaccine performance. Inflammatory signals such as IL-12 can modulate T cell differentiation, promoting the generation of more short-lived effector cells compared to memory precursors (Joshi et al., 2007). The higher levels of IL-12 stimulated by ΔFTL_0883 (Fig. 35) may have shifted T cell development, impairing the development of memory cells. Each of these possibilities is consistent with the reduced IFN-γ observed during re-stimulation of lung cells with antigen *in vitro*. The mechanism(s) accounting for the poor recall responses observed with ΔFTL_0883 is currently being investigated.

The results presented here with the FTL_0883 mutants share common outcomes with studies of other genetically altered *Francisella*. Mutation of *iglC* or *mglA*, genes important for intracellular growth of *Francisella*, or deletion of the *purMCD* purine biosynthesis operon resulted in highly attenuated strains that did not provide better protection than LVS against virulent *Francisella* challenge (Pechous et al., 2008; Twine et al., 2005; West et al., 2008). In contrast, vaccination with a Δ*clpB* mutant in the Schu S4 background is superior to wild-type LVS (Conlan et al., 2009). A greater IFN-γ response was measured four days after challenge of mice vaccinated with the more successful Δ*clpB* mutant than those vaccinated with LVS (Shen et

al., 2010). Coupled with our results, IFN-γ responses measured during restimulation could be a useful predictor of vaccine efficacy.

Several recent studies have shown that IL-17 is also required for control of *F. tularensis* growth and the generation of an effective Th1 response following pulmonary challenge (Cowley et al., 2010; Lin et al., 2009; Markel et al., 2010). Although the role of IL-17 in the immune response to acute *F. tularensis* infection has been characterized (Cowley et al., 2010; Lin et al., 2009; Markel et al., 2010), its role in vaccination against tularemia remains to be elucidated. Paranavitana *et al.* demonstrated that PBMCs from LVS-vaccinated individuals produce high levels of IL-17 following *in vitro* re-stimulation (Paranavitana et al., 2010). Similarly, we have shown that pulmonary vaccination of mice with LVS results in an increase in IL-17 compared to naïve controls (Fig. 37A). Production of IL-17, however, did not correlate with vaccine efficacy since comparable levels of IL-17 were produced by cells from mice receiving wild-type or ΔFTL_0883 vaccinations (Fig. 37A). Additionally, neutralization of IL-17 in mice successfully protected by a Schu S4 Δ*clpB* vaccine did not reduce survival after a pulmonary type A challenge despite increasing bacterial burden (Shen et al., 2010). Therefore, IL-17 alone is not sufficient to predict vaccine efficacy.

Defining an optimal strategy for vaccine development remains a significant challenge for many pathogens. Improving APC stimulation using genetic modifications of LVS in this project failed to improve protection against a virulent *F. tularensis* strain. In addition, modeling vaccination and challenge *in vitro* with human cells did not predict *in vivo* responses in mice. Comparison of different vaccine strains and the protection conferred, however, confirmed IFN-γ production as a potential correlate of protection. A similar experimental approach by Shen *et al.* successfully characterized the immune response to *Francisella* strains that varied in vaccine

efficacy (Shen et al., 2010). Nevertheless, our current study and that of Shen *et al.* are limited by the conditions tested (the number of vaccine and mouse strains used), the limited number of output variables measured (relying primarily on multiplex cytokine measurements), and the timing of sampling (responses tested after challenge *in vitro* or *in vivo*). This leaves open the possibility that more comprehensive investigations could yield additional insights. Recently, a systems-wide analysis of vaccine responses against yellow fever has met with significant success (Pulendran et al., 2010; Querec et al., 2009). In this approach, genome-wide transcriptional studies using microarrays provided a broader assessment of *in vivo* host responses to vaccination (Querec et al., 2009). A seminal application of these concepts to *Francisella* was also recently published by De Pascalis *et al.* (De Pascalis et al., 2012). Here, an *in vitro* lymphocyte-macrophage co-culture was used to model the immune responses elicited by LVS vaccines of varying efficacies (De Pascalis et al., 2012). Analysis of 84 immunologically-relevant genes by real time PCR identified a list of immune mediators whose expression pattern correlated with protection from *F. tularensis* infection, including IFN-γ (De Pascalis et al., 2012). These higher order analyses, which integrate multi-parameter data sets of a variety of measurements, combined with traditional testing of specific hypotheses could yield insight into additional correlates of protection and biological response modifiers that may be exploited during acute infection and vaccination.

5.0 SUMMARY AND DISCUSSION

The innate immune system acts as a first line of defense to limit the replication and dissemination of invading pathogens (Finlay and McFadden, 2006). By delaying the activation of the innate immune response and possessing multiple strategies to avoid host recognition, *F. tularensis* establishes a productive systemic infection resulting in significant morbidity and mortality (Cowley, 2009). Increased understanding of how *F. tularensis* circumvents innate immunity will facilitate the development of novel vaccines and therapeutics. In this thesis, we assessed the contribution of innate host defenses against *F. tularensis* in the context of acute infection and vaccination. Novel findings from this work include determining immunologic parameters of type A *F. tularensis* infection associated with mortality, the first characterization of NK cells in type A *F.tularensis* infection, and evaluation of an LVS strain that better stimulates antigen-presenting cells.

In Chapter 2, a side-by-side comparison of the early host response to an attenuated (LVS) and virulent (Schu S4) *F. tularensis* strain was conducted. A similar analysis was performed previously by Hall and colleagues (Hall et al., 2008), although only a limited number of immunological parameters and timepoints were investigated. By expanding our study to look at additional immune cell populations (NK and T cells), timepoints (two and four dpi), and soluble mediators of the host response (cytokines and chemokines), we identified several unique features of type A *F. tularensis* infection. In the lung, the growth rate of Schu S4 is faster than LVS

during the first 24 hours of infection (Fig. 7). This suggests the enhanced fitness of Schu S4 may be due to either an inherent resistance to innate host defenses or a failure to activate them. Since neither Schu S4 nor LVS elicits proinflammatory cytokine production (Fig. 14) or immune cell recruitment (Fig. 12) during the first two dpi, the latter explanation is unlikely. In support of the resistance hypothesis, Schu S4 is less susceptible to killing by ROS, RNS, and antimicrobial peptides than LVS (Lindgren et al., 2007) (Brian Russo, personal communication). Our laboratory is currently utilizing a Schu S4 mutant that is susceptible to antimicrobial peptides to investigate the role of these molecules in host defense *in vivo*.

Schu S4 also elicits a distinct cytokine and chemokine profile from LVS. Proinflammatory cytokines including IFN-γ and IL-17 are only transiently produced in Schu S4-infected mice, reaching peak levels three dpi then decreasing four dpi, while these cytokines continually increase over time in LVS-infected mice (Fig. 14 and 21). The reduction in cytokines in Schu S4-infected mice did not directly correlate with the decline in cell number since peak production was observed (Fig. 14) when viable cells were already decreasing (Fig. 10). A possible explanation for this loss in cytokines is direct suppression of their production by Schu S4. For example, Bauler *et al.* recently identified a novel Schu S4-specific immune evasion strategy involving the induction of IFN-β, which inhibits IL-12p40 production by human dendritic cells *in vitro* (Bauler et al., 2011). The effects of IFN-β on other cytokines and its role *in vivo* have yet to be determined. In addition to cytokines, Schu S4 and LVS also differ in the chemokine response elicited. High levels of numerous chemokines are produced following Schu S4, but not LVS, infection (Fig. 14). The upregulation of these analytes mimics the classic "cytokine storm" described in different models of sepsis (Sharma et al., 2011). Since the "cytokine storm" is a major contributor of disease pathogenesis in these models (Hotchkiss and

Nicholson, 2006), various therapeutics such as IL-15+IL-15Rα have been tested to limit this response (Inoue et al., 2010). In Schu S4-infected mice, IL-15+IL-15Rα treatment effectively reduces the systemic production of 12 different cytokines and chemokines (Fig. 25G and Table 3), many of which are associated with disease severity and mortality in other models of sepsis (Bozza et al., 2007; Ebong et al., 1999; Walley et al., 1997). Despite these effects of IL-15+IL-15Rα, the progression of disease remains unchanged in Schu S4-infected mice (Fig. 26 and 27). These data suggest that the cytokines and chemokines downregulated by IL-15+IL-15Rα may not contribute to morbidity from type A *F. tularensis* infection. The possibility that other inflammatory mediators not affected by this treatment, e.g. TNF-α, contribute to tularemia pathogenesis remains to be investigated. The ineffectiveness of IL-15+IL-15Rα in this model highlights the need for careful consideration when applying this treatment to sepsis of different etiologies.

Another notable feature of Schu S4 infection is the significant decline in viable lung cells four dpi (Fig. 10). Although cell death correlated with mortality in Schu S4-infected mice, we were unable to demonstrate its direct involvement with death of the host. While treatment with IL-15+IL-15Rα increased total cell numbers in the lung (Fig. 25A), it did not have the desired effect of preventing cell death during Schu S4 infection (Fig. 28). This suggests cell death in Schu S4-infected mice occurs through a novel mechanism, independent of the PUMA and Bim-mediated apoptosis observed in other models of sepsis (Inoue et al., 2010). Even though there is a high frequency of TUNEL-positive cells in Schu S4-infected mice, few caspase-3 positive cells are detected providing further support that cells are not dying through apoptosis (Bosio et al., 2007; Parmely et al., 2009). Direct infection also does not explain death of the cells since there was no detectable costaining of *Francisella* antigen and TUNEL (Fig. 15). Other possible

explanations include the release of bacterial effectors by *F. tularensis* or the induction of bystander cell death by host-produced factors. Understanding the mechanism of cell death will allow evaluation of its contribution to morbidity and mortality during type A *F. tularensis* infection.

In Chapter 2, we observed marked changes in the NK cell population following Schu S4 challenge (Fig. 12D and 13D). Previously, NK cells were shown to contribute to host defense against *F. tularensis* based on studies using the attenuated strain, LVS (Lopez et al., 2004). In addition, NK cells are required for the protective effect of CpG DNA, cationic-liposome DNA complexes, and acai polysaccharides on the type A strain Schu S4 (Elkins et al., 2009 ; Elkins et al., 1999b; Skyberg et al., 2012; Troyer et al., 2009). Based on these findings, we hypothesized NK cells would play a beneficial role in type A *F. tularensis* infection. Modulation of this cell population, however, did not have a demonstrable effect on disease progression following Schu S4 challenge (Chapter 3). This suggests NK cells are dispensable for host resistance to type A *F. tularensis* infection. A potential explanation for the divergent role of NK cells in naïve animals compared to those treated with immunostimulants is poor activation of these cells by Schu S4. Our results indicate this is unlikely since NK cells produce high levels of IFN-γ and granzyme B in naïve animals infected with Schu S4 (Fig. 21-23). Alternatively, stimulation of NK cells prior to three dpi may be essential for host resistance. These immunotherapies may also prevent NK cells from declining during Schu S4 challenge, allowing this cell population to persist in the lung and control the infection. The effects of CpG DNA, cationic-liposome DNA complexes, and acai polysaccharides on NK cell survival remains to be elucidated. The work in Chapter 3 also highlights the constraints of using LVS as a model to study *Francisella* immunology. While LVS does mimic many features of Schu S4 infection as detailed in Chapter 2, there are also distinct

differences between infections with these two strains, such as the contribution of NK cells discussed in Chapter 3. Therefore, it is important to confirm any findings in the LVS mouse model with the virulent strain.

There are also limitations to studying type A *F. tularensis* infection in mice. Mice are highly susceptible to type A *F. tularensis*, succumbing to infection within six days (Metzger et al., 2007). In contrast, pneumonic tularemia in humans can persist for several weeks or months and is not always lethal (Dennis et al., 2001). The rapid time to death in mice makes it difficult to fully characterize the innate and adaptive immune response to type A *F. tularensis*. While Schu S4 infection of other animal species like non-human primates and Fischer 344 rats better reflects human susceptibility to *F. tularensis*, there are limited tools available to study the host response of these animals (Dennis et al., 2001; Ray et al., 2010; Rick Lyons and Wu, 2007). An alternative approach is to improve upon the widely used mouse model of tularemia so it more closely mimics the course of disease in humans. By treating Schu S4-infected mice with a low dose of levofloxacin three dpi, Crane and colleagues prolonged the time to death from five days to three weeks and lowered the mortality rate from 100% to 40% in Schu S4-infected mice (Crane et al., 2012). In this new model, NK cells still declined during the first seven days of infection, as described in Chapter 2 of this thesis, but an increase in this population was observed at subsequent timepoints (Crane et al., 2012). Assessing NK cells at later stages within this model may improve our understanding of their role during infections by type A *F. tularensis*.

In Chapter 4, we further investigated the innate immune response by examining a vaccination/challenge model. We utilized a LVS mutant ΔFTL_0883 that stimulates robust proinflammatory cytokine production and costimulatory molecule expression by DCs (Fig. 35) and macrophages (Russo et al., 2011) to evaluate whether enhanced stimulation of APCs would

improve vaccine efficacy. While ΔFTL_0883 failed to elicit protection against Schu S4 challenge (Table 5), characterization of this mutant provided important knowledge about desired features of an optimal tularemia vaccine. First, protection from type A *F. tularensis* infection requires a robust IFN-γ response. LVS and ΔFTL_0883 significantly differed in their ability to induce the secretion of IFN-γ in an *ex vivo* restimulation assay (Fig. 37). The heightened IFN-γ production measured with LVS (Fig. 37) correlated with a longer median time to death following Schu S4 challenge (Table 5). Studies by Shen *et al.* and De Pascalis *et al.* further support the classification of IFN-γ as a predictor of tularemia vaccine efficacy (De Pascalis et al., 2012; Shen et al., 2010). The superior protection elicited by immunization with a Schu S4 Δ*clpB* mutant compared to LVS was associated with higher levels of IFN-γ four days after Schu S4 challenge (Shen et al., 2010). Similarly, the degree of protection provided by different LVS variants was directly proportional to the expression level of IFN-γ post vaccination (De Pascalis et al., 2012). Second, protective immunity against type A *F. tularensis* is influenced by the duration of antigen exposure. LVS and ΔFTL_0883 exhibit significant differences in bacterial growth *in vivo*. Lower levels of ΔFTL_0883 were detected at all time points in the lung and peripheral organs (Fig. 37). Additionally, ΔFTL_0883 was cleared more rapidly (~10 days) from the lung than LVS (~22 days). The sustained presence of bacteria in LVS-vaccinated mice was associated with a robust recall response and enhanced protection against Schu S4 challenge. Studies with other attenuated LVS mutants both support and contradict this finding. Similar to ΔFTL_0883, LVS Δ*purMCD* was severely attenuated for growth *in vivo* and elicited poor protection from S-chu S4 challenge (Pechous et al., 2006; Pechous et al., 2008). In contrast, mice immunized with LVS Δ*capB*, which is cleared within 10 days like ΔFTL_0883, were completely resistant to Schu S4 (Jia et al., 2010). A possible explanation for this conflicting data is the use of different mouse

models and routes of administration. Utilizing a prime-boost vaccination strategy with ΔFTL_0883 will allow evaluation of the role of additional antigen exposure in the development of adaptive immunity to *F. tularensis*.

Determining the contribution of innate host defenses in immunity to *F. tularensis* is a large problem that can only be answered with multiple experimental approaches. In this thesis, we focused on two specific aspects of the innate immune response: the role of NK cells in type A *F. tularensis* infection and the influence of APC stimulation on tularemia vaccine efficacy. Modulation of NK cells through antibody depletion or IL-15+IL-15α treatment did not alter disease progression. Similarly, activation of APCs with an immunostimulatory LVS mutant did not enhance protection from Schu S4 challenge. Overall, this body of work demonstrated that control of *F. tularensis* is not dependent on one individual aspect of the innate immune response. Thus, virulent strains of *F. tularensis* must possess a large repertoire of strategies to avoid recognition and clearance by the host. Therefore, tularemia pathogenesis would best be investigated using a combined approach of studying the specific bacterial factors involved in immune evasion and the host defenses necessary for control of *F. tularensis*.

APPENDIX A

HISTOPATHOLOGICAL CHANGES IN THE LUNG FOLLOWING TYPE A *F. TULARENSIS* INFECTION

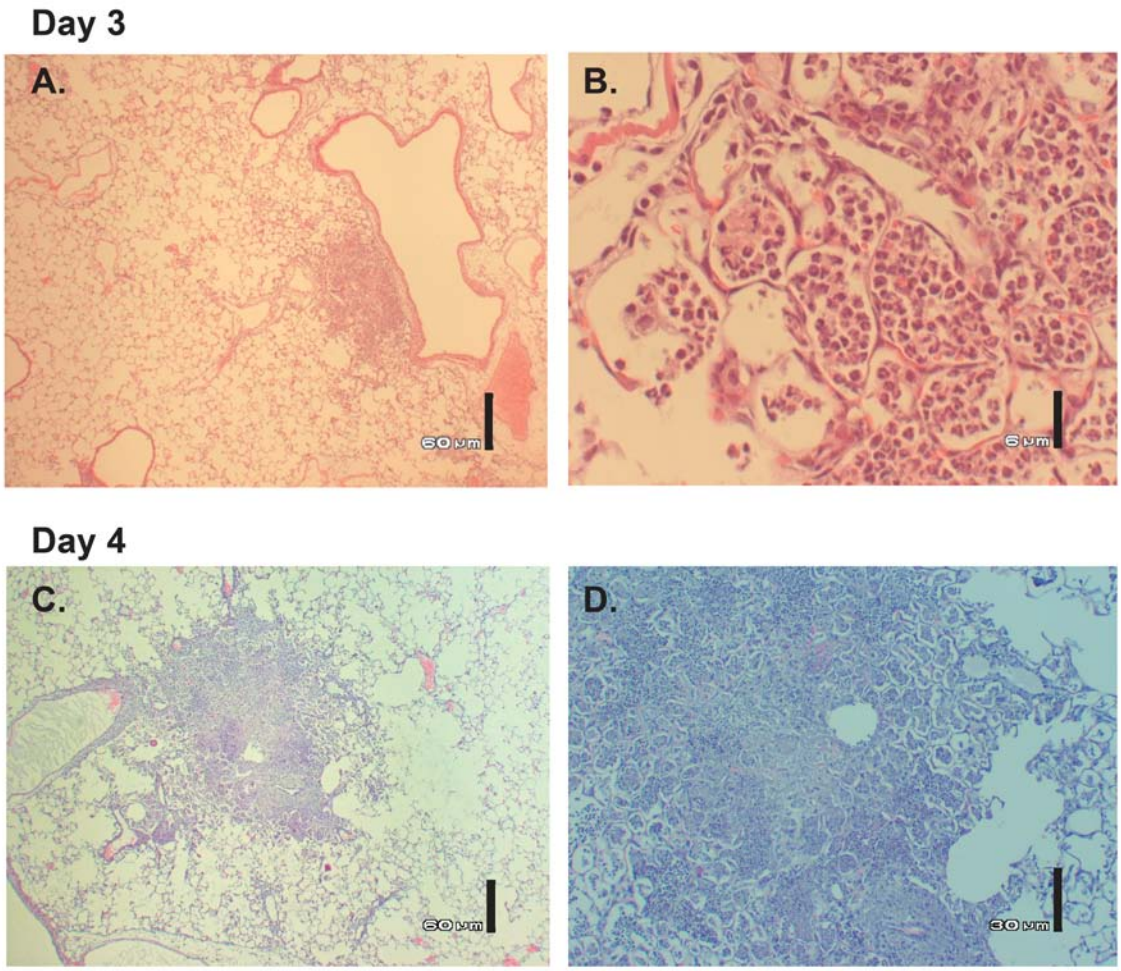

Figure 38. Histopathology of lung tissue from mice infected with the type A *F. tularensis* strain Schu S4.

C57BL/6 mice were infected intratracheally with Schu S4 (100 CFU). Three and four dpi, mice were sacrificed and lungs were fixed by inflating with 0.8 ml of 37% formalin for 5 min. Lungs were then harvested and submerged in 37% formalin for 24 hours. Fixed tissues were placed into histology cassettes and transferred to 10% formalin. Tissue sectioning and hematoxylin and eosin staining was performed by the University of Pittsburgh, School of Medicine Histology Core in the Department of Pathology Development Laboratory. Lung sections from Schu S4-infected mice three (A-B) and four dpi (C-D) showing foci of neutrophilic infiltrates within the alveolar spaces known as pyogranulomas. Scale bars represent 60 μm (A and C), 6 μm (B), and 30 μm (D).

BIBLIOGRAPHY

Abd, H., Johansson, T., Golovliov, I., Sandstrom, G., and Forsman, M. (2003). Survival and growth of *Francisella tularensis* in *Acanthamoeba castellanii*. Appl Environ Microbiol *69*, 600-606.

Abplanalp, A.L., Morris, I.R., Parida, B.K., Teale, J.M., and Berton, M.T. (2009). TLR-dependent control of *Francisella tularensis* infection and host inflammatory responses. PLoS One *4*, e7920.

Alkhuder, K., Meibom, K.L., Dubail, I., Dupuis, M., and Charbit, A. (2009). Glutathione provides a source of cysteine essential for intracellular multiplication of *Francisella tularensis*. PLoS Pathog *5*, e1000284.

Anthony, L.S., Morrissey, P.J., and Nano, F.E. (1992). Growth inhibition of *Francisella tularensis* live vaccine strain by IFN-gamma-activated macrophages is mediated by reactive nitrogen intermediates derived from L-arginine metabolism. J Immunol *148*, 1829-1834.

Apicella, M.A., Post, D.M., Fowler, A.C., Jones, B.D., Rasmussen, J.A., Hunt, J.R., Imagawa, S., Choudhury, B., Inzana, T.J., Maier, T.M., *et al.* (2010). Identification, characterization and immunogenicity of an O-antigen capsular polysaccharide of *Francisella tularensis*. PLoS One *5*, e11060.

Appelberg, R. (2007). Neutrophils and intracellular pathogens: beyond phagocytosis and killing. Trends Microbiol *15*, 87-92.

Badgwell, B., Parihar, R., Magro, C., Dierksheide, J., Russo, T., and Carson, W.E., 3rd (2002). Natural killer cells contribute to the lethality of a murine model of *Escherichia coli* infection. Surgery *132*, 205-212.

Bakshi, C.S., Malik, M., Mahawar, M., Kirimanjeswara, G.S., Hazlett, K.R., Palmer, L.E., Furie, M.B., Singh, R., Melendez, J.A., Sellati, T.J., and Metzger, D.W. (2008). An improved vaccine for prevention of respiratory tularemia caused by *Francisella tularensis* SchuS4 strain. Vaccine *26*, 5276-5288.

Balagopal, A., MacFarlane, A.S., Mohapatra, N., Soni, S., Gunn, J.S., and Schlesinger, L.S. (2006). Characterization of the receptor-ligand pathways important for entry and survival of *Francisella tularensis* in human macrophages. Infect Immun *74*, 5114-5125.

Bandara, A.B., Champion, A.E., Wang, X., Berg, G., Apicella, M.A., McLendon, M., Azadi, P., Snyder, D.S., and Inzana, T.J. (2011). Isolation and mutagenesis of a capsule-like complex (CLC) from *Francisella tularensis*, and contribution of the CLC to *F. tularensis* virulence in mice. PLoS One *6*, e19003.

Bar-Haim, E., Gat, O., Markel, G., Cohen, H., Shafferman, A., and Velan, B. (2008). Interrelationship between dendritic cell trafficking and *Francisella tularensis* dissemination following airway infection. PLoS Pathog *4*, e1000211.

Barel, M., Hovanessian, A.G., Meibom, K., Briand, J.P., Dupuis, M., and Charbit, A. (2008). A novel receptor - ligand pathway for entry of *Francisella tularensis* in monocyte-like THP-1 cells: interaction between surface nucleolin and bacterial elongation factor Tu. BMC Microbiol *8*, 145.

Barker, J.R., Chong, A., Wehrly, T.D., Yu, J.J., Rodriguez, S.A., Liu, J., Celli, J., Arulanandam, B.P., and Klose, K.E. (2009). The *Francisella tularensis* pathogenicity island encodes a secretion system that is required for phagosome escape and virulence. Mol Microbiol *74*, 1459-1470.

Baron, G.S., Myltseva, S.V., and Nano, F.E. (1995). Electroporation of *Francisella tularensis*. Methods Mol Biol *47*, 149-154.

Baron, S.D., Singh, R., and Metzger, D.W. (2007). Inactivated *Francisella tularensis* live vaccine strain protects against respiratory tularemia by intranasal vaccination in an immunoglobulin A-dependent fashion. Infect Immun *75*, 2152-2162.

Barrett, A.D., and Beasley, D.W. (2009). Development pathway for biodefense vaccines. Vaccine *27 Suppl 4*, D2-7.

Barry, E.M., Cole, L.E., and Santiago, A.E. (2009). Vaccines against tularemia. Hum Vaccin *5*, 832-838.

Bauler, T.J., Chase, J.C., and Bosio, C.M. (2011). IFN-beta mediates suppression of IL-12p40 in human dendritic cells following infection with virulent *Francisella tularensis*. J Immunol *187*, 1845-1855.

Ben Nasr, A., Haithcoat, J., Masterson, J.E., Gunn, J.S., Eaves-Pyles, T., and Klimpel, G.R. (2006). Critical role for serum opsonins and complement receptors CR3 (CD11b/CD18) and CR4 (CD11c/CD18) in phagocytosis of *Francisella tularensis* by human dendritic cells (DC): uptake of *Francisella* leads to activation of immature DC and intracellular survival of the bacteria. J Leukoc Biol *80*, 774-786.

Bitsaktsis, C., Rawool, D.B., Li, Y., Kurkure, N.V., Iglesias, B., and Gosselin, E.J. (2009). Differential requirements for protection against mucosal challenge with *Francisella tularensis* in the presence versus absence of cholera toxin B and inactivated *F. tularensis*. J Immunol *182*, 4899-4909.

Bokhari, S.M., Kim, K.J., Pinson, D.M., Slusser, J., Yeh, H.W., and Parmely, M.J. (2008). NK cells and gamma interferon coordinate the formation and function of hepatic granulomas in mice infected with the *Francisella tularensis* live vaccine strain. Infect Immun *76*, 1379-1389.

Bosio, C.M. (2011). The subversion of the immune system by *Francisella tularensis*. Front Microbiol *2*, 9.

Bosio, C.M., Bielefeldt-Ohmann, H., and Belisle, J.T. (2007). Active suppression of the pulmonary immune response by *Francisella tularensis* Schu4. J Immunol *178*, 4538-4547.

Bosio, C.M., and Dow, S.W. (2005). *Francisella tularensis* induces aberrant activation of pulmonary dendritic cells. J Immunol *175*, 6792-6801.

Bozza, F.A., Salluh, J.I., Japiassu, A.M., Soares, M., Assis, E.F., Gomes, R.N., Bozza, M.T., Castro-Faria-Neto, H.C., and Bozza, P.T. (2007). Cytokine profiles as markers of disease severity in sepsis: a multiplex analysis. Crit Care *11*, R49.

Broekhuijsen, M., Larsson, P., Johansson, A., Bystrom, M., Eriksson, U., Larsson, E., Prior, R.G., Sjostedt, A., Titball, R.W., and Forsman, M. (2003). Genome-wide DNA microarray analysis of *Francisella tularensis* strains demonstrates extensive genetic conservation within the species but identifies regions that are unique to the highly virulent *F. tularensis* subsp. *tularensis*. J Clin Microbiol *41*, 2924-2931.

Broms, J.E., Lavander, M., and Sjostedt, A. (2009). A conserved alpha-helix essential for a type VI secretion-like system of *Francisella tularensis*. J Bacteriol *191*, 2431-2446.

Broms, J.E., Sjostedt, A., and Lavander, M. (2010). The Role of the *Francisella Tularensis* Pathogenicity Island in Type VI Secretion, Intracellular Survival, and Modulation of Host Cell Signaling. Front Microbiol *1*, 136.

Brotcke, A., and Monack, D.M. (2008). Identification of fevR, a novel regulator of virulence gene expression in *Francisella novicida*. Infect Immun *76*, 3473-3480.

Brotcke, A., Weiss, D.S., Kim, C.C., Chain, P., Malfatti, S., Garcia, E., and Monack, D.M. (2006). Identification of MglA-regulated genes reveals novel virulence factors in *Francisella tularensis*. Infect Immun *74*, 6642-6655.

Buchan, B.W., McCaffrey, R.L., Lindemann, S.R., Allen, L.A., and Jones, B.D. (2009). Identification of migR, a regulatory element of the *Francisella tularensis* live vaccine strain iglABCD virulence operon required for normal replication and trafficking in macrophages. Infect Immun *77*, 2517-2529.

Bulfone-Paus, S., Ungureanu, D., Pohl, T., Lindner, G., Paus, R., Ruckert, R., Krause, H., and Kunzendorf, U. (1997). Interleukin-15 protects from lethal apoptosis *in vivo*. Nat Med *3*, 1124-1128.

Burke, D.S. (1977). Immunization against tularemia: analysis of the effectiveness of live *Francisella tularensis* vaccine in prevention of laboratory-acquired tularemia. J Infect Dis *135*, 55-60.

Carlson, P.E., Jr., Carroll, J.A., O'Dee, D.M., and Nau, G.J. (2007). Modulation of virulence factors in *Francisella tularensis* determines human macrophage responses. Microb Pathog *42*, 204-214.

Carlson, P.E., Jr., Horzempa, J., O'Dee, D.M., Robinson, C.M., Neophytou, P., Labrinidis, A., and Nau, G.J. (2009). Global transcriptional response to spermine, a component of the intramacrophage environment, reveals regulation of *Francisella* gene expression through insertion sequence elements. J Bacteriol *191*, 6855-6864.

Chakraborty, S., Monfett, M., Maier, T.M., Benach, J.L., Frank, D.W., and Thanassi, D.G. (2008). Type IV pili in *Francisella tularensis*: roles of pilF and pilT in fiber assembly, host cell adherence, and virulence. Infect Immun *76*, 2852-2861.

Chamberlain, R.E. (1965). Evaluation of Live Tularemia Vaccine Prepared in a Chemically Defined Medium. Appl Microbiol *13*, 232-235.

Chan, C.Y., St John, A.L., and Abraham, S.N. (2012). Plasticity in mast cell responses during bacterial infections. Curr Opin Microbiol *15*, 78-84.

Charity, J.C., Costante-Hamm, M.M., Balon, E.L., Boyd, D.H., Rubin, E.J., and Dove, S.L. (2007). Twin RNA polymerase-associated proteins control virulence gene expression in *Francisella tularensis*. PLoS Pathog *3*, e84.

Chase, J.C., Celli, J., and Bosio, C.M. (2009). Direct and indirect impairment of human dendritic cell function by virulent *Francisella tularensis* Schu S4. Infect Immun *77*, 180-195.

Checroun, C., Wehrly, T.D., Fischer, E.R., Hayes, S.F., and Celli, J. (2006). Autophagy-mediated reentry of *Francisella tularensis* into the endocytic compartment after cytoplasmic replication. Proc Natl Acad Sci U S A *103*, 14578-14583.

Chen, W., Kuolee, R., Austin, J.W., Shen, H., Che, Y., and Conlan, J.W. (2005). Low dose aerosol infection of mice with virulent type A *Francisella tularensis* induces severe thymus atrophy and CD4+CD8+ thymocyte depletion. Microb Pathog *39*, 189-196.

Chen, W., KuoLee, R., Shen, H., and Conlan, J.W. (2004). Susceptibility of immunodeficient mice to aerosol and systemic infection with virulent strains of *Francisella tularensis*. Microb Pathog *36*, 311-318.

Chen, W., Shen, H., Webb, A., KuoLee, R., and Conlan, J.W. (2003). Tularemia in BALB/c and C57BL/6 mice vaccinated with *Francisella tularensis* LVS and challenged intradermally, or by aerosol with virulent isolates of the pathogen: protection varies depending on pathogen virulence, route of exposure, and host genetic background. Vaccine *21*, 3690-3700.

Chiavolini, D., Weir, S., Murphy, J.R., and Wetzler, L.M. (2008). Neisseria meningitidis PorB, a Toll-like receptor 2 ligand, improves the capacity of *Francisella tularensis* lipopolysaccharide to protect mice against experimental tularemia. Clin Vaccine Immunol *15*, 1322-1329.

Child, R., Wehrly, T.D., Rockx-Brouwer, D., Dorward, D.W., and Celli, J. (2010). Acid phosphatases do not contribute to the pathogenesis of type A *Francisella tularensis*. Infect Immun *78*, 59-67.

Choi, E. (2002). Tularemia and Q fever. Med Clin North Am *86*, 393-416.

Chong, A., and Celli, J. (2010). The *Francisella* intracellular life cycle: toward molecular mechanisms of intracellular survival and proliferation. Front Microbiol *1*, 138.

Chong, A., Wehrly, T.D., Nair, V., Fischer, E.R., Barker, J.R., Klose, K.E., and Celli, J. (2008). The early phagosomal stage of *Francisella tularensis* determines optimal phagosomal escape and *Francisella* pathogenicity island protein expression. Infect Immun *76*, 5488-5499.

Christopher, G.W., Cieslak, T.J., Pavlin, J.A., and Eitzen, E.M., Jr. (1997). Biological warfare. A historical perspective. JAMA *278*, 412-417.

Clay, C.D., Soni, S., Gunn, J.S., and Schlesinger, L.S. (2008). Evasion of complement-mediated lysis and complement C3 deposition are regulated by *Francisella tularensis* lipopolysaccharide O antigen. J Immunol *181*, 5568-5578.

Clemens, D.L., Lee, B.Y., and Horwitz, M.A. (2004). Virulent and avirulent strains of *Francisella tularensis* prevent acidification and maturation of their phagosomes and escape into the cytoplasm in human macrophages. Infect Immun *72*, 3204-3217.

Clemens, D.L., Lee, B.Y., and Horwitz, M.A. (2005). *Francisella tularensis* enters macrophages via a novel process involving pseudopod loops. Infect Immun *73*, 5892-5902.

Clemens, D.L., Lee, B.Y., and Horwitz, M.A. (2009). *Francisella tularensis* phagosomal escape does not require acidification of the phagosome. Infect Immun *77*, 1757-1773.

Cole, L.E., Yang, Y., Elkins, K.L., Fernandez, E.T., Qureshi, N., Shlomchik, M.J., Herzenberg, L.A., and Vogel, S.N. (2009). Antigen-specific B-1a antibodies induced by *Francisella tularensis* LPS provide long-term protection against *F. tularensis* LVS challenge. Proc Natl Acad Sci U S A *106*, 4343-4348.

Collazo, C.M., Meierovics, A.I., De Pascalis, R., Wu, T.H., Lyons, C.R., and Elkins, K.L. (2009). T cells from lungs and livers of *Francisella tularensis*-immune mice control the growth of intracellular bacteria. Infect Immun *77*, 2010-2021.

Collazo, C.M., Sher, A., Meierovics, A.I., and Elkins, K.L. (2006). Myeloid differentiation factor-88 (MyD88) is essential for control of primary *in vivo Francisella tularensis* LVS infection, but not for control of intra-macrophage bacterial replication. Microbes Infect *8*, 779-790.

Conlan, J.W., Chen, W., Shen, H., Webb, A., and KuoLee, R. (2003). Experimental tularemia in mice challenged by aerosol or intradermally with virulent strains of *Francisella tularensis*: bacteriologic and histopathologic studies. Microb Pathog *34*, 239-248.

Conlan, J.W., KuoLee, R., Shen, H., and Webb, A. (2002). Different host defences are required to protect mice from primary systemic vs pulmonary infection with the facultative intracellular bacterial pathogen, *Francisella tularensis* LVS. Microb Pathog *32*, 127-134.

Conlan, J.W., Shen, H., Golovliov, I., Zingmark, C., Oyston, P.C., Chen, W., House, R.V., and Sjostedt, A. (2009). Differential ability of novel attenuated targeted deletion mutants of *Francisella tularensis* subspecies *tularensis* strain SCHU S4 to protect mice against aerosol challenge with virulent bacteria: Effects of host background and route of immunization. Vaccine.

Conlan, J.W., Shen, H., Golovliov, I., Zingmark, C., Oyston, P.C., Chen, W., House, R.V., and Sjostedt, A. (2010). Differential ability of novel attenuated targeted deletion mutants of *Francisella tularensis* subspecies *tularensis* strain SCHU S4 to protect mice against aerosol challenge with virulent bacteria: effects of host background and route of immunization. Vaccine *28*, 1824-1831.

Conlan, J.W., Sjostedt, A., and North, R.J. (1994). CD4+ and CD8+ T-cell-dependent and -independent host defense mechanisms can operate to control and resolve primary and secondary *Francisella tularensis* LVS infection in mice. Infect Immun *62*, 5603-5607.

Cowley, S.C. (2009). Editorial: Proinflammatory cytokines in pneumonic tularemia: too much too late? J Leukoc Biol *86*, 469-470.

Cowley, S.C., and Elkins, K.L. (2003). Multiple T cell subsets control *Francisella tularensis* LVS intracellular growth without stimulation through macrophage interferon gamma receptors. J Exp Med *198*, 379-389.

Cowley, S.C., and Elkins, K.L. (2011). Immunity to *Francisella*. Front Microbiol *2*, 26.

Cowley, S.C., Goldberg, M.F., Ho, J.A., and Elkins, K.L. (2008). The membrane form of tumor necrosis factor is sufficient to mediate partial innate immunity to *Francisella tularensis* live vaccine strain. J Infect Dis *198*, 284-292.

Cowley, S.C., Hamilton, E., Frelinger, J.A., Su, J., Forman, J., and Elkins, K.L. (2005). CD4-CD8- T cells control intracellular bacterial infections both *in vitro* and *in vivo*. J Exp Med *202*, 309-319.

Cowley, S.C., Meierovics, A.I., Frelinger, J.A., Iwakura, Y., and Elkins, K.L. (2010). Lung CD4-CD8- double-negative T cells are prominent producers of IL-17A and IFN-gamma during primary respiratory murine infection with *Francisella tularensis* live vaccine strain. J Immunol *184*, 5791-5801.

Cowley, S.C., Myltseva, S.V., and Nano, F.E. (1996). Phase variation in *Francisella tularensis* affecting intracellular growth, lipopolysaccharide antigenicity and nitric oxide production. Mol Microbiol *20*, 867-874.

Cowley, S.C., Sedgwick, J.D., and Elkins, K.L. (2007). Differential requirements by CD4+ and CD8+ T cells for soluble and membrane TNF in control of *Francisella tularensis* live vaccine strain intramacrophage growth. J Immunol *179*, 7709-7719.

Crane, D.D., Scott, D.P., and Bosio, C.M. (2012). Generation of a convalescent model of virulent *Francisella tularensis* infection for assessment of host requirements for survival of tularemia. PLoS One *7*, e33349.

Dai, S., Mohapatra, N.P., Schlesinger, L.S., and Gunn, J.S. (2010). Regulation of *Francisella tularensis* virulence. Front Microbiol *1*, 144.

de Bruin, O.M., Ludu, J.S., and Nano, F.E. (2007). The *Francisella* pathogenicity island protein IglA localizes to the bacterial cytoplasm and is needed for intracellular growth. BMC Microbiol *7*, 1.

De Pascalis, R., Chou, A.Y., Bosio, C.M., Huang, C.Y., Follmann, D.A., and Elkins, K.L. (2012). Development of functional and molecular correlates of vaccine-induced protection for a model intracellular pathogen, *F. tularensis* LVS. PLoS Pathog *8*, e1002494.

Deng, K., Blick, R.J., Liu, W., and Hansen, E.J. (2006). Identification of *Francisella tularensis* genes affected by iron limitation. Infect Immun *74*, 4224-4236.

Dennis, D.T., Inglesby, T.V., Henderson, D.A., Bartlett, J.G., Ascher, M.S., Eitzen, E., Fine, A.D., Friedlander, A.M., Hauer, J., Layton, M., *et al.* (2001). Tularemia as a biological weapon: medical and public health management. JAMA *285*, 2763-2773.

Di Santo, E., Meazza, C., Sironi, M., Fruscella, P., Mantovani, A., Sipe, J.D., and Ghezzi, P. (1997). IL-13 inhibits TNF production but potentiates that of IL-6 *in vivo* and *ex vivo* in mice. J Immunol *159*, 379-382.

Drabick, J.J., Narayanan, R.B., Williams, J.C., Leduc, J.W., and Nacy, C.A. (1994). Passive protection of mice against lethal *Francisella tularensis* (live tularemia vaccine strain) infection by the sera of human recipients of the live tularemia vaccine. Am J Med Sci *308*, 83-87.

Duckett, N.S., Olmos, S., Durrant, D.M., and Metzger, D.W. (2005). Intranasal interleukin-12 treatment for protection against respiratory infection with the *Francisella tularensis* live vaccine strain. Infect Immun *73*, 2306-2311.

Ebong, S., Call, D., Nemzek, J., Bolgos, G., Newcomb, D., and Remick, D. (1999). Immunopathologic alterations in murine models of sepsis of increasing severity. Infect Immun *67*, 6603-6610.

Eigelsbach, H.T., and Downs, C.M. (1961). Prophylactic effectiveness of live and killed tularemia vaccines. I. Production of vaccine and evaluation in the white mouse and guinea pig. J Immunol *87*, 415-425.

El Sahly, H.M., Atmar, R.L., Patel, S.M., Wells, J.M., Cate, T., Ho, M., Guo, K., Pasetti, M.F., Lewis, D.E., Sztein, M.B., and Keitel, W.A. (2009). Safety, reactogenicity and immunogenicity of *Francisella tularensis* live vaccine strain in humans. Vaccine *27*, 4905-4911.

Elkins, K.L., Bosio, C.M., and Rhinehart-Jones, T.R. (1999a). Importance of B cells, but not specific antibodies, in primary and secondary protective immunity to the intracellular bacterium *Francisella tularensis* live vaccine strain. Infect Immun *67*, 6002-6007.

Elkins, K.L., Colombini, S.M., Krieg, A.M., and De Pascalis, R. (2009). NK cells activated *in vivo* by bacterial DNA control the intracellular growth of *Francisella tularensis* LVS. Microbes Infect *11*, 49-56.

Elkins, K.L., Colombini, S.M., Meierovics, A.I., Chu, M.C., Chou, A.Y., and Cowley, S.C. (2010). Survival of secondary lethal systemic *Francisella* LVS challenge depends largely on interferon gamma. Microbes Infect *12*, 28-36.

Elkins, K.L., Cooper, A., Colombini, S.M., Cowley, S.C., and Kieffer, T.L. (2002). *In vivo* clearance of an intracellular bacterium, *Francisella tularensis* LVS, is dependent on the p40 subunit of interleukin-12 (IL-12) but not on IL-12 p70. Infect Immun *70*, 1936-1948.

Elkins, K.L., Cowley, S.C., and Bosio, C.M. (2007). Innate and adaptive immunity to *Francisella*. Ann N Y Acad Sci *1105*, 284-324.

Elkins, K.L., Rhinehart-Jones, T., Nacy, C.A., Winegar, R.K., and Fortier, A.H. (1993). T-cell-independent resistance to infection and generation of immunity to *Francisella tularensis*. Infect Immun *61*, 823-829.

Elkins, K.L., Rhinehart-Jones, T.R., Culkin, S.J., Yee, D., and Winegar, R.K. (1996). Minimal requirements for murine resistance to infection with *Francisella tularensis* LVS. Infect Immun *64*, 3288-3293.

Elkins, K.L., Rhinehart-Jones, T.R., Stibitz, S., Conover, J.S., and Klinman, D.M. (1999b). Bacterial DNA containing CpG motifs stimulates lymphocyte-dependent protection of mice against lethal infection with intracellular bacteria. J Immunol *162*, 2291-2298.

Ericsson, M., Tarnvik, A., Kuoppa, K., Sandstrom, G., and Sjostedt, A. (1994). Increased synthesis of DnaK, GroEL, and GroES homologs by *Francisella tularensis* LVS in response to heat and hydrogen peroxide. Infect Immun *62*, 178-183.

Evans, S.E., Scott, B.L., Clement, C.G., Larson, D.T., Kontoyiannis, D., Lewis, R.E., Lasala, P.R., Pawlik, J., Peterson, J.W., Chopra, A.K., *et al.* (2010). Stimulated innate resistance of lung epithelium protects mice broadly against bacteria and fungi. Am J Respir Cell Mol Biol *42*, 40-50.

Eyles, J.E., Hartley, M.G., Laws, T.R., Oyston, P.C., Griffin, K.F., and Titball, R.W. (2008). Protection afforded against aerosol challenge by systemic immunisation with inactivated *Francisella tularensis* live vaccine strain (LVS). Microb Pathog *44*, 164-168.

Feldman, K.A., Enscore, R.E., Lathrop, S.L., Matyas, B.T., McGuill, M., Schriefer, M.E., Stiles-Enos, D., Dennis, D.T., Petersen, L.R., and Hayes, E.B. (2001). An outbreak of primary pneumonic tularemia on Martha's Vineyard. N Engl J Med *345*, 1601-1606.

Feng, C.G., Kaviratne, M., Rothfuchs, A.G., Cheever, A., Hieny, S., Young, H.A., Wynn, T.A., and Sher, A. (2006). NK cell-derived IFN-gamma differentially regulates innate resistance and neutrophil response in T cell-deficient hosts infected with *Mycobacterium tuberculosis*. J Immunol *177*, 7086-7093.

Finlay, B.B., and McFadden, G. (2006). Anti-immunology: evasion of the host immune system by bacterial and viral pathogens. Cell *124*, 767-782.

Forsberg, A., and Guina, T. (2007). Type II secretion and type IV pili of *Francisella*. Ann N Y Acad Sci *1105*, 187-201.

Forslund, A.L., Kuoppa, K., Svensson, K., Salomonsson, E., Johansson, A., Bystrom, M., Oyston, P.C., Michell, S.L., Titball, R.W., Noppa, L., *et al.* (2006). Direct repeat-mediated deletion of a type IV pilin gene results in major virulence attenuation of *Francisella tularensis*. Mol Microbiol *59*, 1818-1830.

Forslund, A.L., Salomonsson, E.N., Golovliov, I., Kuoppa, K., Michell, S., Titball, R., Oyston, P., Noppa, L., Sjostedt, A., and Forsberg, A. (2010). The type IV pilin, PilA, is required for full virulence of *Francisella tularensis* subspecies *tularensis*. BMC Microbiol *10*, 227.

Fortier, A.H., Polsinelli, T., Green, S.J., and Nacy, C.A. (1992). Activation of macrophages for destruction of *Francisella tularensis*: identification of cytokines, effector cells, and effector molecules. Infect Immun *60*, 817-825.

Fortier, A.H., Slayter, M.V., Ziemba, R., Meltzer, M.S., and Nacy, C.A. (1991). Live vaccine strain of *Francisella tularensis*: infection and immunity in mice. Infect Immun *59*, 2922-2928.

Foshay, L. (1950). Tularemia. Annu Rev Microbiol *4*, 313-330.

Foshay, L., Hesselbrock, W.H., Wittenberg, H.J., and Rodenberg, A.H. (1942). Vaccine Prophylaxis against Tularemia in Man. Am J Public Health Nations Health *32*, 1131-1145.

Francis, E. (1925). Tularemia. JAMA *84*, 1243-1250.

Francis, E. (1928). A Summary of Present Knowledge of Tularaemia. Medicine *7*, 411-432.

Frazer, L.C., O'Connell, C.M., Andrews, C.W., Jr., Zurenski, M.A., and Darville, T. (2011). Enhanced neutrophil longevity and recruitment contribute to the severity of oviduct pathology during *Chlamydia muridarum* infection. Infect Immun *79*, 4029-4041.

Fulop, M., Manchee, R., and Titball, R. (1995). Role of lipopolysaccharide and a major outer membrane protein from *Francisella tularensis* in the induction of immunity against tularemia. Vaccine *13*, 1220-1225.

Fulop, M., Mastroeni, P., Green, M., and Titball, R.W. (2001). Role of antibody to lipopolysaccharide in protection against low- and high-virulence strains of *Francisella tularensis*. Vaccine *19*, 4465-4472.

Gil, H., Benach, J.L., and Thanassi, D.G. (2004). Presence of pili on the surface of *Francisella tularensis*. Infect Immun *72*, 3042-3047.

Gil, H., Platz, G.J., Forestal, C.A., Monfett, M., Bakshi, C.S., Sellati, T.J., Furie, M.B., Benach, J.L., and Thanassi, D.G. (2006). Deletion of TolC orthologs in *Francisella tularensis* identifies roles in multidrug resistance and virulence. Proc Natl Acad Sci U S A *103*, 12897-12902.

Golovliov, I., Baranov, V., Krocova, Z., Kovarova, H., and Sjostedt, A. (2003). An attenuated strain of the facultative intracellular bacterium *Francisella tularensis* can escape the phagosome of monocytic cells. Infect Immun *71*, 5940-5950.

Golovliov, I., Ericsson, M., Akerblom, L., Sandstrom, G., Tarnvik, A., and Sjostedt, A. (1995). Adjuvanticity of ISCOMs incorporating a T cell-reactive lipoprotein of the facultative intracellular pathogen *Francisella tularensis*. Vaccine *13*, 261-267.

Golovliov, I., Ericsson, M., Sandstrom, G., Tarnvik, A., and Sjostedt, A. (1997). Identification of proteins of *Francisella tularensis* induced during growth in macrophages and cloning of the gene encoding a prominently induced 23-kilodalton protein. Infect Immun *65*, 2183-2189.

Gueders, M.M., Paulissen, G., Crahay, C., Quesada-Calvo, F., Hacha, J., Van Hove, C., Tournoy, K., Louis, R., Foidart, J.M., Noel, A., and Cataldo, D.D. (2009). Mouse models of asthma: a comparison between C57BL/6 and BALB/c strains regarding bronchial responsiveness, inflammation, and cytokine production. Inflamm Res *58*, 845-854.

Gunn, J.S., and Ernst, R.K. (2007). The structure and function of *Francisella* lipopolysaccharide. Ann N Y Acad Sci *1105*, 202-218.

Hager, A.J., Bolton, D.L., Pelletier, M.R., Brittnacher, M.J., Gallagher, L.A., Kaul, R., Skerrett, S.J., Miller, S.I., and Guina, T. (2006). Type IV pili-mediated secretion modulates *Francisella* virulence. Mol Microbiol *62*, 227-237.

Hall, J.D., Craven, R.R., Fuller, J.R., Pickles, R.J., and Kawula, T.H. (2007). *Francisella tularensis* replicates within alveolar type II epithelial cells *in vitro* and *in vivo* following inhalation. Infect Immun *75*, 1034-1039.

Hall, J.D., Kurtz, S.L., Rigel, N.W., Gunn, B.M., Taft-Benz, S., Morrison, J.P., Fong, A.M., Patel, D.D., Braunstein, M., and Kawula, T.H. (2009). The impact of chemokine receptor CX3CR1 deficiency during respiratory infections with Mycobacterium tuberculosis or *Francisella tularensis*. Clin Exp Immunol *156*, 278-284.

Hall, J.D., Woolard, M.D., Gunn, B.M., Craven, R.R., Taft-Benz, S., Frelinger, J.A., and Kawula, T.H. (2008). Infected-host-cell repertoire and cellular response in the lung following inhalation of *Francisella tularensis* Schu S4, LVS, or U112. Infect Immun *76*, 5843-5852.

Hall, L.J., Clare, S., and Dougan, G. (2010). NK cells influence both innate and adaptive immune responses after mucosal immunization with antigen and mucosal adjuvant. J Immunol *184*, 4327-4337.

Hazlett, K.R., Caldon, S.D., McArthur, D.G., Cirillo, K.A., Kirimanjeswara, G.S., Magguilli, M.L., Malik, M., Shah, A., Broderick, S., Golovliov, I., *et al.* (2008). Adaptation of *Francisella tularensis* to the mammalian environment is governed by cues which can be mimicked *in vitro*. Infect Immun *76*, 4479-4488.

Henry, T., Kirimanjeswara, G.S., Ruby, T., Jones, J.W., Peng, K., Perret, M., Ho, L., Sauer, J.D., Iwakura, Y., Metzger, D.W., and Monack, D.M. (2010). Type I IFN signaling constrains IL-17A/F secretion by gammadelta T cells during bacterial infections. J Immunol *184*, 3755-3767.

Hinman, A.R. (1998). Global progress in infectious disease control. Vaccine *16*, 1116-1121.

Hood, A.M. (1977). Virulence factors of *Francisella tularensis*. J Hyg (Lond) *79*, 47-60.

Hornick, R.B., and Eigelsbach, H.T. (1966). Aerogenic immunization of man with live Tularemia vaccine. Bacteriol Rev *30*, 532-538.

Horzempa, J., Carlson, P.E., Jr., O'Dee, D.M., Shanks, R.M., and Nau, G.J. (2008a). Global transcriptional response to mammalian temperature provides new insight into *Francisella tularensis* pathogenesis. BMC Microbiol *8*, 172.

Horzempa, J., O'Dee, D.M., Shanks, R.M., and Nau, G.J. (2010). *Francisella tularensis* DeltapyrF mutants show that replication in nonmacrophages is sufficient for pathogenesis *in vivo*. Infect Immun *78*, 2607-2619.

Horzempa, J., Tarwacki, D.M., Carlson, P.E., Jr., Robinson, C.M., and Nau, G.J. (2008b). Characterization and application of a glucose-repressible promoter in *Francisella tularensis*. Appl Environ Microbiol *74*, 2161-2170.

Hotchkiss, R.S., Coopersmith, C.M., and Karl, I.E. (2005). Prevention of lymphocyte apoptosis--a potential treatment of sepsis? Clin Infect Dis *41 Suppl 7*, S465-469.

Hotchkiss, R.S., and Karl, I.E. (2003). The pathophysiology and treatment of sepsis. N Engl J Med *348*, 138-150.

Hotchkiss, R.S., and Nicholson, D.W. (2006). Apoptosis and caspases regulate death and inflammation in sepsis. Nat Rev Immunol *6*, 813-822.

Huntley, J.F., Conley, P.G., Rasko, D.A., Hagman, K.E., Apicella, M.A., and Norgard, M.V. (2008). Native outer membrane proteins protect mice against pulmonary challenge with virulent type A *Francisella tularensis*. Infect Immun *76*, 3664-3671.

Inoue, S., Unsinger, J., Davis, C.G., Muenzer, J.T., Ferguson, T.A., Chang, K., Osborne, D.F., Clark, A.T., Coopersmith, C.M., McDunn, J.E., and Hotchkiss, R.S. (2010). IL-15 prevents apoptosis, reverses innate and adaptive immune dysfunction, and improves survival in sepsis. J Immunol *184*, 1401-1409.

Jia, Q., Lee, B.Y., Bowen, R., Dillon, B.J., Som, S.M., and Horwitz, M.A. (2010). A *Francisella tularensis* live vaccine strain (LVS) mutant with a deletion in capB, encoding a putative capsular

biosynthesis protein, is significantly more attenuated than LVS yet induces potent protective immunity in mice against *F. tularensis* challenge. Infect Immun *78*, 4341-4355.

Jia, Q., Lee, B.Y., Clemens, D.L., Bowen, R.A., and Horwitz, M.A. (2009). Recombinant attenuated *Listeria monocytogenes* vaccine expressing *Francisella tularensis* IglC induces protection in mice against aerosolized Type A *F. tularensis*. Vaccine *27*, 1216-1229.

Joshi, N.S., Cui, W., Chandele, A., Lee, H.K., Urso, D.R., Hagman, J., Gapin, L., and Kaech, S.M. (2007). Inflammation directs memory precursor and short-lived effector CD8(+) T cell fates via the graded expression of T-bet transcription factor. Immunity *27*, 281-295.

Kadull, P.J., Reames, H.R., Coriell, L.L., and Foshay, L. (1950). Studies on tularemia. V. Immunization of man. J Immunol *65*, 425-435.

Karttunen, R., Surcel, H.M., Andersson, G., Ekre, H.P., and Herva, E. (1991). *Francisella tularensis*-induced *in vitro* gamma interferon, tumor necrosis factor alpha, and interleukin 2 responses appear within 2 weeks of tularemia vaccination in human beings. J Clin Microbiol *29*, 753-756.

Katz, J., Zhang, P., Martin, M., Vogel, S.N., and Michalek, S.M. (2006). Toll-like receptor 2 is required for inflammatory responses to *Francisella tularensis* LVS. Infect Immun *74*, 2809-2816.

Keim, P., Johansson, A., and Wagner, D.M. (2007). Molecular epidemiology, evolution, and ecology of *Francisella*. Ann N Y Acad Sci *1105*, 30-66.

Ketavarapu, J.M., Rodriguez, A.R., Yu, J.J., Cong, Y., Murthy, A.K., Forsthuber, T.G., Guentzel, M.N., Klose, K.E., Berton, M.T., and Arulanandam, B.P. (2008). Mast cells inhibit intramacrophage *Francisella tularensis* replication via contact and secreted products including IL-4. Proc Natl Acad Sci U S A *105*, 9313-9318.

Kim, T.H., Pinkham, J.T., Heninger, S.J., Chalabaev, S., and Kasper, D.L. (2012). Genetic modification of the O-polysaccharide of *Francisella tularensis* results in an avirulent live attenuated vaccine. J Infect Dis *205*, 1056-1065.

Kirimanjeswara, G.S., Golden, J.M., Bakshi, C.S., and Metzger, D.W. (2007). Prophylactic and therapeutic use of antibodies for protection against respiratory infection with *Francisella tularensis*. J Immunol *179*, 532-539.

Koskela, P., and Herva, E. (1982). Cell-mediated and humoral immunity induced by a live *Francisella tularensis* vaccine. Infect Immun *36*, 983-989.

Koskela, P., and Salminen, A. (1985). Humoral immunity against *Francisella tularensis* after natural infection. J Clin Microbiol *22*, 973-979.

Krocova, Z., Hartlova, A., Souckova, D., Zivna, L., Kroca, M., Rudolf, E., Macela, A., and Stulik, J. (2008). Interaction of B cells with intracellular pathogen *Francisella tularensis*. Microb Pathog *45*, 79-85.

KuoLee, R., Harris, G., Conlan, J.W., and Chen, W. (2011). Role of neutrophils and NADPH phagocyte oxidase in host defense against respiratory infection with virulent *Francisella tularensis* in mice. Microbes Infect *13*, 447-456.

Kuroda, E., Kito, T., and Yamashita, U. (2002). Reduced expression of STAT4 and IFN-gamma in macrophages from BALB/c mice. J Immunol *168*, 5477-5482.

Kuroda, E., and Yamashita, U. (2003). Mechanisms of enhanced macrophage-mediated prostaglandin E2 production and its suppressive role in Th1 activation in Th2-dominant BALB/c mice. J Immunol *170*, 757-764.

Lai, X.H., Golovliov, I., and Sjostedt, A. (2001). *Francisella tularensis* induces cytopathogenicity and apoptosis in murine macrophages via a mechanism that requires intracellular bacterial multiplication. Infect Immun *69*, 4691-4694.

Lai, X.H., Golovliov, I., and Sjostedt, A. (2004). Expression of IglC is necessary for intracellular growth and induction of apoptosis in murine macrophages by *Francisella tularensis*. Microb Pathog *37*, 225-230.

Lai, X.H., and Sjostedt, A. (2003). Delineation of the molecular mechanisms of *Francisella tularensis*-induced apoptosis in murine macrophages. Infect Immun *71*, 4642-4646.

Lambrecht, B.N., Prins, J.B., and Hoogsteden, H.C. (2001). Lung dendritic cells and host immunity to infection. Eur Respir J *18*, 692-704.

Larsson, P., Oyston, P.C., Chain, P., Chu, M.C., Duffield, M., Fuxelius, H.H., Garcia, E., Halltorp, G., Johansson, D., Isherwood, K.E., *et al.* (2005). The complete genome sequence of *Francisella tularensis*, the causative agent of tularemia. Nat Genet *37*, 153-159.

Lauriano, C.M., Barker, J.R., Yoon, S.S., Nano, F.E., Arulanandam, B.P., Hassett, D.J., and Klose, K.E. (2004). MglA regulates transcription of virulence factors necessary for *Francisella tularensis* intraamoebae and intramacrophage survival. Proc Natl Acad Sci U S A *101*, 4246-4249.

Lavine, C.L., Clinton, S.R., Angelova-Fischer, I., Marion, T.N., Bina, X.R., Bina, J.E., Whitt, M.A., and Miller, M.A. (2007). Immunization with heat-killed *Francisella tularensis* LVS elicits protective antibody-mediated immunity. Eur J Immunol *37*, 3007-3020.

Le-Barillec, K., Magalhaes, J.G., Corcuff, E., Thuizat, A., Sansonetti, P.J., Phalipon, A., and Di Santo, J.P. (2005). Roles for T and NK cells in the innate immune response to *Shigella flexneri*. J Immunol *175*, 1735-1740.

Le Nouen, C., Hillyer, P., Munir, S., Winter, C.C., McCarty, T., Bukreyev, A., Collins, P.L., Rabin, R.L., and Buchholz, U.J. (2010). Effects of human respiratory syncytial virus, metapneumovirus, parainfluenza virus 3 and influenza virus on CD4+ T cell activation by dendritic cells. PLoS One *5*, e15017.

Lee, B.Y., Horwitz, M.A., and Clemens, D.L. (2006). Identification, recombinant expression, immunolocalization in macrophages, and T-cell responsiveness of the major extracellular proteins of *Francisella tularensis*. Infect Immun *74*, 4002-4013.

Lee, U., Santa, K., Habu, S., and Nishimura, T. (1996). Murine asialo GM1+CD8+ T cells as novel interleukin-12-responsive killer T cell precursors. Jpn J Cancer Res *87*, 429-432.

Leiby, D.A., Fortier, A.H., Crawford, R.M., Schreiber, R.D., and Nacy, C.A. (1992). *In vivo* modulation of the murine immune response to *Francisella tularensis* LVS by administration of anticytokine antibodies. Infect Immun *60*, 84-89.

Lembo, A., Pelletier, M., Iyer, R., Timko, M., Dudda, J.C., West, T.E., Wilson, C.B., Hajjar, A.M., and Skerrett, S.J. (2008). Administration of a synthetic TLR4 agonist protects mice from pneumonic tularemia. J Immunol *180*, 7574-7581.

Lenco, J., Hubalek, M., Larsson, P., Fucikova, A., Brychta, M., Macela, A., and Stulik, J. (2007). Proteomics analysis of the *Francisella tularensis* LVS response to iron restriction: induction of the *F. tularensis* pathogenicity island proteins IglABC. FEMS Microbiol Lett *269*, 11-21.

Lenco, J., Pavkova, I., Hubalek, M., and Stulik, J. (2005). Insights into the oxidative stress response in *Francisella tularensis* LVS and its mutant DeltaiglC1+2 by proteomics analysis. FEMS Microbiol Lett *246*, 47-54.

Lin, Y., Ritchea, S., Logar, A., Slight, S., Messmer, M., Rangel-Moreno, J., Guglani, L., Alcorn, J.F., Strawbridge, H., Park, S.M., *et al.* (2009). Interleukin-17 is required for T helper 1 cell immunity and host resistance to the intracellular pathogen *Francisella tularensis*. Immunity *31*, 799-810.

Lindemann, S.R., Peng, K., Long, M.E., Hunt, J.R., Apicella, M.A., Monack, D.M., Allen, L.A., and Jones, B.D. (2011). *Francisella tularensis* Schu S4 O-antigen and capsule biosynthesis gene mutants induce early cell death in human macrophages. Infect Immun *79*, 581-594.

Lindgren, H., Golovliov, I., Baranov, V., Ernst, R.K., Telepnev, M., and Sjostedt, A. (2004a). Factors affecting the escape of *Francisella tularensis* from the phagolysosome. J Med Microbiol *53*, 953-958.

Lindgren, H., Shen, H., Zingmark, C., Golovliov, I., Conlan, W., and Sjostedt, A. (2007). Resistance of *Francisella tularensis* strains against reactive nitrogen and oxygen species with special reference to the role of KatG. Infect Immun *75*, 1303-1309.

Lindgren, H., Stenman, L., Tarnvik, A., and Sjostedt, A. (2005). The contribution of reactive nitrogen and oxygen species to the killing of *Francisella tularensis* LVS by murine macrophages. Microbes Infect *7*, 467-475.

Lindgren, H., Stenmark, S., Chen, W., Tarnvik, A., and Sjostedt, A. (2004b). Distinct roles of reactive nitrogen and oxygen species to control infection with the facultative intracellular bacterium *Francisella tularensis*. Infect Immun *72*, 7172-7182.

Loegering, D.J., Drake, J.R., Banas, J.A., McNealy, T.L., Mc Arthur, D.G., Webster, L.M., and Lennartz, M.R. (2006). *Francisella tularensis* LVS grown in macrophages has reduced ability to stimulate the secretion of inflammatory cytokines by macrophages *in vitro*. Microb Pathog *41*, 218-225.

Lopez, M.C., Duckett, N.S., Baron, S.D., and Metzger, D.W. (2004). Early activation of NK cells after lung infection with the intracellular bacterium, *Francisella tularensis* LVS. Cell Immunol *232*, 75-85.

Lu, Z., Madico, G., Roche, M.I., Wang, Q., Hui, J.H., Perkins, H.M., Zaia, J., Costello, C.E., and Sharon, J. (2012). Protective B cell epitopes of *Francisella tularensis* O-polysaccharide in a mouse model of respiratory tularemia. Immunology.

Ludu, J.S., de Bruin, O.M., Duplantis, B.N., Schmerk, C.L., Chou, A.Y., Elkins, K.L., and Nano, F.E. (2008). The *Francisella* pathogenicity island protein PdpD is required for full virulence and associates with homologues of the type VI secretion system. J Bacteriol *190*, 4584-4595.

Mahawar, M., Kirimanjeswara, G.S., Metzger, D.W., and Bakshi, C.S. (2009). Contribution of citrulline ureidase to *Francisella tularensis* strain Schu S4 pathogenesis. J Bacteriol *191*, 4798-4806.

Malik, M., Bakshi, C.S., McCabe, K., Catlett, S.V., Shah, A., Singh, R., Jackson, P.L., Gaggar, A., Metzger, D.W., Melendez, J.A., *et al.* (2007). Matrix metalloproteinase 9 activity enhances host susceptibility to pulmonary infection with type A and B strains of *Francisella tularensis*. J Immunol *178*, 1013-1020.

Malik, M., Bakshi, C.S., Sahay, B., Shah, A., Lotz, S.A., and Sellati, T.J. (2006). Toll-like receptor 2 is required for control of pulmonary infection with *Francisella tularensis*. Infect Immun *74*, 3657-3662.

Mares, C.A., Ojeda, S.S., Morris, E.G., Li, Q., and Teale, J.M. (2008). Initial delay in the immune response to *Francisella tularensis* is followed by hypercytokinemia characteristic of severe sepsis and correlating with upregulation and release of damage-associated molecular patterns. Infect Immun *76*, 3001-3010.

Mariathasan, S., Weiss, D.S., Dixit, V.M., and Monack, D.M. (2005). Innate immunity against *Francisella tularensis* is dependent on the ASC/caspase-1 axis. J Exp Med *202*, 1043-1049.

Markel, G., Bar-Haim, E., Zahavy, E., Cohen, H., Cohen, O., Shafferman, A., and Velan, B. (2010). The involvement of IL-17A in the murine response to sub-lethal inhalational infection with *Francisella tularensis*. PLoS One *5*, e11176.

McCaffrey, R.L., and Allen, L.A. (2006). *Francisella tularensis* LVS evades killing by human neutrophils via inhibition of the respiratory burst and phagosome escape. J Leukoc Biol *80*, 1224-1230.

McCaffrey, R.L., Schwartz, J.T., Lindemann, S.R., Moreland, J.G., Buchan, B.W., Jones, B.D., and Allen, L.A. (2010). Multiple mechanisms of NADPH oxidase inhibition by type A and type B *Francisella tularensis*. J Leukoc Biol *88*, 791-805.

McCrumb, F.R. (1961). Aerosol Infection of Man with *Pasteurella Tularensis*. Bacteriol Rev *25*, 262-267.

McLendon, M.K., Apicella, M.A., and Allen, L.A. (2006). *Francisella tularensis*: taxonomy, genetics, and Immunopathogenesis of a potential agent of biowarfare. Annu Rev Microbiol *60*, 167-185.

Meibom, K.L., Forslund, A.L., Kuoppa, K., Alkhuder, K., Dubail, I., Dupuis, M., Forsberg, A., and Charbit, A. (2009). Hfq, a novel pleiotropic regulator of virulence-associated genes in *Francisella tularensis*. Infect Immun *77*, 1866-1880.

Metzger, D.W., Bakshi, C.S., and Kirimanjeswara, G. (2007). Mucosal immunopathogenesis of *Francisella tularensis*. Ann N Y Acad Sci *1105*, 266-283.

Michell, S.L., Dean, R.E., Eyles, J.E., Hartley, M.G., Waters, E., Prior, J.L., Titball, R.W., and Oyston, P.C. (2010). Deletion of the Bacillus anthracis capB homologue in *Francisella tularensis* subspecies *tularensis* generates an attenuated strain that protects mice against virulent tularaemia. J Med Microbiol *59*, 1275-1284.

Mills, C.D., Kincaid, K., Alt, J.M., Heilman, M.J., and Hill, A.M. (2000). M-1/M-2 macrophages and the Th1/Th2 paradigm. J Immunol *164*, 6166-6173.

Mohapatra, N.P., Soni, S., Bell, B.L., Warren, R., Ernst, R.K., Muszynski, A., Carlson, R.W., and Gunn, J.S. (2007). Identification of an orphan response regulator required for the virulence of *Francisella* spp. and transcription of pathogenicity island genes. Infect Immun *75*, 3305-3314.

Mohapatra, N.P., Soni, S., Reilly, T.J., Liu, J., Klose, K.E., and Gunn, J.S. (2008). Combined deletion of four *Francisella novicida* acid phosphatases attenuates virulence and macrophage vacuolar escape. Infect Immun *76*, 3690-3699.

Molins, C.R., Delorey, M.J., Yockey, B.M., Young, J.W., Sheldon, S.W., Reese, S.M., Schriefer, M.E., and Petersen, J.M. (2010). Virulence differences among *Francisella tularensis* subsp. *tularensis* clades in mice. PLoS One *5*, e10205.

Munir, S., Hillyer, P., Le Nouen, C., Buchholz, U.J., Rabin, R.L., Collins, P.L., and Bukreyev, A. (2011). Respiratory syncytial virus interferon antagonist NS1 protein suppresses and skews the human T lymphocyte response. PLoS Pathog *7*, e1001336.

Nano, F.E., Zhang, N., Cowley, S.C., Klose, K.E., Cheung, K.K., Roberts, M.J., Ludu, J.S., Letendre, G.W., Meierovics, A.I., Stephens, G., and Elkins, K.L. (2004). A *Francisella tularensis* pathogenicity island required for intramacrophage growth. J Bacteriol *186*, 6430-6436.

Nau, G.J., Guilfoile, P., Chupp, G.L., Berman, J.S., Kim, S.J., Kornfeld, H., and Young, R.A. (1997). A chemoattractant cytokine associated with granulomas in tuberculosis and silicosis. Proc Natl Acad Sci U S A *94*, 6414-6419.

Nigrovic, L.E., and Wingerter, S.L. (2008). Tularemia. Infect Dis Clin North Am *22*, 489-504, ix.

Nishikado, H., Mukai, K., Kawano, Y., Minegishi, Y., and Karasuyama, H. (2011). NK cell-depleting anti-asialo GM1 antibody exhibits a lethal off-target effect on basophils *in vivo*. J Immunol *186*, 5766-5771.

Oh, S., Perera, L.P., Terabe, M., Ni, L., Waldmann, T.A., and Berzofsky, J.A. (2008). IL-15 as a mediator of CD4+ help for CD8+ T cell longevity and avoidance of TRAIL-mediated apoptosis. Proc Natl Acad Sci U S A *105*, 5201-5206.

Oyston, P.C. (2008). *Francisella tularensis*: unravelling the secrets of an intracellular pathogen. J Med Microbiol *57*, 921-930.

Oyston, P.C. (2009). *Francisella tularensis* vaccines. Vaccine *27 Suppl 4*, D48-51.

Oyston, P.C., and Quarry, J.E. (2005). Tularemia vaccine: past, present and future. Antonie Van Leeuwenhoek *87*, 277-281.

Oyston, P.C., Sjostedt, A., and Titball, R.W. (2004). Tularaemia: bioterrorism defence renews interest in *Francisella tularensis*. Nat Rev Microbiol *2*, 967-978.

Pammit, M.A., Budhavarapu, V.N., Raulie, E.K., Klose, K.E., Teale, J.M., and Arulanandam, B.P. (2004). Intranasal interleukin-12 treatment promotes antimicrobial clearance and survival in pulmonary *Francisella tularensis* subsp. *novicida* infection. Antimicrob Agents Chemother *48*, 4513-4519.

Paranavitana, C., Zelazowska, E., DaSilva, L., Pittman, P.R., and Nikolich, M. (2010). Th17 cytokines in recall responses against *Francisella tularensis* in humans. J Interferon Cytokine Res *30*, 471-476.

Park, M.K., Amichay, D., Love, P., Wick, E., Liao, F., Grinberg, A., Rabin, R.L., Zhang, H.H., Gebeyehu, S., Wright, T.M., *et al.* (2002). The CXC chemokine murine monokine induced by IFN-gamma (CXC chemokine ligand 9) is made by APCs, targets lymphocytes including activated B cells, and supports antibody responses to a bacterial pathogen *in vivo*. J Immunol *169*, 1433-1443.

Parmely, M.J., Fischer, J.L., and Pinson, D.M. (2009). Programmed cell death and the pathogenesis of tissue injury induced by type A *Francisella tularensis*. FEMS Microbiol Lett *301*, 1-11.

Parsa, K.V., Butchar, J.P., Rajaram, M.V., Cremer, T.J., Gunn, J.S., Schlesinger, L.S., and Tridandapani, S. (2008). *Francisella* gains a survival advantage within mononuclear phagocytes by suppressing the host IFNgamma response. Mol Immunol *45*, 3428-3437.

Pasetti, M.F., Cuberos, L., Horn, T.L., Shearer, J.D., Matthews, S.J., House, R.V., and Sztein, M.B. (2008). An improved *Francisella tularensis* live vaccine strain (LVS) is well tolerated and highly immunogenic when administered to rabbits in escalating doses using various immunization routes. Vaccine *26*, 1773-1785.

Pechous, R., Celli, J., Penoske, R., Hayes, S.F., Frank, D.W., and Zahrt, T.C. (2006). Construction and characterization of an attenuated purine auxotroph in a *Francisella tularensis* live vaccine strain. Infect Immun *74*, 4452-4461.

Pechous, R.D., McCarthy, T.R., Mohapatra, N.P., Soni, S., Penoske, R.M., Salzman, N.H., Frank, D.W., Gunn, J.S., and Zahrt, T.C. (2008). A *Francisella tularensis* Schu S4 purine auxotroph is highly attenuated in mice but offers limited protection against homologous intranasal challenge. PLoS One *3*, e2487.

Pechous, R.D., McCarthy, T.R., and Zahrt, T.C. (2009). Working toward the future: insights into *Francisella tularensis* pathogenesis and vaccine development. Microbiol Mol Biol Rev *73*, 684-711.

Phillips, N.J., Schilling, B., McLendon, M.K., Apicella, M.A., and Gibson, B.W. (2004). Novel modification of lipid A of *Francisella tularensis*. Infect Immun *72*, 5340-5348.

Pierini, L.M. (2006). Uptake of serum-opsonized *Francisella tularensis* by macrophages can be mediated by class A scavenger receptors. Cell Microbiol *8*, 1361-1370.

Pietras, E.M., Miller, L.S., Johnson, C.T., O'Connell, R.M., Dempsey, P.W., and Cheng, G. (2011). A MyD88-dependent IFNgammaR-CCR2 signaling circuit is required for mobilization of monocytes and host defense against systemic bacterial challenge. Cell Res *21*, 1068-1079.

Poquet, Y., Kroca, M., Halary, F., Stenmark, S., Peyrat, M.A., Bonneville, M., Fournie, J.J., and Sjostedt, A. (1998). Expansion of Vgamma9 Vdelta2 T cells is triggered by *Francisella tularensis*-derived phosphoantigens in tularemia but not after tularemia vaccination. Infect Immun *66*, 2107-2114.

Pulendran, B., Li, S., and Nakaya, H.I. (2010). Systems vaccinology. Immunity *33*, 516-529.

Pyles, R.B., Jezek, G.E., and Eaves-Pyles, T.D. (2010). Toll-like receptor 3 agonist protection against experimental *Francisella tularensis* respiratory tract infection. Infect Immun *78*, 1700-1710.

Qin, A., Scott, D.W., Thompson, J.A., and Mann, B.J. (2009). Identification of an essential *Francisella tularensis* subsp. *tularensis* virulence factor. Infect Immun *77*, 152-161.

Querec, T.D., Akondy, R.S., Lee, E.K., Cao, W., Nakaya, H.I., Teuwen, D., Pirani, A., Gernert, K., Deng, J., Marzolf, B., *et al.* (2009). Systems biology approach predicts immunogenicity of the yellow fever vaccine in humans. Nat Immunol *10*, 116-125.

Quill, H., and Giovanni, M. (2004). Working with dangerous bugs. Nat Immunol *5*, 765-767.

Rawool, D.B., Bitsaktsis, C., Li, Y., Gosselin, D.R., Lin, Y., Kurkure, N.V., Metzger, D.W., and Gosselin, E.J. (2008). Utilization of Fc receptors as a mucosal vaccine strategy against an intracellular bacterium, *Francisella tularensis*. J Immunol *180*, 5548-5557.

Ray, H.J., Chu, P., Wu, T.H., Lyons, C.R., Murthy, A.K., Guentzel, M.N., Klose, K.E., and Arulanandam, B.P. (2010). The Fischer 344 rat reflects human susceptibility to *Francisella* pulmonary challenge and provides a new platform for virulence and protection studies. PLoS One *5*, e9952.

Raynaud, C., Meibom, K.L., Lety, M.A., Dubail, I., Candela, T., Frapy, E., and Charbit, A. (2007). Role of the wbt locus of *Francisella tularensis* in lipopolysaccharide O-antigen biogenesis and pathogenicity. Infect Immun *75*, 536-541.

Reilly, T.J., Baron, G.S., Nano, F.E., and Kuhlenschmidt, M.S. (1996). Characterization and sequencing of a respiratory burst-inhibiting acid phosphatase from *Francisella tularensis*. J Biol Chem *271*, 10973-10983.

Rhinehart-Jones, T.R., Fortier, A.H., and Elkins, K.L. (1994). Transfer of immunity against lethal murine *Francisella* infection by specific antibody depends on host gamma interferon and T cells. Infect Immun *62*, 3129-3137.

Rick Lyons, C., and Wu, T.H. (2007). Animal models of *Francisella tularensis* infection. Ann N Y Acad Sci *1105*, 238-265.

Rodriguez, A.R., Yu, J.J., Murthy, A.K., Guentzel, M.N., Klose, K.E., Forsthuber, T.G., Chambers, J.P., Berton, M.T., and Arulanandam, B.P. (2011). Mast cell/IL-4 control of *Francisella tularensis* replication and host cell death is associated with increased ATP production and phagosomal acidification. Mucosal Immunol *4*, 217-226.

Rubin, E.J., Akerley, B.J., Novik, V.N., Lampe, D.J., Husson, R.N., and Mekalanos, J.J. (1999). *In vivo* transposition of mariner-based elements in enteric bacteria and mycobacteria. Proc Natl Acad Sci U S A *96*, 1645-1650.

Rubinstein, M.P., Kovar, M., Purton, J.F., Cho, J.H., Boyman, O., Surh, C.D., and Sprent, J. (2006). Converting IL-15 to a superagonist by binding to soluble IL-15R{alpha}. Proc Natl Acad Sci U S A *103*, 9166-9171.

Russo, B.C., Horzempa, J., O'Dee, D.M., Schmitt, D.M., Brown, M.J., Carlson, P.E., Jr., Xavier, R.J., and Nau, G.J. (2011). A *Francisella tularensis* locus required for spermine responsiveness is necessary for virulence. Infect Immun *79*, 3665-3676.

Ryden, P., Bjork, R., Schafer, M.L., Lundstrom, J.O., Petersen, B., Lindblom, A., Forsman, M., Sjostedt, A., and Johansson, A. (2012). Outbreaks of tularemia in a boreal forest region depends on mosquito prevalence. J Infect Dis *205*, 297-304.

Salomonsson, E., Kuoppa, K., Forslund, A.L., Zingmark, C., Golovliov, I., Sjostedt, A., Noppa, L., and Forsberg, A. (2009). Reintroduction of two deleted virulence loci restores full virulence to the live vaccine strain of *Francisella tularensis*. Infect Immun *77*, 3424-3431.

Salomonsson, E.N., Forslund, A.L., and Forsberg, A. (2011). Type IV Pili in *Francisella* - A Virulence Trait in an Intracellular Pathogen. Front Microbiol *2*, 29.

Sanapala, S., Yu, J.J., Murthy, A.K., Li, W., Guentzel, M.N., Chambers, J.P., Klose, K.E., and Arulanandam, B.P. (2012). Perforin- and Granzyme-Mediated Cytotoxic Effector Functions Are Essential for Protection against *Francisella tularensis* following Vaccination by the Defined *F. tularensis* subsp. *novicida* {Delta} fopC Vaccine Strain. Infect Immun *80*, 2177-2185.

Sandstrom, G. (1994). The tularaemia vaccine. J Chem Technol Biotechnol *59*, 315-320.

Sandstrom, G., Lofgren, S., and Tarnvik, A. (1988). A capsule-deficient mutant of *Francisella tularensis* LVS exhibits enhanced sensitivity to killing by serum but diminished sensitivity to killing by polymorphonuclear leukocytes. Infect Immun *56*, 1194-1202.

Santiago, A.E., Cole, L.E., Franco, A., Vogel, S.N., Levine, M.M., and Barry, E.M. (2009). Characterization of rationally attenuated *Francisella tularensis* vaccine strains that harbor deletions in the guaA and guaB genes. Vaccine *27*, 2426-2436.

Santic, M., Asare, R., Skrobonja, I., Jones, S., and Abu Kwaik, Y. (2008). Acquisition of the vacuolar ATPase proton pump and phagosome acidification are essential for escape of *Francisella tularensis* into the macrophage cytosol. Infect Immun *76*, 2671-2677.

Santic, M., Molmeret, M., and Abu Kwaik, Y. (2005a). Modulation of biogenesis of the *Francisella tularensis* subsp. *novicida*-containing phagosome in quiescent human macrophages and its maturation into a phagolysosome upon activation by IFN-gamma. Cell Microbiol *7*, 957-967.

Santic, M., Molmeret, M., Klose, K.E., Jones, S., and Kwaik, Y.A. (2005b). The *Francisella tularensis* pathogenicity island protein IglC and its regulator MglA are essential for modulating phagosome biogenesis and subsequent bacterial escape into the cytoplasm. Cell Microbiol *7*, 969-979.

Santic, M., Pavokovic, G., Jones, S., Asare, R., and Kwaik, Y.A. (2009). Regulation of apoptosis and anti-apoptosis signalling by *Francisella tularensis*. Microbes Infect *12*, 126-134.

Saslaw, S., Eigelsbach, H.T., Prior, J.A., Wilson, H.E., and Carhart, S. (1961). Tularemia vaccine study. II. Respiratory challenge. Arch Intern Med *107*, 702-714.

Schmerk, C.L., Duplantis, B.N., Howard, P.L., and Nano, F.E. (2009). A *Francisella novicida* pdpA mutant exhibits limited intracellular replication and remains associated with the lysosomal marker LAMP-1. Microbiology *155*, 1498-1504.

Schmitt, D.M., O'Dee, D.M., Horzempa, J., Carlson, P.E., Jr., Russo, B.C., Bales, J.M., Brown, M.J., and Nau, G.J. (2012). A *Francisella tularensis* live vaccine strain that improves stimulation of antigen-presenting cells does not enhance vaccine efficacy. PLoS One *7*, e31172.

Schulert, G.S., and Allen, L.A. (2006). Differential infection of mononuclear phagocytes by *Francisella tularensis*: role of the macrophage mannose receptor. J Leukoc Biol *80*, 563-571.

Schwartz, J.T., Barker, J.H., Kaufman, J., Fayram, D.C., McCracken, J.M., and Allen, L.A. (2012). *Francisella tularensis* inhibits the intrinsic and extrinsic pathways to delay constitutive apoptosis and prolong human neutrophil lifespan. J Immunol *188*, 3351-3363.

Sharma, J., Mares, C.A., Li, Q., Morris, E.G., and Teale, J.M. (2011). Features of sepsis caused by pulmonary infection with *Francisella tularensis* Type A strain. Microb Pathog *51*, 39-47.

Shen, H., Harris, G., Chen, W., Sjostedt, A., Ryden, P., and Conlan, W. (2010). Molecular immune responses to aerosol challenge with *Francisella tularensis* in mice inoculated with live vaccine candidates of varying efficacy. PLoS One *5*, e13349.

Sherwood, E.R., Enoh, V.T., Murphey, E.D., and Lin, C.Y. (2004). Mice depleted of CD8+ T and NK cells are resistant to injury caused by cecal ligation and puncture. Lab Invest *84*, 1655-1665.

Sjostedt, A. (2007). Tularemia: history, epidemiology, pathogen physiology, and clinical manifestations. Ann N Y Acad Sci *1105*, 1-29.

Sjostedt, A., Conlan, J.W., and North, R.J. (1994). Neutrophils are critical for host defense against primary infection with the facultative intracellular bacterium *Francisella tularensis* in mice and participate in defense against reinfection. Infect Immun *62*, 2779-2783.

Skyberg, J.A., Rollins, M.F., Holderness, J.S., Marlenee, N.L., Schepetkin, I.A., Goodyear, A., Dow, S.W., Jutila, M.A., and Pascual, D.W. (2012). Nasal Acai polysaccharides potentiate innate immunity to protect against pulmonary *Francisella tularensis* and *Burkholderia pseudomallei* Infections. PLoS Pathog *8*, e1002587.

Slight, S.R., Lin, Y., Messmer, M., and Khader, S.A. (2011). *Francisella tularensis* LVS-induced Interleukin-12 p40 cytokine production mediates dendritic cell migration through IL-12 Receptor beta1. Cytokine *55*, 372-379.

Small, P.L., Isberg, R.R., and Falkow, S. (1987). Comparison of the ability of enteroinvasive *Escherichia coli, Salmonella typhimurium, Yersinia pseudotuberculosis,* and *Yersinia enterocolitica* to enter and replicate within HEp-2 cells. Infect Immun *55*, 1674-1679.

Staples, J.E., Kubota, K.A., Chalcraft, L.G., Mead, P.S., and Petersen, J.M. (2006). Epidemiologic and molecular analysis of human tularemia, United States, 1964-2004. Emerg Infect Dis *12*, 1113-1118.

Stenmark, S., Lindgren, H., Tarnvik, A., and Sjostedt, A. (2003). Specific antibodies contribute to the host protection against strains of *Francisella tularensis* subspecies *holarctica*. Microb Pathog *35*, 73-80.

Stenmark, S., Sunnemark, D., Bucht, A., and Sjostedt, A. (1999). Rapid local expression of interleukin-12, tumor necrosis factor alpha, and gamma interferon after cutaneous *Francisella tularensis* infection in tularemia-immune mice. Infect Immun *67*, 1789-1797.

Stonier, S.W., and Schluns, K.S. (2010). Trans-presentation: a novel mechanism regulating IL-15 delivery and responses. Immunol Lett *127*, 85-92.

Su, J., Yang, J., Zhao, D., Kawula, T.H., Banas, J.A., and Zhang, J.R. (2007). Genome-wide identification of *Francisella tularensis* virulence determinants. Infect Immun *75*, 3089-3101.

Surcel, H.M., Syrjala, H., Karttunen, R., Tapaninaho, S., and Herva, E. (1991). Development of *Francisella tularensis* antigen responses measured as T-lymphocyte proliferation and cytokine production (tumor necrosis factor alpha, gamma interferon, and interleukin-2 and -4) during human tularemia. Infect Immun *59*, 1948-1953.

Svensson, K., Larsson, P., Johansson, D., Bystrom, M., Forsman, M., and Johansson, A. (2005). Evolution of subspecies of *Francisella tularensis*. J Bacteriol *187*, 3903-3908.

Telepnev, M., Golovliov, I., Grundstrom, T., Tarnvik, A., and Sjostedt, A. (2003). *Francisella tularensis* inhibits Toll-like receptor-mediated activation of intracellular signalling and secretion of TNF-alpha and IL-1 from murine macrophages. Cell Microbiol *5*, 41-51.

Telepnev, M., Golovliov, I., and Sjostedt, A. (2005). *Francisella tularensis* LVS initially activates but subsequently down-regulates intracellular signaling and cytokine secretion in mouse monocytic and human peripheral blood mononuclear cells. Microb Pathog *38*, 239-247.

Thatte, A., DeWitte-Orr, S.J., Lichty, B., Mossman, K.L., and Ashkar, A.A. (2011). A critical role for IL-15 in TLR-mediated innate antiviral immunity against genital HSV-2 infection. Immunol Cell Biol *89*, 663-669.

Thomas, R.M., Titball, R.W., Oyston, P.C., Griffin, K., Waters, E., Hitchen, P.G., Michell, S.L., Grice, I.D., Wilson, J.C., and Prior, J.L. (2007). The immunologically distinct O antigens from *Francisella tularensis* subspecies *tularensis* and *Francisella novicida* are both virulence determinants and protective antigens. Infect Immun *75*, 371-378.

Titball, R.W., and Oyston, P.C. (2003). A vaccine for tularaemia. Expert Opin Biol Ther *3*, 645-653.

Torres, V.J., VanCompernolle, S.E., Sundrud, M.S., Unutmaz, D., and Cover, T.L. (2007). *Helicobacter pylori* vacuolating cytotoxin inhibits activation-induced proliferation of human T and B lymphocyte subsets. J Immunol *179*, 5433-5440.

Trambley, J., Bingaman, A.W., Lin, A., Elwood, E.T., Waitze, S.Y., Ha, J., Durham, M.M., Corbascio, M., Cowan, S.R., Pearson, T.C., and Larsen, C.P. (1999). Asialo GM1(+) CD8(+) T cells play a critical role in costimulation blockade-resistant allograft rejection. J Clin Invest *104*, 1715-1722.

Trevisanato, S.I. (2007). The 'Hittite plague', an epidemic of tularemia and the first record of biological warfare. Med Hypotheses *69*, 1371-1374.

Troyer, R.M., Propst, K.L., Fairman, J., Bosio, C.M., and Dow, S.W. (2009). Mucosal immunotherapy for protection from pneumonic infection with *Francisella tularensis*. Vaccine *27*, 4424-4433.

Twine, S., Bystrom, M., Chen, W., Forsman, M., Golovliov, I., Johansson, A., Kelly, J., Lindgren, H., Svensson, K., Zingmark, C., *et al.* (2005). A mutant of *Francisella tularensis* strain SCHU S4 lacking the ability to express a 58-kilodalton protein is attenuated for virulence and is an effective live vaccine. Infect Immun *73*, 8345-8352.

Valentino, M.D., Hensley, L.L., Skrombolas, D., McPherson, P.L., Woolard, M.D., Kawula, T.H., Frelinger, J.A., and Frelinger, J.G. (2009). Identification of a dominant CD4 T cell epitope in the membrane lipop rotein Tul4 from *Francisella tularensis* LVS. Mol Immunol *46*, 1830-1838.

Vinogradov, E., Perry, M.B., and Conlan, J.W. (2002). Structural analysis of *Francisella tularensis* lipopolysaccharide. Eur J Biochem *269*, 6112-6118.

Walley, K.R., Lukacs, N.W., Standiford, T.J., Strieter, R.M., and Kunkel, S.L. (1997). Elevated levels of macrophage inflammatory protein 2 in severe murine peritonitis increase neutrophil recruitment and mortality. Infect Immun *65*, 3847-3851.

Wang, X., Karbarz, M.J., McGrath, S.C., Cotter, R.J., and Raetz, C.R. (2004). MsbA transporter-dependent lipid A 1-dephosphorylation on the periplasmic surface of the inner membrane: topography of *Francisella novicida* LpxE expressed in Escherichia coli. J Biol Chem *279*, 49470-49478.

Wang, X., Ribeiro, A.A., Guan, Z., Abraham, S.N., and Raetz, C.R. (2007). Attenuated virulence of a *Francisella* mutant lacking the lipid A 4'-phosphatase. Proc Natl Acad Sci U S A *104*, 4136-4141.

Wang, X., Ribeiro, A.A., Guan, Z., McGrath, S.C., Cotter, R.J., and Raetz, C.R. (2006). Structure and biosynthesis of free lipid A molecules that replace lipopolysaccharide in *Francisella tularensis* subsp. *novicida*. Biochemistry *45*, 14427-14440.

Warren, H.S., and Smyth, M.J. (1999). NK cells and apoptosis. Immunol Cell Biol *77*, 64-75.

Watanabe, H., Numata, K., Ito, T., Takagi, K., and Matsukawa, A. (2004). Innate immune response in Th1- and Th2-dominant mouse strains. Shock *22*, 460-466.

Wayne Conlan, J., and Oyston, P.C. (2007). Vaccines against *Francisella tularensis*. Ann N Y Acad Sci *1105*, 325-350.

Wayne Conlan, J., Shen, H., Kuolee, R., Zhao, X., and Chen, W. (2005). Aerosol-, but not intradermal-immunization with the live vaccine strain of *Francisella tularensis* protects mice against subsequent aerosol challenge with a highly virulent type A strain of the pathogen by an alphabeta T cell- and interferon gamma- dependent mechanism. Vaccine *23*, 2477-2485.

Wehrly, T.D., Chong, A., Virtaneva, K., Sturdevant, D.E., Child, R., Edwards, J.A., Brouwer, D., Nair, V., Fischer, E.R., Wicke, L., *et al.* (2009). Intracellular biology and virulence determinants of *Francisella tularensis* revealed by transcriptional profiling inside macrophages. Cell Microbiol *11*, 1128-1150.

Weiss, D.S., Brotcke, A., Henry, T., Margolis, J.J., Chan, K., and Monack, D.M. (2007). *In vivo* negative selection screen identifies genes required for *Francisella* virulence. Proc Natl Acad Sci U S A *104*, 6037-6042.

West, T.E., Pelletier, M.R., Majure, M.C., Lembo, A., Hajjar, A.M., and Skerrett, S.J. (2008). Inhalation of *Francisella novicida* Delta mglA causes replicative infection that elicits innate and adaptive responses but is not protective against invasive pneumonic tularemia. Microbes Infect *10*, 773-780.

Wherry, W.B., Lamb, B.H. (1914). Infection of man with Bacterium tularense. J Infect Dis *15*, 331-340.

Wickstrum, J.R., Hong, K.J., Bokhari, S., Reed, N., McWilliams, N., Horvat, R.T., and Parmely, M.J. (2007). Coactivating signals for the hepatic lymphocyte gamma interferon response to *Francisella tularensis*. Infect Immun *75*, 1335-1342.

Woolard, M.D., Wilson, J.E., Hensley, L.L., Jania, L.A., Kawula, T.H., Drake, J.R., and Frelinger, J.A. (2007). *Francisella tularensis*-infected macrophages release prostaglandin E2 that blocks T cell proliferation and promotes a Th2-like response. J Immunol *178*, 2065-2074.

Wu, T.H., Hutt, J.A., Garrison, K.A., Berliba, L.S., Zhou, Y., and Lyons, C.R. (2005). Intranasal vaccination induces protective immunity against intranasal infection with virulent *Francisella tularensis* biovar A. Infect Immun *73*, 2644-2654.

Yee, D., Rhinehart-Jones, T.R., and Elkins, K.L. (1996). Loss of either CD4+ or CD8+ T cells does not affect the magnitude of protective immunity to an intracellular pathogen, *Francisella tularensis* strain LVS. J Immunol *157*, 5042-5048.

Zarrella, T.M., Singh, A., Bitsaktsis, C., Rahman, T., Sahay, B., Feustel, P.J., Gosselin, E.J., Sellati, T.J., and Hazlett, K.R. (2011). Host-adaptation of *Francisella tularensis* alters the bacterium's surface-carbohydrates to hinder effectors of innate and adaptive immunity. PLoS One *6*, e22335.

Zhang, D., Kuolee, R., Harris, G., Zhang, Q., Conlan, J.W., and Chen, W. (2008). Lymphotoxin-alpha plays only a minor role in host resistance to respiratory infection with virulent type A *Francisella tularensis* in mice. Mediators Inflamm *2008*, 239740.